2003

Effect on Heartbeat of Drosophila melanogaster of Mutations in the Calcium Channel Encoding cacophony Gene and its Interaction with the RNA Helicase Mutant maleless^napts

Vanessa McGowan

EFFECT ON HEARTBEAT OF *Drosophila melanogaster* OF MUTATIONS IN THE CALCIUM CHANNEL ENCODING *cacophony* GENE AND ITS INTERACTION WITH THE RNA HELICASE MUTANT *maleless*^{napts}

By

Vanessa McGowan

B.S. University of Maine, 2000

A THESIS

Submitted in Partial Fulfillment of the

Requirements for the Degree of

Master of Science

(in Zoology)

The Graduate School

The University of Maine

December, 2003

Advisory Committee:

Harold B. Dowse, Professor of Zoology and Cooperating Professor of Mathematics, Advisor

John M. Ringo, Professor of Biology

Erik Johnson, Ph.D.

EFFECT ON HEARTBEAT OF *Drosophila melanogaster* OF MUTATIONS IN THE CALCIUM CHANNEL ENCODING *cacophony* GENE AND ITS INTERACTION WITH THE RNA HELICASE MUTANT *maleless*^{napts}

By Vanessa McGowan Ray

Thesis Advisor: Dr. Harold B. Dowse

An Abstract of the Thesis Presented
in Partial Fulfillment of the Requirements for the
Degree of Master of Science
(in Zoology)
December, 2003

There is a lack of information concerning the genetics of heart disease, especially of those due to aberrant pacemaker activity. *Drosophila melanogaster* is an ideal candidate for research in this area because of its suitability to genetic manipulation and its accessible genetic database. What is most compelling, however, is that the genesis of heartbeat is *Drosophila* is strikingly similar to that in many other organisms, including mammals.

The myogenic heart of *Drosophila melanogaster* is stimulated to contract by a caudal pacemaker, which is regulated by ion channel interactions. A voltage-gated calcium channel of P/Q- or N-type is implicated in the pacemaker by pharmacological studies. The voltage-gated calcium channel α_1 subunit encoding gene in *Drosophila*, *cacophony* (*cac*), was identified as a candidate for this role. After examining heartbeat of the *cac* alleles *cac*^{s} and *cac*^{ts2} I report that they have increased heart rates and

rhythmicities, potentially due to altered inactivation of the calcium channels they encode affecting pacemaking.

The gene with which the RNA helicase mutant *no action potential*$^{temperature\text{-}sensitive}$ (*mle*^{napts}) interacts, causing arrhythmic heartbeat, has yet to be uncovered. *mle*^{napts} is an allele of the dosage compensation gene *maleless* (*mle*). It is possible that *mle*^{napts} is interacting with *cac* to cause deviations in heartbeat phenotype from wild-type. By characterizing heartbeat of *cac ; mle*^{napts} double mutants I determine that the genes interact, but in an unresolved manner.

ACKNOWLEDGMENTS

I would like to thank the Association of Graduate Students for helping fund this project through research grant awards. I would also like to thank the members of my advisory committee for the time and energy they committed to helping me mold this project and thesis into its present form. I also appreciate the example they set for fulfilling the requirements placed on research scientists in academia.

There are other people who deserve recognition for their contribution to my personal development throughout my time as a graduate student. During my time as a graduate student I gained valuable experience as a teaching assistant. Because of this commitment, I had the privilege of working closely with the laboratory coordinator, Kevin Tracewski. I thank him not only for his professional guidance and steadfast support, but also for his insight on life planning.

As an athlete on the University of Maine's cross country and track & field teams I forged a strong bond with my coach, Mark Lech. He has been one of my biggest advocates, and I have relied on him for advice and guidance in personal and athletic matters.

Above all, my family has always supported me in my endeavors, personally, emotionally, and sometimes financially. My parents, sisters, and husband, Benjamin, have been terrific listeners and morale coaches.

TABLE OF CONTENTS

LIST OF TABLES

LIST OF FIGURES

Chapter 1

EFFECT ON HEARTBEAT OF *Drosophila melanogaster* OF MUTATIONS IN THE CALCIUM CHANNEL ENCODING *cacophony* GENE

INTRODUCTION

Background Information on *cacophony*: Alleles and their Phenotypes

The Discovery of the cacophony *gene: Courtship Song*

cacophony [*cac*] was the first *Drosophila melanogaster* (fruit fly) courtship song mutant isolated through screening after ethyl methansulfonate (EMS) mutagenesis (Schilcher, 1976). Male flies create the song by intermittently beating their wings in a patterned way (Chang and Miller, 1978; Speith and Ringo, 1983; Wheeler *et al.*, 1989; Kawasaki, 2000). Certain viable mutants of *cac* (cac^{s}, cac^{ts2}) exhibit qualitative abnormalities in various he pattern and amplitude of this song parameters (Schilcher, 1976, Kulkarni and Hall, 1987; Peixoto and Hall, 1998; Jeziorski *et al.*, 2000; Peixoto *et al.*, 2000; Chan *et al.*, 2002). Specifically, cac^{s} mutants recessively exhibit an extended (~11 ms), often polycyclic, and uncoordinated ("broken") pulse song that contrasts the 4 ms, mono- or bicyclic pulse song of wild-type flies (Schilcher, 1976; Kulkarni and Hall, 1987; Wheeler *et al.*, 1989; Hall, 1994; Yamamoto *et al.*, 1997; Fletcher *et al.*, 1998; Peixoto and Hall, 1998; Smith *et al.*, 1998; Peixoto *et al.*, 2000; Chan *et al.*, 2002). The interpulse interval (IPI) in mutants is increased from ~35 ms to ~44 ms, which is thought

to be partially due to extended pulse duration (Schilcher, 1976; Wheeler *et al.*, 1989; Yamamoto *et al.*, 1997; Smith *et al.*, 1998; Peixoto and Hall, 1998; Peixoto *et al.*, 2000; Chan *et al.*, 2002). The amplitude of cac^{s} song pulses (PA) is also aberrant, at 50-100% greater than wild-type (Schilcher, 1976; and Kulkarni and Hall, 1987; Wheeler *et al.*, 1989; Yamamoto *et al.*, 1997; Peixoto and Hall, 1998; Smith *et al.*, 1998; Peixoto *et al.*, 2000). Intrapulse frequency (IPF) and sine song frequency (SSF) appear to be unaffected by the cac^{s} mutation (Wheeler *et al.*, 1989; Yamamoto *et al.*, 1997; Peixoto and Hall, 1998); however, bouts of the latter occur less frequently (Schilcher, 1976). cac^{ts2} flies show temperature-dependent song defects in cycles per pulse (CPP), PA, and IPI that resemble those of cac^{s} across temperature (Chan *et al.*, 2002). At the highest temperature tested, 30°C, CPP is 35% higher and PA is 50% greater than wild-type song parameters (Chan *et al.*, 2002). cac^{ts2} exhibits an additional song defect in that IPF is lower (25% at 30°C) than wild-type (Chan *et al.*, 2002).

The impact of deviations within courtship song potentially may have very large consequences. Many aspects of the courtship song are unique to species and so it potentially represents a mechanism of speciation within the *Drospholid* group (Peixoto and Hall, 1998; Smith *et al.*, 1998; Peixoto *et al.*, 2000; Greenspan and Ferveur, 2000). The hypothesis that mutations in *cac* may be involved in speciation is suggested by the fact that CPP, IPI, and IPF, altered by mutations in this gene, are song parameters that commonly differ among *Drosophila* species (Ewing and Bennet-Clark, 1968; Chang and Miller, 1978; Wheeler *et al.*, 1989; Peixoto and Hall, 1998; Peixoto *et al.*, 2000; Greenspan and Ferveur, 2000). Also, alterations in courtship song of *cac* mutants are not "pathologically" defective to the point of rendering it ineffective; however, they affect

song quality by changing the patterning of certain components (Peixoto and Hall, 1998; Greenspan and Ferveur, 2000; Chan *et al.*, 2002).

cac *Alleles: Visual and Lethal Mutants*

To date, thirty-nine alleles of *cac* have been identified, most of which are recessive lethals (FlyBase, 2003), suggesting that the *cac* gene's polypeptide product has a vital role in *Drosophila*. Two families of *cac* alleles lack song defects and are instead composed of lethal (lethal(1)L13, now cac^{L-}) and visual (n*ightblind-A* [*nbA*], now cac^{nbA}) mutants (Pak, 1970; Heisenberg and Götz, 1975; Kulkarni and Hall, 1987; Fletcher *et al.*, 1998; Peixoto *et al.*, 2000; Jeziorski *et al.*, 2000). These three behavioral mutant classes are within a single genetic locus that is variably spliced resulting in different developmental and structural functions of the cac product(Kulkarni and Hall, 1987; Smith *et al.*, 1996; Smith *et al.*, 1998; Kawasaki *et al.*, 2000). This implies that cac^{L-} mutations are within a common exon whereas mutations affecting either song or vision occur in differentially spliced transcript regions (Kulkarni and Hall, 1987 The *cac* locus was physically defined by deficiencies spanning a 17-23 kb region of the X chromosome that failed to complement all three mutations (Kulkarni and Hall, 1987).

Initially cac^{L-} and cac^{nbA} were not thought to be allelic to *cac* because of large phenotypic differences. cac^{nbA} causes defects in the kinetics and amplitude of the electroretinogram (ERG) (Kulkarni and Hall, 1987; Homyk and Pye, 1989; Smith *et al.* 1998) as well as abnormal light thresholds for optomotor and phototactic behaviors (Pak, 1979; Heisenberg and Götz, 1975; Smith *et al.*, 1998). However, mutants of these two behavioral classes fail to complement, firmly establishing their allelism (Homyk and Pye,

1989). Although *cac* and *nbA* initially did not appear to complement for song or vision (Homyk and Pye, 1989; Hall, 1994), further studies elucidated that several heteroallelic combinations of *cac* mutants involving cac^{s} have mild electroretinogram (ERG) abnormalities involving a novel rebound component, and certain genetic combinations involving a cac^{nbA} family allele (cac^{P73}) exhibit subtle song defects (Smith *et al.*, 1998). cac^{ts2} was found to be slightly defective in ERG analyses as well, but in a temperature-dependent fashion (Chan *et al.*, 2002). The structure of the ERG is normal, however the amplitude of light-on transient spikes is significantly smaller at low temperature (~22°C) (Chan *et al.*, 2002). Additionally, the amplitude of light-coincident photoreceptor potentials (LCRPs) and light-off transient spikes are slightly but not significantly low, and these deficits are restored to normal at higher temperature (~30°C) Chan *et al.*, 2002). The most obvious defect occurs at high temperature, where repolarization intervals are drastically increased (Chan *et al.*, 2002).

The connection to cac^{L-} alleles came even later, when it was discovered that the onset of embryonic lethality in cac^{L-} (Kulkarni and Hall, 1987) is consistent with the time of the first peak of *cac* expression (Smith *et al.*, 1996). *cac* is expressed in the nervous system, showing peaks during *Drosophila* development in first instar larvae, midpupae, and late pupae (Smith *et al.*, 1996). Since this coincidence was revealed, the failure of these two mutant classes to complement was reported, establishing that they are allelic (Kulkarni and Hall, 1987). Recent research by Kawasaki *et al.* (2002) demonstrated rescue of lethality with a wild-type *cac* transgene, thus reinforcing that cac^{L-} is an allele of *cac* and the causal agent of lethality.

Pleiotropic Effects of cac *Mutations: Courtship Defects*

The courtship defect of mutations in the *cac* gene is genetically separable from its song abnormality (Kulkarni and Hall, 1987; Peixoto and Hall, 1998; Smith *et al.*, 1998). Schilcher's (1976) and later Kulkarni and Hall's (1987) studies found wingless cac^s flies to have lower mating success than wild-type flies in the same state (Yamamoto *et al.*, 1997). This result was deduced based on a parallel comparison using intact flies, which suggested that the cac^s mutant's song abnormalities may actually improve its chance of mating success, although not to wild-type levels because of other behavioral factors like hampered locomotor ability that will be discussed in more detail (Schilcher, 1976; Kulkarni and Hall, 1987; Yamamoto *et al.*, 1997). Later studies revealed that the courtship decrement originally observed in intact cac^s males (Schilcher, 1976; Kulkarni and Hall, 1987) was due to genetic background effects. cac^s decreases courtship initiation latency and enhances copulation duration (30% longer than wild-type) (Chan *et al.*, 2002). The ameliorated fitness hypothesis for winged cac^s flies is that its loud song stimulates females more than normal (Schilcher, 1976), which enables it to overcome its locomotor deficit (Sturtevant, 1915; Kulkarni and Hall, 1987) and its decrease in number of female-arousing sine song bouts (Schilcher, 1976).

Another factor that adds confusion to this discussion is that the cac^s mutant's initially reported mating decrement (Schilcher, 1976) was expected because of the positive relationship between IPI abnormalities and increased mating latencies (Wheeler *et al.*, 1989). However, because IPI does not solely measure increments of silence between trains, which may be wild-type in cac^s, and because females may respond to this

parameter specifically, it is believable that intact cac^{s} males are not deficient in this aspect of courtship (Wheeler *et al.*, 1989).

That the cac^{ts2} courtship defect is independent of temperature, unlike this mutant's song defect, confirms that different phenotypes are caused by issues of expression (Chan *et al.*, 2002). In contrast to intact cac^{s} flies, mating success of cac^{ts2} flies is reduced, especially when they are wingless (Chan *et al.*, 2002). In this condition the mating success of cac^{ts2} flies is three times lower than that of wild-type (Chan *et al.*, 2002). In terms of specific courtship parameters, though, they are only significantly slower than wild-type to initiate courtship, and only when de-winged (Chan *et al.*, 2002). Despite these results, wing condition (winged or wingless) does not statistically impact courtship initiation latency in cac^{ts2} flies (Chan *et al.*, 2002). Therefore, cac^{ts2} flies' courtship disadvantage must be due to additional behavioral defects, like their motor deficit (Sturtevant, 1915; Chan *et al.*, 2002). In summation, courtship phenotypes are quite different between *cac* mutants, with cac^{s} showing enhancements and cac^{ts2} exhibiting detrimental effects.

Pleiotropic Effects of cac *Mutations: Motor Defects*

The *cac* gene was discovered to have pleiotropic effects because its alleles influence many behavioral phenotypes besides courtship and the associated song. For example, some *cac* mutants have recessive temperature-sensitive motor defects that are exhibited as lack of coordinated movements, spinning behavior, and paralysis (Peixoto and Hall, 1998; Dellinger *et al.*, 2000). Peixoto and Hall (1998) reported that cac^{s} showed all of these phenotypic defects at temperatures over 36°C. In particular, paralysis

occurred at temperature ≥46°C (Peixoto and Hall, 1998). If the flies were maintained at elevated temperatures for long periods of time (> 1 hr for 1-day-old flies and less for older flies) they usually died (Peixoto and Hall, 1998). The cac^{ts2} mutant's gross motor behavior defect (paralysis) was characterized by Dellinger *et al.* (2000). In this study cac^{ts2} flies became paralyzed at lower temperatures (38°C) than cac^{s} flies (46°C) (Peixoto and Hall, 1998; Chan *et al.*, 2002). At 38°C it took cac^{s} flies approximately 20 minutes to become paralyzed, whereas it only took cac^{ts2} flies about a minute (Dellinger *et al.*, 2000). However, cac^{s} flies are temperature-dependent for paralysis and cac^{ts2} flies sharply exhibit it only beyond the restrictive temperature (38°) (Dellinger *et al.*, 2000). For this phenotype cac^{s} does not complement cac^{ts2} but instead appears to dominate it because at 38°C behavior is like that of cac^{s} flies (Dellinger *et al.*, 2000). Like cac^{s} flies, cac^{ts2} flies exhibit the other locomotor defects when temperature reaches 36°C (Peixoto and Hall, 1998; Dellinger *et al.*, 2000). The locomotor defects associated with the cac^{ts2} allele include a long recovery time after mechanical shock in a temperature-independent fashion (Chan *et al.*, 2002).

Behavioral Exclusions of cac *Mutants*

The *cac* mutations do not appear to affect factors underlying flight (Yamamoto *et al.*, 1997), circadian rhythms, longevity, or thoracic morphology (Kulkarni and Hall, 1987). Other exclusions to *cac* mutants' array of behavioral defects are somewhat surprising. Mediocre light-induced responses of certain *cac* mutants (ERG) have been described (Smith *et al.*, 1998; Chan *et al.*, 2002). This makes it likely that the same *cac* mutants would be defective in regard to other visually mediated responses like optomotor

cytoplasmic linker, and potentially S4 segments also contribute to voltage-dependent inactivation (Ashcroft, 2000). Independent of the underlying process, voltage-mediated inactivation renders channels incapable of opening so that they do not activate in response to subsequent depolarization (de Leon *et al.*, 1995).

Calcium-dependent inactivation occurs more rapidly than voltage-dependent inhibition, but it is less efficient in terminating channel activity (DeMaria *et al.*, 2001). Feedback inhibition by local intracellular Ca^{2+} in certain channels (L-, P/Q, and R-types, but not in N-type) (Zühlke *et al.*, 1999; Lee *et al.*, 1999; DeMaria *et al.*, 2001) depends on two crucial motifs in the proximal third section of the C-terminus (de Leon *et al.*, 1995) called the Ca^{2+} inactivation (CI) region (Hering *et al.*, 2000). Evidently, inactivation does not depend solely on an EF hand, a Ca^{2+} binding motif consisting of 29 amino acids (de Leon *et al.*, 1995), but also requires a critical section located C-terminal to it called the 'IQ' domain (Zhou *et al.*, 1997; Zühlke *et al.*, 1999; Peterson *et al.*, 2000; DeMaria *et al.*, 2001; Kawasaki *et al.*, 2002; Brooks *et al.*, 2003). One model for the Ca^{2+}-dependent inactivation mechanism is that calcium binds the EF hand's helix-loop-helix, causing a conformational change to occur that closes the channel (Chan *et al.*, 2002). However, a study by Zhou *et al.* (1997) showed that calcium binds somewhere in the C-terminus besides the EF hand. Zhou *et al.* (1997) defined a segment of ~18 amino acids C-terminal to the EF hand, spanning ~160 amino acids, and including the IQ domain. The IQ motif in the C-terminus, specifically, is a calmodulin (CaM) interaction domain composed of ~8 amino acids with a consensus sequence of IQEYFRKF (Peterson *et al.*, 2000). The isoleucine and glutamine residues within the IQ motif are essential to bind CaM in a Ca^{2+}-dependent manner (Hering *et al.*, 2000). To trigger inactivation,

Ca^{2+} putatively binds multivalently to two sites in the N-terminal domain of the constitutively tethered (potentially to the channel's N-terminus) CaM prosthetic group (Jeziorski *et al.*, 2000) close to the inner mouth of the channel yet outside of the conduction pathway, causing it to complex with the IQ domain while providing resistance to Ca^{2+} chelators (de Leon *et al.*, 1995; Zhou *et al.*, 1997; Zühlke *et al.*, 1999; Hering *et al.*, 2000; Peterson *et al.*, 2000; DeMaria *et al.*, 2001; Kawasaki *et al.*, 2002; Brooks *et al.*, 2003). CaM's interaction with calcium channels is terminal-specific in that its C-terminal lobe also interacts with the IQ motif but in a facilitatory capacity, promoting rapid channel activation in response to local Ca^{2+} increases (Zühlke *et al.*, 1999; DeMaria *et al.*, 2001). In contrast, CaM's N-terminal lobe triggers inactivation more slowly and in response to rises in general cellular Ca^{2+} concentration (DeMaria *et al.*, 2001).. Note that a CaM binding domain ('CBD') that lies distal to the IQ motif (Peterson *et al.*, 2000) in the proximal third of the C terminus was originally thought to fulfill the Ca^{2+}-CaM interaction function in P/Q-type channels (Lee *et al.*, 1999), but it has since been discredited in favor of the IQ motif (DeMaria *et al.*, 2001). The theory of IQ domain involvement in Ca^{2+}-inactivation relegates the EF hand to having a modulatory impact on the process, probably by supporting necessary conformational changes (Hering *et al.*, 2000), or by affecting calcium binding (Peterson *et al.*, 2000). Support for this assignation comes from mutagenic and chimeric channel studies that confirm that the EF hand's consensus Ca^{2+}-binding motif fails to act as the Ca^{2+} sensor (Zhou *et al.*, 1997) but that a cluster of four hydrophobic amino acids (VVTL) within the *F* helix is crucial for inactivation, the essential chemistry has been functionally mapped to the second valine (Peterson *et al.*, 2000). Clusters of this type often transduce Ca^{2+}

binding into sequential interactions that allow for the functional consequences of EF-hand domains (Peterson *et al.,* 2000). A putative model detailing interactions between EF hand and IQ domains to allow for inactivation is suggested by Peterson *et al.* (2000). Potentially, Ca^{2+}-induced CaM binding the IQ motif could induce conformational changes in the EF hand, which by causing exposure of hydrophobic patches to target sites on the channel would result in inactivation (de Leon *et al.*, 1995; Peterson *et al.,* 2000).

The contribution to voltage-dependent inactivation of conserved residues (E1537 – Hering *et al.,* 2000, and E1535 - Peterson *et al.,* 2000) within the EF hand of L-type channels, perhaps as part of a putative inactivation ball, suggests commonality in molecular determinants of inactivation mechanisms. The C-terminus also contains a cAMP-dependent protein kinase phosphorylation site between IVS6 and the EF hand that is conserved in all identified calcium channels and therefore may have a universal function, perhaps related to voltage dependence (Loughney *et al.*, 1989; Smith *et al.*, 1996). In addition, Ca^{2+}-dependent channel inactivation may be modulated by I-II and II-III interdomain linkers, by proteins that interact with them and other intracellular loops (Hering *et al.,* 2000), and/or by distal portions of the carboxyl tail (Peterson *et al.,* 2000). By whatever means Ca^{2+} causes inactivation, it does so by shifting the pattern of channel gating from a high opening frequency, rapidly activating mode (mode 1) to an infrequently opening, slowly activating mode (mode Ca^{2+}) (de Leon *et al.*, 1995).

The other four subunits modify channel function by interacting with the α_1 subunit (Snutch *et al.*, 1990; Neely *et al.*, 1993; Jeziorski *et al.*, 2000; Hille, 2001; Krauss, 2001). They impact channel properties by affecting current density and enhancing magnitude, mediating pharmacological sensitivity (Neely *et al.*, 1993),

modulating voltage dependence, and altering kinetic properties (Jeziorski *et al.*, 2000; Ashcroft, 2000; Hering *et al.*, 2000; Peterson *et al.*, 2000). Extracellular portions of regulatory subunits are often glycosylated (Jeziorski *et al.*, 2000) and some intracellular parts possess regulatory phosphorylation sites, which may affect channel kinetics (Loughney *et al.*, 1989; Nunoki *et al.*, 1989; Krauss, 2001).

Specifically, the β subunit improves coupling of voltage sensing to pore opening, which results in increased Ca^{2+} current amplitude (Neely *et al.*, 1993). β subunits also regulate the rate and voltage dependence of activation and inactivation of channels (Smith *et al.*, 1996; Hering *et al.*, 1998; Hering *et al.*, 2000; Jeziorski *et al.*, 2000; Peterson *et al.*, 2000). The β subunit is bound to α_1 by a conserved sequence of eighteen amino acids in the cytoplasmic linker between domains I and II (Smith, 1996; Peixoto *et al.*, 1997; Ashcroft, 2000; Jeziorski *et al.*, 2000).

Types of Voltage-Gated Calcium Channels

There are two major electrophysiological categories of mammalian voltage-gated calcium channels (Day *et al.*, 1997; Jeziorski *et al.*, 2000). Type I are activated by small depolarizations (positive to –70 mV) (Dascal *et al.*, 1986; Fozzard and Arnsdorf, 1992; Gielow *et al.*, 1995) and are thus called LVA channels, for low voltage activating (Ashcroft, 2000; Hille, 2001). These channels characteristically have tiny, transient currents and are therefore classified by Tsien *et al.* (1987) as T-type channels (Ashcroft, 2000; Hille, 2001). They generally activate (open) and deactivate (close) quickly and completely, and rapidly inactivate in a voltage-dependent manner (Dascal *et al.*, 1986; Ashcroft, 2000; Hille, 2001). T-type channels are usually responsible for generation of

rhythmic pacemaker activity in vertebrate cardiac muscle and some nerve cells (Olivera *et al.,* 1994; Ashcroft, 2000). They are selectively sensitive to blockage by synthetic funnel-web toxin (sFTX) (Olivera *et al.,* 1994), and Ni^{2+} (Hüser *et al.*, 2000; Terrar and Rigg, 2000; Lipsius *et al.*, 2001), and non-specifically to amiloride (Johnson *et al.*, 1998), octanol, and flunarizine (Gielow *et al.,* 1995). T-type channels of *Drosophila* have subtle physiological differences from those of vertebrates in that they have higher activation thresholds (positive to –30 mV) and slower inactivation (Gielow *et al.,* 1995).

In contrast, type II channels are high voltage activating (HVA) and so they only open in reaction to large depolarizations (Dascal *et al.*, 1986; Hille, 2001). There are at least four HVA channel sub-types according to Tsien *et al.* (1987) (L, P/Q, N, and R) that have slightly different kinetics and pharmacologies (Ashcroft, 2000; Hille, 2001). L-type channels are named for their large and long conductances. They open slowly at membrane potentials positive to –30 mV (Gielow *et al.,* 1995) and close quickly but are persistent, meaning that they inactivate very slowly (Dascal *et al.*, 1986; Ashcroft, 2000; Hille, 2001). Inactivation in L-type channels is more calcium-dependent than any other type of calcium channel (Ashcroft, 2000). L-type HVA channel currents compose the primary Ca^{2+} conductance in vertebrate cardiac, skeletal, and smooth muscle (Dascal *et al.*, 1986; Gielow *et al.*, 1995), and are also prominent in endocrine cells and continuously secreting synapses (Ashcroft, 2000; Jeziorski *et al.*, 2000; Hille, 2001). In *Drosophila*, they provide the dominating Ca^{2+} current underlying muscular action potentials (Littleton and Ganetzky, 2000). They have extracellular binding domains at IIIS5-S6, and IVS5-S6 (Smith *et al.*, 1996) that are highly sensitive to antagonists like ω-Agatoxin (ω-Aga) IIIA, ω-conotoxin (ω-CTx) GVIA (Greenberg *et al.*, 1989),

calciseptine (Olivera *et al.*, 1994), use-dependently to phenylalkylamines (PAAs) like verapamil, (-)q-devapamil (qDev), (-)gallopamil and D-600, benzothiazepines (BTZs) like diltiazem, and in a voltage-based manner to 1,4-dihydropyridines (DHPs) (Snutch *et al.*, 1990) like the blockers nifedipine (Dascal *et al.*, 1986), isradipine (Jeziorski *et al.*, 2000), nitrendipine and PN200-110, and the agonist BAY K8644 (Nunoki *et al.*, 1989; Gielow *et al.*, 1995; Eberl *et al.*, 1998; Hering *et al.*, 1998; Jeziorski *et al.*, 2000; Hille, 2001). The C-terminus of one well-characterized channel in *Drosophila* (Dmca1D) also contains part of a DHP binding domain and a PAA binding domain (Eberl *et al.*, 1998). Most channel characteristics are based on vertebrate subtypes, and unfortunately invertebrate Ca^{2+} currents do not correspond precisely to these profiles (Jeziorski *et al.*, 2000). For instance, *Drosophila* L-type channels have a slight pharmacological deviation from those of vertebrates by being less sensitive to verapamil (Gielow *et al.*, 1995). *Drosophila* neuronal currents are generally more sensitive to PAAs than DHPs, whereas L-type channels in muscle are more effectively blocked by DHPs (Jeziorski *et al.*, 2000).

Other HVA channels subtypes, N (for neuronal), P/Q (P for Purkinje cell and Q for cerebellar granule cell), and R (for resistant to toxins), can be grouped together functionally but are pharmacologically distinct (Hille, 2001). P- and Q-types are usually grouped as one channel type because they may employ the same α_1 subunit (Day *et al.*, 1997); however, P-type channels inactivate more slowly than Q-types (Hering *et al.*, 2000). Non-L-type HVA channels are only found in invertebrate and vertebrate neural tissue (Jeziorski *et al.*, 2000), and in certain endocrine cells (Ashcroft, 2000). N-type channels are sensitive to ω-CTx GVIA (Greenberg *et al.*, 1989), MVIIA and less severely to MVIIC, while P/Q-type are blocked by ω-Aga IVA and ω-CTx MVIIC, and less so by

ω-Aga IIIA and FTX, and R-type are mostly insensitive to both (Olivera *et al.,* 1994; Ashcroft, 2000; Jeziorski *et al.* 2000; Hille, 2001). There is evidence of an additional HVA channel type, labeled O-type by Olivera *et al.* (1994), characterized as regulating norepinephrine release in rat brain hippocampus cells, and being highly sensitive to ω-CTx MVIIC and less inhibited by ω-Aga IVA. Its similarity to P/Q channel types prompted the proposal of an "OPQ" channel subfamily (Olivera *et al.,* 1994); however, this grouping is not widely recognized. It is important to note that spider (ω-Aga) toxins have greater potency in invertebrate tissues than those from fish-hunting snails (ω-CTx), probably due to these organisms respective predatory targets (Jeziorski *et al.*, 2000).

Non-L-type HVA channels exhibit certain properties, like single channel conductance, and degree of inactivation, that are intermediate between T- and L- type channels (Olivera *et al.,* 1994; Hille, 2001). For example, they partially inactivate but not very quickly (Hille, 2001). Ordered according to their inactivation time courses, R-type channels are fastest, N-types are intermediate, and P/Q-types are slowest (Hering *et al.,* 2000). They are more similar to LVA T-type channels in that they open quickly at negative potentials and are resistant to dihydropyridines (Olivera *et al.,* 1994; Hille, 2001). However, they are similar to L-type channels in that they conduct Ba^{2+} better than Ca^{2+}, have peak currents at relatively positive potentials, are blocked more readily by Cd^{2+} than Ni^{2+} (Tsien *et al.*, 1987; Nunoki *et al.*, 1989), and are insensitive to amiloride and octanol (Olivera *et al.,* 1994; Hille, 2001). They are also blocked by phenylalkylamines (Smith *et al.*, 1996) and are weakly sensitive to benzothiazepines, but unlike L-type channels they are not stereoselective (Greenberg *et al.*, 1989; Hering *et al.*, 1996). N, P/Q, and R channels are distinguished from T- and L-types by certain unique

channel kinetics. Specifically, they close slowly, have a high activation range (positive to –20 mV), and a huge inactivation range (-120 to –30 mV) (Hille, 2001).

Snutch *et al.* (1990) created a molecular classification system for vertebrate voltage-gated calcium channel α_1 subunits that corresponds with Tsien *et al.*'s (1987) phenomenological nomenclature for the channels they compose (Day *et al.*, 1997; Peixoto and Hall, 1998; Ashcroft, 2000; Jeziorski *et al.*, 2000; Hille, 2001). Most of Snutch *et al.*'s (1990) channel classes have been expressed but exceptions are noted as follows (Hille, 2001). According to Snutch *et al.*'s (1990) system, T-type channels contain one of three α_1 subunits genes, α_{1G} ($Ca_v3.1$), α_{1H} ($Ca_v3.2$) (only one cloned), and α_{1I} ($Ca_v3.3$); L-type channels are made of either an α_{1C} (cardiac - $Ca_v1.2$), α_{1D} (brain, soma and dendrites - $Ca_v1.3$), α_{1F} ($Ca_v1.4$) (only one not yet cloned), or α_{1S} (skeletal - $Ca_v1.1$) subunit, N-type channels have α_{1B} subunits (brain, synapses - $Ca_v2.2$), P/Q-type are composed of α_{1A} subunits (brain, synapses - $Ca_v2.1$), and R-type are categorized as having α_{1E} subunits (brain, soma and dendrites - $Ca_v2.3$) (Peixoto *et al.*, 1997; Day *et al.*, 1997; Fletcher *et al.*, 1998; Hering *et al.*, 1998; Ashcroft, 2000; Jeziorski *et al.*, 2000; Lipsius *et al.*, 2001; Hille, 2001; Chan *et al.*, 2002). Since then, a new nomenclature based on nucleotide sequence was introduced to replace the Snutch *et al.* (1990) system (Hille, 2001). This system is shown in brackets (Ca_v#) beside the corresponding Snutch *et al.* (1990) classes, and is organized into three families of channels based on phylogeny: LVA T-types, HVA L-types, and HVA non-L-types (Hille, 2001).

Diversity of Voltage-Gated Calcium Channels

There is much pharmacological and electrophysiological evidence of voltage-gated calcium channel diversity in *Drosophila* (Greenberg *et al.*, 1989; Gielow *et al.*, 1995; Smith *et al.*, 1996; Fletcher *et al.*, 1998; Jeziorski *et al.*, 2000; MacPherson *et al.*, 2001). Ion channel differences are caused by several additive factors that allow for varying channel properties (Hering *et al.*, 2000). The entire α_1 subunit of calcium channels is the single gene product of one of several genes in a multi-gene family (Day *et al.*, 1997; Eberl, 1998; Fletcher *et al.*, 1998; Jeziorski *et al.*, 2000; MacPherson *et al.*, 2001), which allows for isoforms with different electrophysiologies and spatial and temporal expression patterns to exist (Moczydloswki *et al.*, 1988; Koch *et al.*, 1990; Snutch *et al.*, 1990; Olivera *et al.*, 1994; Jeziorski *et al.*, 2000; Hille, 2001; Kawasaki *et al.*, 2002). For example, there is evidence of as many as eight pharmacological classes of calcium channels that are probably derived from a much reduced number of genes, which suggests that α_1 subunits in different tissues have distinct pharmacological sensitivities (MacPherson *et al.*, 2001). In *Drosophila* there are at least two distinct, non redundant α_1 subunits proteins, Dmca1A (N-type/α_{1A}) on the X (Smith *et al.*, 1996; Peixoto *et al.*, 1997), and Dmca1D (L-type/α_{1D}) on the second chromosome (Eberl *et al.*, 1998; Rubin *et al.*, 2000). There is evidence of at least two more calcium channel α_1 subunit genes that may or may not be vital and non-redundant, one of which is a T-type (α_{1G}) channel and the other is a calcium channel class that diverges from those of vertebrates (Rubin *et al.*, 2000; Littleton and Ganetzky, 2000; Kawasaki *et al.*, 2002).

Like for α_1 subunits, many genes code for other calcium channel subunits so that the number of possible subunit combinations increases channel number factorially

(Olivera *et al.*, 1994; Eberl *et al.*, 1998; Ashcroft, 2000; Jeziorski *et al.*, 2000; MacPherson *et al.*, 2001). There is one β subunit gene, three α_2/δ genes (α_2 and δ are derived from the same gene product), and putatively one γ gene in the *Drosophila* genome (Rubin *et al.*, 2000; Littleton and Ganetzky, 2000). Alternative splicing further increases transcript possibilities (Fletcher *et al.*, 1998; Hering *et al.*, 2000; Jeziorski *et al.*, 2000; MacPherson *et al.*, 2001). For one particular α_1 subunit encoding gene (*cac*), there are at least thirty predicted exons that are alternatively spliced to potentially contribute to ion channel diversity (Smith *et al.*, 1996; Peixoto *et al.*, 1997; Smith *et al.*, 1998). The physiological heterogeneity of ion channels is also increased by RNA editing (Peixoto *et al.*, 1997; Smith *et al.*, 1998; Palladino *et al.*, 2000; Hille, 2001; Chan *et al.*, 2002; Kawasaki *et al.*, 2002) and posttranslational modification (Nunoki *et al.*, 1989; Koch *et al.*, 1990; Jeziorski *et al.*, 2000; Hille, 2001; Kawasaki *et al.*, 2002).

Roles of Voltage-Gated Calcium Channels

Calcium is a potent intracellular signaling ion in the cell (Jeziorski *et al.*, 2000) and so it is kept at very low levels, as low as $\sim 10^{-4}$ the extracellular concentration (Fozzard and Arnsdorf, 1992; Ashcroft, 2000; Markou and Theophilidis, 2000; Hille, 2001). Towards this goal, it is important that voltage-gated calcium channels have strict ionic selectivity (Irisawa *et al.*, 1993), more than a 1000-fold for Ca^{2+} (Krauss, 2001), owing to a small minimum pore radius (Hille, 2001). Voltage-gated calcium channels allow excitable cells to transduce electrical energy into intracellular action (Dascal *et al.*, 1986; Fletcher *et al.*, 1998; Hille, 2001). An increase in intracellular calcium may cause muscular contraction, enzymatic activity, synaptic transmission (Greenberg *et al.*, 1989;

Lee *et al.*, 1999; Kawasaki *et al.*, 2000; Kawasaki *et al.*, 2002; Jiang *et al.*, 2003a), membrane excitability (Dascal *et al.*, 1986l; Snutch *et al.*, 1990; Strong *et al.*, 1993; Gielow *et al.*, 1995), gene expression (Fletcher *et al.*, 1998; Zühlke *et al.*, 1999; Jeziorski *et al.*, 2000), and rhythmic potentials, among other functions (Tsien *et al.*, 1987; Hille 2001; Smith *et al.*, 1996; Smith *et al.*, 1998; Hering *et al.*, 2000). Intracellular calcium is necessary for the contractile machinery of the heart, so that an increase in concentration could stimulate heart rate purely due to improved Ca^{2+} availability (Johnson *et al.*, 2002). Intracellular calcium is specifically important for pacemaker activity because it influences gating of certain calcium and potassium channels directly, and through various heterotrimeric guanine nucleotide-binding regulatory protein (G-protein) coupled signaling pathways (Hille, 2001). For example, intracellular calcium interacts with the calcium-calmodulin dependent protein kinase II (CaMKII) signaling pathway, thereby mediating the activities of some calcium and potassium channels involved in pacemaking (Johnson *et al.*, 2002; Rigg *et al.*, 2003).

Molecular Characterization of *cacophony*

The cac *Gene Transcript* – Dmca1A

cac is located on the X chromosome at meiotic map position 1-36.7, according to a report by Kulkarni and Hall (1987). Cytogenetic studies using deficiencies suggest it is found on the distal portion of the X chromosome from polytene chromosome region 11A1 to 11A2 (Kulkarni and Hall, 1987; Dellinger *et al.*, 2000). The *cac* gene is distributed over more than 45 kb of genomic sequence (Peixoto *et al.*, 1997; Peixoto *et*

al., 2000) and encodes a single 10.5 kb transcript class that is preferentially expressed in the nervous system and alternately spliced for functional heterogeneity (Smith *et al.*, 1996; MacPherson *et al.*, 2001). A representative mRNA of 6522 nucleotides (U55776) containing a solitary open reading frame (ORF) of 5553 nucleotides was derived from one assembled contig (Smith *et al.*, 1996). It translates into a polypeptide composed of 1851 amino acids (P91645) that form a predicted 212 kD voltage-gated calcium channel α_1 subunit protein called Dmca1A (Smith *et al.*, 1996; Peixoto *et al.*, 2000). Prior to genetic and molecular information, the basis for the theory that *cac* encodes the α_1 subunit of a family of voltage-gated calcium channels was the momentary spastic fit phenotype, among others, exhibited by mutants (Hall, 1994).

Dmca1A is classified as the α_1 subunit of a non-L-type HVA calcium channel (Jeziorski *et al.*, 2000) because its protein transcript has poorly conserved dihydropyridine binding sites (MacPherson *et al.*, 2001) and exhibits five conserved protein kinase C (PKC) phosphorylation sites in the S4-S5 loops that are exclusive to non-L-type calcium channels (Smith *et al.*, 1996). The proximity of the PKC sites to the S4 domain suggests that they may affect voltage sensing (Smith *et al.*, 1996). Grouping Dmca1A in a specific analogous vertebrate channel class is problematic because it appears that non-L-type invertebrate channels diverged after the evolutionary separation of vertebrates and invertebrates (Smith *et al.*, 1996; Jeziorski *et al.*, 2000). The *cac* gene can be most closely classified according to Tsien *et al.*'s (1987) calcium channel-type nomenclature as a P/Q-type high voltage-gated calcium channel because of its similarity to this class of channel (Smith *et al.*, 1996; Littleton and Ganetzky, 2000; MacPherson *et al.*, 2001; Kawasaki *et al.*, 2002). According to Snutch *et al.*'s (1990) calcium channel α_1

subunit identification, Dmca1A has channel characteristics closest to vertebrate α_{1A} subunits, which is consistent with its sequence homology grouping (Kawasaki *et al.*, 2002). However, *cac* is also closely related to α_{1B} subunits (Snutch *et al.*, 1990), and N-type (Tsien *et al.*, 1987) channels (Smith *et al.*, 1996; Peixoto *et al.*, 1997; Littleton and Ganetzky, 2000; Jeziorski *et al.*, 2000; Kawasaki *et al.*, 2002). Therefore, *cac* can be best described as intermediate between these two channel types (P/Q- and N-types). Direct functional analysis of *cac* calcium channels is necessary to determine specific calcium channel characteristics (Brooks *et al.*, 2003).

The Dmca1A amino acid sequence contains regions resembling different ion channel components, some of which are not specific to voltage-gated calcium channels. Namely, the *cac* transcript has a region resembling a calcium channel (Littleton and Ganetzky, 2000; MacPherson *et al.*, 2001), an EF-hand family, a phenylalkylamine binding fragment, a cation channel transmembrane (TM) region, a non-ligand gated cation channel (Smith *et al.*, 1996), a calcium and sodium channel pore region (S4-S6), and a sodium channel α subunit (FlyBase, 2003). This subtle ambiguity alludes to the evolutionary history of this channel class (Nunoki *et al.*, 1989; Snutch *et al.*, 1990; Jeziorski *et al.*, 2000) that helps identify functional significances of various components by analogy (Loughney *et al.*, 1989; Strong *et al.*, 1993; Ashcroft, 2000; Hille, 2001; Jiang *et al.*, 2003a).

cac *Transcript Diversity*

The diversity of *cac* mutant phenotypes, as well as their complex complementation and interaction patterns (Kulkarni and Hall, 1987; Peixoto *et al.*, 1997;

Smith *et al.*, 1998; Peixoto and Hall, 1998; Kawasaki *et al.*, 2000; Dellinger *et al.*, 2000), suggest multiple cellular roles for Dmca1A. Phenogenetic analyses suggest that these functions are at least partially separable (Smith *et al.*, 1998), and that most identified *cac* alleles are homozygous lethals (FlyBase, 2003) implies that the role of calcium channel(s) incorporating Dmca1A are crucial in *Drosophila.*

The diversity of *cac* functions is due to regulation of temporal, spatial, and tissue-specific expression (Engel and Wu, 1992; Smith *et al.*, 1998), and to the existence of different Dmca1A isoforms (Gielow *et al.*, 1995; Smith *et al.*, 1996; Smith *et al.*, 1998; Palladino *et al.*, 2000; Chan *et al.*, 2002). Differential transcript splicing (Jeziorski *et al.*, 2000; MacPherson *et al.*, 2001), and posttranscriptional and posttranslational modifications (Nunoki *et al.*, 1989) provide complexity at the molecular level and help to explain *cac* alleles' involved complementation patterns (Kulkarni and Hall, 1987; Smith *et al.*, 1998; Kawasaki *et al.*, 2000). However, despite the existence of multiple *cac* transcripts (Kawasaki *et al.*, 2002), there appears to be little (five sites) natural polymorphic variation (Robbins *et al.*, 1999) even in noncoding *cac* DNA, and absolutely no variation in Dmca1A amino acid sequence samples from closely related species (Peixoto *et al.*, 2000; Chan *et al.*, 2002).

Alternative splicing contributes to transcript heterogeneity. *cac* has 34 predicted exons (Smith *et al.*, 1996; Smith *et al.*, 1998), 32 of which contain coding sequences (Peixoto *et al.*, 1997). Two very short exons (3 bp and 6 bp) are optional and three pairs of exons are mutually exclusive (Peixoto *et al.*, 1997; Jeziorski *et al.*, 2000). Dmca1A's optional splice site in the IVS3/IVS4 extracellular loop generates four transcript variants with unknown functional significance (Peixoto *et al.*, 1997), besides being unnecessary

for Dmca1A's role in neurotransmitter release (Kawasaki *et al.*, 2002). The splice site is conserved in mammalian α_1 subunit genes in which analogous exonic inclusions create channels with heterogeneous channel activation, inactivation, and pharmacological properties (Kawasaki *et al.*, 2002). However, it remains to be seen if these optional exons have analogous functions in *Drosophila*.

The other three alternative splices have more obvious significance. Differences in the mutually exclusive exons encoding the IS3/IS4 loop and the IS4 segment likely affect channel electrophysiologies (Peixoto *et al.*, 1997). Variability in the IS3/IS4 loop section of the two exons may alter activation kinetics (Peixoto *et al.*, 1997; Jeziorski *et al.*, 2000). Also, alternative exons differ in their number of positively charged residues, which could affect voltage sensing (Peixoto *et al.*, 1997).

Another mutually exclusive splice site concerns part of the loop between domains I and II (Smith *et al.*, 1996; Peixoto *et al.*, 1997). Recently it was discovered that these exons are optional as well (Kawasaki *et al.*, 2002). One alternative exon (I-IIb) is more common and encodes a β subunit binding region and an overlapping domain that binds $G_{\beta\gamma}$ subunits (Smith *et al.*, 1998; Jeziorski *et al.*, 2000; Kawasaki *et al.*, 2002). The other exon (I-IIa) may be specific to the eye (Smith *et al.*, 1998), has a poorly conserved β subunit binding domain and lacks the heterotrimeric G-protein subunit binding motif (Smith *et al.*, 1998). It is possible that exon I-IIa may be altered in cac^{nbA} mutants by virtue of its expression being linked to eye tissue. Because the resulting isoforms are so distinct they may bind different β subunits, or none at all, and they may also lack G-protein interaction, thus altering channel modulation (Peixoto *et al.*, 1997; Smith *et al.*, 1998; Jeziorski *et al.*, 2000; Kawasaki *et al.*, 2002).

The last known mutually exclusive splice site involves two differently sized exons (12 bp and 60 bp) in the sequence encoding the *cac* C-terminus (Kawasaki *et al.*, 2002). The position of this splice site just C-terminal to the IQ domain suggests that splice variants may have differing calcium/calmodulin binding but neither appear to be necessary for Dmca1A's function in neurotransmitter release (Kawasaki *et al.*, 2002).

Published *cac* sequence has twelve detected post-transcriptional modification sites, all of which are A to G transitions (Smith *et al.*, 1996; Smith *et al.*, 1998; Palladino *et al.*, 2000; Chan *et al.*, 2002; Kawasaki *et al.*, 2002; Brooks *et al.*, 2003) that often lie within functionally critical regions such as transmembrane segments or connecting loops (Jeziorski *et al.*, 2000). The alterations are hydrolytic deaminations of adenosine to inosine during RNA editing by the sole *Drosophila* adenosine deaminase acting on double-stranded RNA (dADAR) (Palladino *et al.*, 2000; Hanrahan *et al.*, 2000). Specific editing of this sort alters coding sequences to potentially allow for functional diversity of α_1 subunits (Jeziorski *et al.*, 2000), while nonspecific editing would occur at a higher frequency with the intent of preventing extensively modified transcripts from leaving the nucleus and potentially protecting against double-stranded RNA (dsRNA) viruses (Smith *et al.*, 1996; Peixoto *et al.*, 1997; Smith *et al.*, 1998; Palladino *et al.*, 2000; Hanrahan *et al.*, 2000; Kawasaki *et al.*, 2002). The importance of editing *cac* transcripts resides in "fine-tuning" and maintenance of the nervous system to modulate adult behaviors (Palladino *et al.*, 2000). However, RNA editing is not required for nervous system development or basic function (Palladino *et al.*, 2000; Kawasaki *et al.*, 2002).

cac cDNAs show multiple evidence of posttranslational modification, including consensus sequences for N-glycosylation (one site), cAMP-dependent protein kinase

phosphorylation (nine sites), and protein kinase C (PKC) phosphorylation (fifteen sites) (Smith *et al.*, 1996; Kawasaki *et al.*, 2002). Thirteen potential phosphorylation sites are clustered in the C-terminus, suggesting that they may be involved in channel function (Smith *et al.*, 1996), perhaps in an inactivation influencing capacity (Loughney *et al.*, 1989). An example of the impact of posttranslational modification on Dmca1A is that phosphorylation by PKC has been shown to increase baseline Ca^{2+} currents and reduce direct G-protein inhibition of calcium channels (Kawasaki *et al.*, 2002).

Molecular Lesions of cac *Mutants*

Both *cac* alleles used in this study (cac^{s} and cac^{ts2}) have mutations in regions implicated in inactivation. Specifically, the cac^{s} mutation appears to have abnormal voltage-dependent inactivation (Hering *et al.*, 1996; Smith *et al.*, 1996; Smith *et al.*, 1998; Chan *et al.*, 2002), whereas the cac^{ts2} alteration may have altered calcium-dependent inactivation (Zhou *et al.*, 1997; Dellinger *et al.*, 2000; Kawasaki *et al.*, 2000; Chan *et al.*, 2002; Kawasaki *et al.*, 2002).

The cac^{s} mutation involves a nucleotide substitution of a T for an A in the sequence encoding transmembrane domain IIIS6 of Dmca1A calcium channel α_1 subunit proteins (Smith *et al.*, 1998). The transversion results in an amino acid substitution of a phenylalanine (F) for an isoleucine (I) that would presumably affect all splice variants because it occurs in exon 19, which is ubiquitous to all Dmca1A isoforms (Smith *et al.*, 1996; Smith *et al.*, 1998). This phenylalanine is highly conserved, not only in calcium channels but also in analogous subunits of sodium and some potassium channels (Smith *et al.*, 1998). As previously mentioned, S6 segments, and IIIS6 especially, are implicated

in fast voltage-dependent inactivation of calcium channels (Hering *et al.*, 1996; Hering *et al.*, 2000; Chan *et al.*, 2002), which is why altered inactivation most likely underlies the various phenotypes of cac^{s} mutants. It may cause the activity dependence of the cac^{s} synaptic defect (Kawasaki *et al.*, 2000) and its song defect (Dellinger *et al.*, 2000; Chan *et al.*, 2002), as will be explained in greater detail.

The cac^{ts2} mutation involves a C for T nucleotide transition that causes a proline (P) to serine (S) substitution in the second of a pair of highly conserved proline residues three amino acids from the EF hand domain towards the C-terminus, where in other channels calcium traditionally binds (Chan *et al.*, 2002; Kawasaki *et al.*, 2002). As previously mentioned, the EF hand and adjacent residues, including a calcium/CaM binding domain (IQ) are involved in calcium-mediated channel inactivation (Chan *et al.*, 2002; Kawasaki *et al.*, 2002).

According to Chan *et al.*'s (2002) theory of Ca^{2+}-dependent inactivation based on calcium binding at the EF hand domain, the amino acid change in cac^{ts2} mutants alters the EF hand's local 3D structure, which would affect its function more critically as temperature increases. Kawasaki *et al.*'s (2002) theory of Ca^{2+} binding a CaM group associated with the IQ domain suggests that the proline pair where cac^{ts2} is mutated may participate in calcium-dependent inactivation by assisting in necessary folding transitions (Kawasaki *et al.*, 2002). It is possible that abnormal folding of this region due to the proline to serine change in cac^{ts2} affects the channel's ability to inactivate so that its function is compromised under the stress of increased temperature (Kawasaki *et al.*, 2002). Altered inactivation in Dmca1A calcium channels would impact any processes in

which this channel is involved, like neurotransmission (Kawasaki *et al.*, 2002), and song production (Chan *et al.*, 2002), as will be more thoroughly explained.

Heartbeat of *Drosophila melanogaster*

Synaptic Physiology of cac *Mutants*

A potentially functionally related phenotype to behavioral defects of *cac* mutants was discovered when Dmca1A was found to be involved in synaptic transmission (Peixoto *et al.*, 2000; Kawasaki *et al.*, 2000; Littleton and Ganetzky, 2000). Initially, similarities between Dmca1A and vertebrate calcium channel α_1 subunits involved in presynaptic neuromuscular transmission (α_{1A} – $Ca_v2.1$; α_{1B} – $Ca_v2.2$) (Day *et al.*, 1997; Lee *et al.*, 1999) suggested the *cac* gene's participation in neurotransmission (Olivera *et al.*, 1994; Smith *et al.*, 1996; Hering *et al.*, 2000; Kawasaki *et al.*, 2002). Neural studies reinforced this suspicion through phenotypic characterization of an interaction between cac^{ts2} and a presynaptic vesicle fusion priming protein (N-ethylmaleimide-sensitive fusion protein (NSF1)) mutant, *comatose* (*comt*) (Dellinger *et al.*, 2000). Furthermore, synaptic electrophysiology studies at the dorsal longitudinal flight muscle (DLM) and the intracoxal lateral levator muscle (ICLM) suggested that a calcium channel that Dmca1A participates in is primarily responsible for fast Ca^{2+}-triggered neurotransmitter release at these synapses (Kawasaki *et al.*, 2000; Kawasaki *et al.*, 2002). This was deduced based on cac^{s} and cac^{ts2} mutants' recessive and reversible decreased synaptic current phenotypes (Kawasaki, 2000; Kawasaki *et al.*, 2002). Analyses of synaptic electrophysiology revealed that cac^{s} flies' reduction of DLM and ICLM synaptic currents

is activity-dependent but temperature-insensitive (Kawasaki *et al.*, 2000). In contrast, the cac^{ts2} mutation causes sharply temperature-sensitive current reduction at these neuromuscular synapses (Kawasaki *et al.*, 2000; Kawasaki *et al.*, 2002). The effect has a restrictive temperature of 33°C and its severity is temperature-dependent (Kawasaki *et al.*, 2000; Kawasaki *et al.*, 2002). The complementation pattern for synaptic electrophysiology is somewhat complex in that cac^{ts2} rescues the cac^{s} mutant phenotype at 20°C (at which temperature the cac^{ts2} phenotype is not evident) but at 36°C the cac^{s} phenotype dominates (Kawasaki *et al.*, 2000).

Voltage-gated calcium channels were originally thought to trigger neurotransmitter release in *Drosophila* in an analogous way to vertebrates, via coupling calcium influxes to fast synaptic vesicle fusion using synaptic protein interaction domains (SYNPRINTs) (Kawasaki *et al.*, 2000; Kawasaki *et al.*, 2002). However, because a SYNPRINT domain has yet to be identified in *Drosophila* (Kawasaki *et al.*, 2000; Littleton and Ganetzky, 2000), and *cac* fulfills its presynaptic role in vesicle fusion without such a domain being identified, *Drosophila* either contain a divergent SYNPRINT domain or more probably have a novel mechanism for coupling calcium influx to neurotransmitter release (Littleton and Ganetzky, 2000; Kawasaki *et al.*, 2002).

The *cac* gene's synaptic role may help explain certain other phenotypic aberrances seen in mutants of this gene. For example, ERG abnormalities in *cac* visual mutants (cac^{nbA}, cac^{s}, cac^{ts2}) are probably due in part to defective transmission from cells of the retina to those in the lamina (Heisenberg and Götz, 1975; Smith *et al.*, 1998). The underlying cause of this problem may be reduced Ca^{2+}-triggered release of neurotransmitter containing vesicles due to defective membrane calcium channels in *cac*

mutants, as seen in peripheral neuromuscular synapses (Kawasaki *et al.*, 2000; Dellinger *et al.*, 2000; Kawasaki *et al.*, 2002; Brooks *et al.,* 2003). Motor problems that occur at elevated temperatures may be due to increased spontaneous neural activity at high temperatures that in turn exacerbates the cac^{s} allele's activity-dependent reduction in synaptic transmission (Kawasaki, 2000). This same aberrance in Dmca1A's role in exocytosis at central (Smith *et al.*, 1996) and peripheral synapses (Kawasaki *et al.*, 2000) may cause the alterations in song pattern seen in certain *cac* mutants (cac^{s}, cac^{ts2}) (Dellinger *et al.*, 2000; Chan *et al.*, 2002; Kawasaki *et al.*, 2002).

Dmca1A has also been shown to be involved in transport in a much different capacity from synaptic transmission. *cac* is expressed in non-excitable Malpighian tubules, which suggests its potential role in epithelial fluid transport (MacPherson *et al.*, 2001). From its putative localization on the basolateral surface of principal cells in the main segment of the tubule, Dmca1A may provide a calcium signal for fluid transport induced by CAP_{2b}, and be involved in the thapsigargin and cyclic 3',5'-guanosine monophosphate (cGMP) responses of these cells (MacPherson *et al.*, 2001).

The Heart of Drosophila melanogaster

The current work concerns heartbeat of *Drosophila*. The heart is a tubular dorsal vessel responsible for movement of hemolymph throughout the body (McCann, 1969; Poulson, 1994; Curtis *et al.*, 1999; Markou and Theophilidis, 2000). It is a simple tubular peristaltic pump (Jones, 1977; Markou and Theophilidis, 2000) consisting of a single layer of cells that extends from the last abdominal segment to the anterior region of the brain (Rizki, 1978; Curtis *et al.*, 1999). The heart is structurally subdivided into an

anterior aorta and a caudal muscular heart that contains the heartbeat-initiating pacemaker (Rizki, 1978; Curtis *et al.*, 1999; Markou and Theophilidis, 2000; Papaefthimiou and Theophilidis, 2001). Openings in the walls of the heart proper, called ostia, allow hemolymph to enter the heart vessel to be pumped out an opening at the anterior end (McCann, 1969; Rizki, 1978; Curtis *et al.*, 1999; Markou and Theophilidis, 2000).

The caudal pacemaker (Rizki, 1978; Gu and Singh, 1995) generates heartbeat myogenically (Dowse *et al.*, 1995; Johnson *et al.*, 1997) to create waves of contraction that pass anteriorly in the dorsal vessel (McCann, 1969; Rizki, 1978; Curtis *et al.*, 1999; Markou and Theophilidis, 2000; Papaefthimiou and Theophilidis, 2001). The possibility of a second, more anterior pacemaker in the region of the cardiovascular valve is suggested by reversals in contraction seen occasionally in larvae and consistently in early pupae (McCann, 1969; Rizki, 1978). Although pacemaking is evident in slow response fibers (Fozzard and Arnsdorf, 1992) of *Drosophila* (Dowse *et al.*, 1995; Johnson *et al.*, 1998), pacemaker cells are morphologically indistinguishable from other myocardial cells (Curtis *et al.*, 1999; Markou and Theophilidis, 2000). To explain the ability of isolated heart segments to maintain intrinsic frequency, Markou and Theophilidis (2000) hypothesized that the pacemaker is actually made of single long cell(s), potentially derived from muscle fibers, that run along the length of the heart. This is in contrast to sinus nodal cells of vertebrates, which are readily identifiable by structure as well as composition (Navaratnam, 1987; Fozzard and Arnsdorf, 1992; Hüser *et al.*, 2000; Lipsius *et al.*, 2001).

Heartbeat is triphasic, consisting of contraction (systole), relaxation (diastole), and pause (diastasis) (Jones, 1977; Rizki, 1978). Heart rate is determined by the duration of diastasis (Markou and Theophilidis, 2000) and is modulated by temperature (Irisawa *et al.*, 1993; Dowse *et al.*, 1995), small peptide hormones (Johnson *et al.*, 2000), and neurotransmitters (Metcalf *et al.*, 1964; Miller, 1985; Dascal *et al.*, 1986; Johnson *et al.*, 1997; Hille, 2001). Cardioactive substances alter heart rate and sometimes rhythmicity by altering pacemaker ion channel kinetics either by directbinding or indirect modulation through signaling pathways (Johnson *et al.*, 1997; Johnson *et al.*, 2000; Johnson *et al.*, 2002).

Ion Channels of the Drosophila *Cardiac Pacemaker*

cac calcium channel(s)'s participation in neurotransmission is the key to solving neurally implicated phenotypes. This information becomes important to determine the source of Dmca1A mutants' heartbeat abnormalities because the heart of *Drosophila* is myogenic (Dowse *et al.*, 1995), and so its activity is independent of nervous stimulation (Markou and Theophilidis, 2000; Papaefthimiou and Theophilidis, 2001). Therefore, *cac* influences heartbeat by a mechanism other than direct neurotransmission. Prior work by this lab suggests that *cac* fulfills this role by participating in cardiac pacemaking (Johnson *et al.*, 1997; Johnson *et al.*, 1998; E. Johnson, unpublished data).

A study of pertussis toxin's (PTX) effect of increasing heart rate may suggest the involvement of a voltage-gated calcium channel in pacemaking (*Johnson et al.,* 2002). Certain compounds have opposite roles in *Drosophila* and vertebrate hearts (Johnson *et al.,* 1997). For example, certain G-proteins are involved in modulation of heartbeat

agonists in vertebrates (Johnson *et al.*, 1997) but in *Drosophila* it may be essential for normal pacemaker activity to have G-proteins inhibit calcium channels (Johnson *et al.*, 1997; Johnson *et al.*, 2002). Because pertussis toxin inhibits Gi/o proteins putatively expressed in cardiac tissue that directly inhibit voltage-gated calcium channels (Guillén *et al.*, 1990; Simon *et al.*, 1991; Ashcroft, 2000; DeMaria *et al.*, 2001), it appears that inhibiting this protein may increase heart rate (Johnson *et al.*, 2002).

Differences in protein action are not surprising considering other deviations in signaling pathway effects between *Drosophila* and vertebrates. Vertebrate hearts are stimulated by neurotransmitters (Hüser *et al.*, 2000; Lipsius *et al.*, 2001) through liberating cyclic adenosine 3',5'-monophosphate (cAMP) signaling pathway (Dascal *et al.*, 1986; Nunoki *et al.*, 1989; Koch *et al.*, 1990; Johnson *et al.*, 1997; Ashcroft, 2000; Hille, 2001) that modulates pacemaker ion channels (ex. I_h) (Rigg *et al.*, 2003), but pharmacological evidence and studies of *dunce* (*dnc*) and *rutabaga* (*rut*) mutants indicate that this pathway is not involved in heartbeat modulation in *Drosophila* (Dowse *et al.*, 1995; Johnson *et al.*, 1997; Johnson *et al.*, 2002). Also, acetylcholine accelerates certain insect hearts, including *Drosophila*'s, via the nervous system but inhibits those of vertebrates by decreasing cAMP levels (Dascal *et al.*, 1986; Johnson *et al.*, 1997; Rigg *et al.*, 2003).

That the cardiac pacemaker requires participation of a voltage-gated calcium channel is supported by several studies using various organisms. A study by Markou and Theophilidis (2000) established that rhythmic pacemaker potentials in the heart of *Tenebrio molitor* depend on Ca^{2+} influx. Work on the auditory organ of lower vertebrates further establishes the critical role of Ca^{2+} channels in oscillatory mechanisms

(Hille, 2001). Purportedly, hair cells respond to specific frequencies of sound through a process called electrical tuning whereby their membrane potentials tend to oscillate due to interacting ion channel currents (Hille, 2001). When sound reaches hair cells it causes a slight membrane depolarization that activates L-type calcium channels to create an inward Ca^{2+} current, further depolarizing the membrane (Hille, 2001). Increased intracellular Ca^{2+} concentrations open calcium-activated potassium channels (BK) encoded by a *slowpoke* (*slo*) homolog, as delayed rectifier channels (Kv) are simultaneously activated by increased membrane potential (Hille, 2001). The outward release of K^+ by these channels hyperpolarizes the membrane so that the cycle can recommence (Hille, 2001). Cochlear oscillations not only provide precedent for implicating calcium and potassium channels in these phenomena, but also serve as a base for modeling the *Drosophila* cardiac pacemaker. The interaction of calcium and potassium channels to generate cellular excitability is illustrated even more relevantly by *Drosophila* larval muscle that contains two calcium channels (L- and T-types) and four potassium channel currents (I_A, I_K, I_{CF}, and I_{CS}) (Gielow *et al.*, 1995). In addition to cochlear and larval studies, early work by Thompson (1977) on *Tritonia diomedia* neurons and by Elkins *et al.* (1986) on *Drosophila* dorsal longitudinal flight muscles (DLMs) to distinguish potassium channel currents, combined with pharmacological identification of ion channels involved in heartbeat by this lab (Johnson *et al.*, 1998) allow the hypothetical determination of pacemaker ion channel activities in *Drosophila*.

The oscillatory interactions of ion channels in excitable cells are innate, allowing pacemaker action potentials to be spontaneous (Fozzard and Arnsdorf, 1992; Hille, 2001) and regenerative so that sinoatrial cells of the heart exhibit repetitive self-excitation, or

"automaticity" (Fozzard and Arnsdorf, 1992; Irisawa *et al.*, 1993; Hüser *et al.*, 2000; Lipsius *et al.*, 2001). It appears that two ion channel types are crucial to the activity of the *Drosophila* cardiac pacemaker: potassium and calcium channels. Four ion channel genes have been identified as necessary for normal heartbeat through analysis of mutant heartbeat and pharmacology (Johnson *et al.*, 1998; Johnson *et al.*, 2000). Three of the channels allow the passage of K^+ and the other carries a Ca^{2+} current (Johnson *et al.*, 2000). The actions of these ion channels permit formulating a putative model for the cardiac pacemaker of *Drosophila* (Johnson *et al.*, 1997; Johnson *et al.*, 1998).

A slow delayed-rectifier potassium channel current (I_{Kr}) containing an α subunit encoded by *ether à go-go* (*eag*) (Kaplan and Trout, 1968; Warmke *et al.*, 1991; Engel and Wu, 1992; Brüggeman *et al.*, 1993) creates a hyperpolarizing leak (E. Johnson, personal communication). The *eag* encoded subunit may contribute to four separate potassium currents (I_A, I_K, I_{CF}, and I_{CS}) either physically (Warmke *et al.*, 1991; Zhong and Wu, 1991; Engel and Wu, 1992; Warmke and Ganetzky, 1994) or electrophysiologically (Brüggeman *et al.*, 1993), which makes it difficult to selectively block the delayed-rectifier K^+ current (I_{Kr}). However, there is evidence that the *eag* current is blocked by quinidine (Zhong and Wu, 1991; Brüggeman *et al.*, 1993; Johnson *et al.*, 1998) and is more sensitive to tetraethylammonium (TEA) than other potassium channels (Thompson, 1977; Moczydlowksi *et al.*, 1988; Atkinson *et al.*, 1991). The decay of the hyperpolarizing K^+ efflux has the effect of depolarizing sino-atrial cells so that a voltage-gated calcium channel, the α_1 subunit of which may be encoded by *cacophony* (*cac*) (von Schilcher, 1976; Smith *et al.*, 1996; Smith *et al.*, 1998), opens to allow Ca^{2+} to enter the cell. This current is blocked by ω-conotoxin (ω-CgTx) MVIIC, an antagonist of N-

(Ashcroft, 2000; Hille, 2001) and P/Q-type calcium channels, and importantly this agent is effective at disrupting the normal heartbeat of *Drosophila* (Olivera *et al.*, 1994).

The influx of Ca^{2+} simultaneously activates a calcium-activated potassium channel (Markou and Theophilidis, 2000) homologous to mammalian BK-type, encoded by *slowpoke* (*slo*) (Elkins *et al.*, 1986), that carries a large and long K^+ current (I_{CF}) (Atkinson *et al.*, 1991; Rubin *et al.*, 2000; Littleton and Ganetzky, 2000; Hille, 2001) blocked by charybdotoxin (CTX) (Moczydlowski *et al.*, 1988), and a fast voltage-gated potassium channel (K_V, A-type) encoded by *Shaker* (*Sh*) (Kaplan and Trout, 1968; Warmke and Ganetzky, 1994; Timpe *et al.*, 1998) and blocked by 4-aminopyridine (4-AP) (Thompson, 1977; Moczydlowki *et al.*, 1988; Engel and Wu, 1992). The efflux of potassium repolarizes the membrane (Thompson, 1977; Elkins *et al.*, 1986; Fozzard and Arnsdorf, 1992; Irisawa *et al.*, 1993; Littleton and Ganetzky, 2000; Lipsius *et al.*, 2001). The *eag* channel is also activated by the calcium depolarization, but in a more delayed fashion. The K^+ current carried by this channel type eventually triggers the pacemaker potential, thereby recommencing the oscillatory process.

There is a second calcium channel necessary for normal heartbeat, an L-type (HVA) calcium channel encoded by Dmca1D (Eberl *et al.*, 1988) that is responsible for Ca^{2+}-dependent conduction (Jeziorski *et al.*, 2000) and excitation-contraction coupling (Nunoki *et al.*, 1989; Fozzard and Arnsdorf, 1992; Littleton and Ganetzky, 2000). Because mutants in this gene have normal pacemaker activity but abnormal EKGs, it is probable that this calcium channel is involved in beat conduction but not in pacemaking (Johnson *et al.*, 1997). Pharmacological evidence supports these results because injections of L-type channel blockers verapamil (phenylalkylamine) and nifedipine

(dihydropyridine) did not interfere with beat generation but uncoupled the pacemaker from the rest of the myocardium, which ceased to contract (Johnson *et al.,* 1998). Data from the same study excludes T-type calcium channels from involvement in pacemaking because an antagonist to this channel type, amiloride (Irisawa *et al.*, 1993; Gielow *et al.,* 1995), had no effect on the heart (Johnson *et al.,* 1998). Because L-type and T-type channels are not candidates for pacemaker involvement, and based on pharmacological evidence (Johnson *et al.,* 1998), the *cac* calcium channel is the prime suspect for fulfilling this function.

Perspectives: Importance of *Drosophila* Research

All living organisms and their constituent cells are descended from a common ancestor that evolved through changes in the genetic code. There is a high amount of evolutionary conservation among all organisms at the genetic level (Alberts *et al.*, 1994). This commonality enables us to use knowledge of one organism as a basis for study in others.

The concept of extrapolating information from simple to more complex organisms is the basis for much biological and molecular genetic research (Keating and Sanguinetti, 1996), in which *Drosophila* occupies a central role (Suzuki *et al.*, 1971; Fletcher *et al.*, 1998; Rubin *et al.*, 2000; Papaefthimiou and Theophilidis, 2001). Because of its high reproduction rate, easy maintenance, and substantial genetic database, it has long been esteemed as an ideal organism for study (Davenport, 1941; Kaplan and Trout, 1968; McCann, 1969; Guillén *et al.*, 1990; Fletcher *et al.*, 1998; Rubin *et al.*, 2000; Jeziorski *et*

al., 2000). The tradition of *Drosophila* research provides massive amounts of information to the current investigator (Simon *et al.*, 1991). The genome of *Drosophila* has been completely mapped and sequenced (Adams *et al.*, 2000), and its development intensely studied (Rubin *et al.*, 2000; Gilbert, 2000). Perhaps more than any other model organism, *Drosophila* has revealed the path of conduction from genetic code to adult multicellular organism and provided insight into the molecular biology of higher eukaryotes, including *Homo sapiens* (humans) (Fletcher *et al.*, 1998; Rubin *et al.*, 2000; Papaefthimiou and Theophilidis, 2001; Alberts *et al.*, 2002). As a continuation of this trend, *Drosophila* heart research provides insight into the hearts of vertebrates (McCann, 1969; Papaefthimiou and Theophilidis, 2001). More specifically, the pacemakers that are responsible for the genesis of heartbeat may be highly comparable between *Drosophila* and humans.

Similarities Between Cardiac Physiologies of Homo sapiens *and* Drosophila

Although at maturity vertebrate hearts appear structurally distinct from those of invertebrates, they are phylogenetically related and appear similar at embryological stages in development (Park *et al.*, 1998; Kardong, 2002). After three weeks of gestation the heart of a human embryo is comparable to that of a fruit fly larva, consisting of a tube-like dorsal vessel (Gilbert, 2000). There are even homologous transcription factors essential for proper heart development in fruit flies and humans. *tinman* (*tin*) (Kim and Nirenberg, 1989; Bodmer, 1993) and NKX2-5 (Schott *et al*, 1998) are related homeobox-containing genes necessary for cardiac development in their respective organisms (Park *et al.*, 1998; Barinaga, 1998; Gilbert, 2000).

The genesis of heartbeat in *Drosophila* and *Homo sapiens* is also strikingly similar. In both organisms heartbeat is initiated by specialized cardiac tissue capable of pacemaker function due to the additive effects of several ion channels (Fozzard and Arnsdorf, 1992; Irisawa *et al.*, 1993; Guyton and Hall, 1996; Johnson *et al.*, 1998; Terrar and Rigg, 2000; Hüser *et al.*, 2000; Rigg *et al.*, 2000; Lipsius *et al.*, 2001). Because of this, heartbeat in both organisms is produced myogenically, and nervous stimulation serves to modulate myocardial performance (Rizki, 1978; Fozzard and Arnsdorf, 1992; Irisawa *et al.*, 1993; Dowse *et al.*, 1995; Johnson *et al.*, 1997; Hüser *et al.*, 2000; Johnson *et al.*, 2001). The compelling similarities that exist between the cardiac pacemakers of such divergent species are due to the ubiquitous nature (Hille, 2001), and evolutionarily conserved structure (Strong *et al.*, 1993) of ion channels, especially at the molecular level (Nunoki *et al.*, 1989; Loughney *et al.*, 1989; Snutch *et al.*, 1990; Amichot *et al.*, 1993; Littleton and Ganetzky, 2000; Jeziorski *et al.*, 2000). Organisms from protozoa to humans respond to a variety of stimuli via ion channels in their cell membranes (Hille, 2001). Ionic currents due to ion channels opening interact to produce action potentials in excitable cells (Amichot *et al.*, 1993), and are responsible for pacemaking in invertebrate and vertebrate hearts (Fozzard and Arnsdorf, 1992; Irisawa *et al.*, 1993; Guyton and Hall, 1996; Ashcroft, 2000; Hüser *et al.*, 2000; Terrar and Rigg, 2000; Rigg *et al.*, 2000; Papaefthimiou and Theophilidis, 2001; Lipsius *et al.*, 2001; Hille, 2001).

Importance of Pacemaker Research

With the realization over a decade ago that the primary cause of fatalities in developed countries is heart disease came a plethora of studies concerning mutations that

directly impair the heart (Keating and Sanguinetti, 1996; Barinaga, 1998; Clancy and Rudy, 1999). Although heritable conditions are fairly rare, gathering information about them is beneficial because it may be translated to treat similar, more common heart ailments that develop throughout adulthood (Barinaga, 1998). Towards this goal, several genes have been identified as critical to proper heart function, and many mutations in these have been implicated in heart abnormalities (Keating and Sanguinetti, 1996; Barinaga, 1998). However, not much is known about heart diseases caused by pacemaker abnormalities despite the fact that cardiac arrhythmias are a major contributor to sudden cardiac death (Curran *et al.*, 1995; Keating and Sanguinetti, 1996; Hüser *et al.*, 2000). The only known pacemaker ion channel diseases involve potassium and sodium channels (Keating and Sanguinetti, 1996; Barinaga, 1998; Clancy and Rudy, 1999), and there is a lack of information concerning the contribution of calcium channels to these pathologies even though excessive Ca^{2+} influx and intracellular accumulation are pivotal to the instigation of cardiac arrhythmias (Fozzard and Arnsdorf, 1992; Hüser *et al.*, 2000; Terrar and Rigg, 2000).

There is increasing information concerning genetic diseases caused by calcium channel mutations affecting the body outside of heart function (Fletcher *et al.*, 1998; Ashcroft, 2000). Mutations in calcium channel α_1 subunit genes, specifically, alter channel activities, and cause heritable nerve and muscle disorders (Warmke and Ganetzky, 1994; Jeziorski *et al.*, 2000) like hypokalaemic periodic paralysis (HypoPP – mutant CACNA1S), malignant hyperthermia susceptibility type-5 (MHS5 – mutant CACNA1S), incomplete X-linked congenital stationary night blindness (mutant CACNA1F), familial hemiplegic migraine (FHM – mutant CACNA1A), episodic ataxia

type-2 (EA-2 – mutant CACNA1A), spinocerebellar ataxia type-6 (SCA-6 – mutant CACNA1A) (Rubin *et al.*, 2000), amyotrophic lateral sclerosis (ALS – several potential α_1 calcium channel mutants, including CACNA1A and CACNA1S, C, D, or F) (Day *et al.*, 1997), absence epilepsy (in mice), and muscular dysgenesis (in mice - mutant CACNA1S) in vertebrates (Ashcroft, 2000; Fletcher *et al.*, 1998; Hering *et al.*, 1998; Hering *et al.*, 2000; Weinreich and Jentsch, 2000; Brooks *et al.*, 2003). Furthermore, many of these diseases are associated with altered calcium channel inactivation (Hering *et al.*, 2000) like those seen in *cac* mutants used in this study. Therefore, determining how mutations in calcium channels contribute to heart disease, using *Drosophila* as a model, is the next step to understanding the impact of this channel class on heritable cardiac arrhythmias.

The effects of *Drosophila* mutations analogous to those causing certain vertebrate diseases have already been described. For instance, an enhancer of motor defects in the cac^{ts2} calcium channel mutant, $cac^{E(TS2)1}$, worsens paralysis in a dominant fashion, and maps genetically to the second homology domain's P-loop, as does the lesion causing familial hemiplegic migraine (Brooks *et al.*, 2003). Actually, many human ion channel genes were isolated using homologous *Drosophila* channel transcripts because of the large correspondence between membrane proteins of vertebrates and insects (Loughney *et al.*, 1989; Atkinson *et al.*, 1991; Warmke *et al.*, 1991; Amichot *et al.*, 1993; Olivera *et al.*, 1994; Warmke and Ganetzky, 1994; Littleton and Ganetzky, 2000). These examples, along with previous studies presented by this lab (Dowse *et al.*, 1995; Johnson *et al.*, 1997; Johnson *et al.*, 1998; Johnson *et al.*, 2000; Johnson *et al.*, 2001; Johnson *et al.*, 2002) set precedents for using *Drosophila* to garner information about the impact of

altered components of pacemaking on the heart (Papaefthimiou and Theophilidis, 2001). *Drosophila* is a good model for gathering this fundamental neurobiological data about mutational effects (Jeziorski *et al.*, 2000; Littleton and Ganetzky, 2000) because its genome contains homologous genes for close to three-quarters (177 of 289) of identified human disease genes (Rubin *et al.*, 2000). Therefore, research to elucidate the roles of ion channels in *Drosophila* pacemaker function could potentially be extrapolated to human research (Jeziorski *et al.*, 2000; Papaefthimiou and Theophilidis, 2001).

Further rationale for this line of research comes from evidence that pacemaking in the hearts of *Drosophila* and humans are at least partly due to homologous ion channel activities (Johnson *et al.* 1998). For example, a mutation of the *Drosophila ether à go-go* (*eag*) gene (Kaplan and Trout, 1968; Brüggeman *et al.*, 1993) causes lengthening of heartbeat (Johnson *et al.*, 1998) that parallels common type 2 hereditary long QT syndrome (LQTS) in humans (Keating and Sanguinetti, 1996), caused by a mutation in the homologous HERG gene (Warmke and Ganetzky, 1994; Curran *et al.*, 1995; Robbins *et al.*, 1999; Barinaga, 1998; Sanguinetti *et al.*, 1995; Littleton and Ganetzky, 2000). Because the potassium channel subunit encoded by HERG is responsible for a delayed rectifier K^+ current (I_{Kr}) (Sanguinetti *et al.*, 1995), mutations of this gene disturb repolarization of sinus node cells (Curran *et al.*, 1995; Keating and Sanguinetti, 1996). The extension of the cardiac potential reaches as far as the ventricles, hence the prolonged QT interval that is the disease's namesake, causing a ventricular tacchycardia called torsade de pointes (Curran *et al.*, 1995; Sanguinetti *et al.*, 1995). This distinctive arrhythmia may degenerate into ventricular fibrillation, potentially resulting in sudden cardiac death (Curran *et al.*, 1995; Sanguinetti *et al.*, 1995).

reflex and phototaxis. Some *cac* mutants, like cac^{nbA} alleles, support this hypothesis; however, others do not. Although an early study found cac^{s} flies to be subnormal in a Y-tube phototaxis assay, this effect was attributed to the mutant's general temperature-dependent locomotor sluggishness (Kulkarni and Hall, 1987). Later studies revealed that not only was cac^{s} wild-type for Y-tube phototaxis (Chan *et al.*, 2002), but also for optomotor ability and countercurrent phototaxis (Smith *et al.*, 1998). The cac^{ts2} mutation does not appear to affect visually mediated behavior either. Slight phototaxis reluctance after exposure to high temperature was attributed to cac^{ts2} flies' temperature-dependent depressed locomotor activity (~30% as active as wild-type at 29°C) that parallels observations of cac^{s} flies (Chan *et al.*, 2002).

Calcium Channel Information

Composition of Voltage-Gated Calcium Channels

Ion channels are transmembrane proteins that function as selective pores (Miller, 1978), allowing the passage of specific ions across a cell's membrane (Strong *et al.*, 1993). Voltage-gated calcium channels are heteromultimeric complexes (Neely *et al.*, 1993) composed of a primary $\alpha_1$subunit, and four accessory subunits (Snutch *et al.*, 1990; Day *et al.*, 1997; Jeziorski *et al.*, 2000), three of which are transmembrane (α_2, δ, γ), and one is intracellular (β) (Hering *et al.*, 1998; Ashcroft, 2000; Littleton and Peixoto *et al.*, 2000; Ganetzky, 2000; Hering *et al.*, 2000; Jeziorski *et al.*, 2000; Hille, 2001; Krauss, 2001; Brooks *et al.*, 2003). The α_1 subunit is the largest and arguably the most important as it forms the channel pore, senses changes in transmembrane potential, and

acts as a receptor for many drugs and toxins (Olivera *et al.,* 1994; Ashcroft, 2000; Jeziorski *et al.*, 2000). The α_1 subunit is made up of four homologous domains (I-IV) each consisting of ~300-400 residues that are linked by cytoplasmic loops (Kawasaki *et al.,* 2002). Each domain is formed by six transmembrane α-helical segments (S1-S6) (Koch *et al.*, 1990; Snutch *et al.*, 1990; Peixoto *et al.*, 2000; Jeziorski *et al.*, 2000; Hille, 2001). The amino (N) and carboxylic acid (C) termini are found intracellularly, and along with connecting loops, contain several protein interaction domains that participate in channel regulation and modulation (Zhou *et al.*, 1997; Kawasaki *et al.*, 2002; Brooks *et al.,* 2003).

Each domain segment has a specific functional role, some of which have been characterized. For instance, the S1 segment of domain I (IS1) is involved in determining the rate of channel activation and peak current (Eberl *et al.*, 1998). Additionally, various conserved sequences within the cytoplasmic linker of domains I and II mediate second messenger signaling by binding $G_{\beta\gamma}$ subunits (Ashcroft, 2000; Jeziorski *et al.*, 2000). The extracellular loop between IS3 and IS4 has a critical role in channel activation kinetics (Peixoto *et al.*, 1997).

More general characteristics of channel electrophysiology are due to the combinatorial roles of domain segments. For example, a widely accepted feature of members of the cation channel family is that S4 segments are responsible for voltage sensing (Snutch *et al.*, 1990; Koch *et al.*, 1990; Atkinson *et al.*, 1991; Warmke *et al.*, 1991; Strong *et al.*, 1993; Jeziorski *et al.*, 2000; Lewin, 2000; Krauss, 2001; Hille, 2001). This phenomenon has recently been described in detail based on the crystal structure of a bacterial voltage-gated potassium channel (KvAP) (Jiang *et al.*, 2003a and 2003b;

Sigworth, 2003). Apparently, a helix-turn-helix 'paddle' structure formed not only of the N-terminal half of the fourth helix (S4) but also of the C-terminal half of the third helix (3b) controls voltage gating (Jiang *et al.*, 2003a and 2003b; Sigworth, 2003). The α-helical hairpin paddle juts into the membrane interior in a tangential orientation to the channel's axis, and is able to move a large distance from internal to external membrane surface and beyond because of its flexible connection to the channel core at the S3 loop and the S4-S5 linker (Jiang *et al.*, 2003a and 2003b; Sigworth, 2003). Because of its charged amino acid residues, it moves through the membrane's electric field in reaction to voltage changes (Jiang *et al.*, 2003a; Sigworth, 2003). The S4 helix's conserved pattern of positively charged amino acids (Snutch *et al.*, 1990; Koch *et al.*, 1990; Atkinson *et al.*, 1991; Strong *et al.*, 1993) every third or fourth residue (Jeziorski *et al.*, 2000), separated by hydrophobic residues, for a total of four to eight arginines (R) and lysines (K) (less frequently) (Warmke *et al.*, 1991; Lewin, 2000; Krauss, 2001; Hille, 2001; Jiang *et al.*, 2003b) account for the gating charge, with the first four arginines being functionally critical (Jiang *et al.*, 2003a). The combined movement of residues from all four domains explains the finding that voltage sensing is due to at least twelve and maybe as many as fourteen charged particles moving through the membrane in response to voltage changes (Jiang *et al.*, 2003a and 2003b; Sigworth, 2003). In addition, conserved acidic residues in S2 and S3 segments allow salt bridges to form with S4 arginines, contributing to gating charge movement (Jiang *et al.*, 2003a) and/or pore formation (Koch *et al.*, 1990; Jiang *et al.*, 2003b). There is speculation that the voltage-sensing paddles may cause channel opening by pulling S5 segments, , away from the pore's center as they move through the lipid membrane from interior to exterior in

response to depolarization (Jiang *et al.*, 2003a and 2003b). Because S5 segments form a cuff around S6 segments they move as a single unit, which would cause S6 helices' glycine-gating hinges to bend in response to widening of the S5 layer, thereby opening the channel pore (Jiang *et al.*, 2003a and 2003b). This hypothesis is plausible, though it contradicts conventional models; however, precise details of the motions of the voltage sensor and of its relationship to channel opening have yet to be elucidated experimentally (Jiang *et al.*, 2003a and 2003b; Sigworth, 2003).

The last two helices (S5 and S6) flank a hydrophobic intramembrane loop (P-loop) (Hering *et al.*, 2000; Brooks *et al.*, 2003) that determines ion selectivity (Jiang *et al.*, 2003a), two short segments of which (SS1 and SS2) form the walls of the ion pore (Jeziorski *et al.*, 2000; Krauss, 2001; Kawasaki *et al.*, 2002). A ring within the ion pore formed from conserved negatively charged glutamates in each SS2 section is a high-affinity binding site for Ca^{2+}, and is responsible for calcium channels' exclusive Ca^{2+} selectivity (Smith *et al.*, 1996; Ashcroft, 2000; Jeziorski *et al.*, 2000). SS1 and SS2 transmembrane stretches as a whole are highly conserved (Smith *et al.*, 1996). They are not organized in the usual hydrophobic α-helical structure and could be an extended β-hairpin (Lewin, 2000). Together, the SS1 and SS2 segments of all four domains form a pore that has four-fold symmetry about the axis (Hille, 2001; Jiang *et al.*, 2003a). Below the selectivity filter S6 helices line the ion pathway and are thus considered the inner helices, while S5 helices are the outer helices because they encircle the pore proper (Jiang *et al.*, 2003a). These two segments are together considered the channel's core (Jiang *et al.*, 2003a). The channel core is loosely surrounded by a concentric layer of S1 and S2

helices, while S3 and S4 are localized at the channel's outer perimeter (Jiang *et al.*, 2003a and 2003b; Sigworth, 2003)

Calcium channels are inactivated by voltage and/or by calcium itself (Zhou *et al.*, 1997; Kawasaki *et al.*, 2002). Contributors to inactivation at the molecular level are poorly identified in calcium channels in contrast to sodium and potassium channels (Hering *et al.*, 2000). However, reminiscent of *Shaker* potassium channels, an N- (Lewin, 2000) or C-terminal, or I-II linker structure resembling a ball and chain may control the state of the channel in reaction to voltage by acting as a plug on the cytoplasmic side (Hering *et al.*, 1998; Hering *et al.*, 2000). A more parsimonious hypothesis for voltage-dependent inactivation is that it may result from conformational distortions in the putative inverted 'teepee' arrangement of S6 segments, specifically affecting the region near the inner channel mouth where they come into contact as they cross (Hering *et al.*, 1998; Hering *et al.*, 2000). This theory of inactivation is supported by a potassium channel crystal structure (Hering *et al.*, 1998) and evidence that noncovalent interactions between pore-lining S5 and S6 segments and their adjacent intracellular and extracellular sequences, and putatively pore-forming regions of S5-S6 linkers appear to be involved in fast voltage-dependent channel inactivation (Zhang *et al.*, 1994; Hering *et al.*, 1996; Hering *et al.*, 1998; Hering *et al.*, 1998; Hering *et al.*, 2000; Chan *et al.*, 2002). Channel inactivation kinetics are based on the presence of a hierarchy of crucial amino acids in these regions (Hering *et al.*, 1996), especially those proximal to the channel mouth (Hering *et al.*, 1998). The most important determinant of inactivation in these regions may be nine amino acids within segment IS6 (Zhang *et al.*, 1994; Ashcroft, 2000). An arginine residue located within the $G_{\beta\gamma}$ binding site of the I-II

Some ion channels contributing to pacemaker activity may not be homologous across organisms; nevertheless, they are related evolutionarily (Atkinson *et al.*, 1991; Gielow *et al.*, 1995; Littleton and Ganetzky, 2000; Rigg *et al.*, 2000; Hille, 2001). Voltage-gated calcium, sodium, and potassium channels share many kinetic properties, are structurally similar at the level of amino acid sequence, and are highly conserved throughout evolution, which suggests some preservation of *in vivo* functions across organisms (Moczydlowksi *et al.*, 1988; Loughney *et al.*, 1989; Amichot *et al.*, 1993; Warmke and Ganetzky, 1994; Littleton and Ganetzky, 2000; Hille, 2001). Therefore, even if not all ion channels involved in pacemaking are homologous between *Drosophila* and humans, insight into invertebrate channel function will be beneficial in its applicability to vertebrates (Rigg *et al.*, 2000).

Importance of Studying cac *Heartbeat Mutants*

The purpose of studying the effect of *cac* mutants on heartbeat is twofold. New information will increase understanding of the biological role of this calcium channel gene (Smith *et al.*, 1998), which has uses as far-reaching as designing strategies to control harmful insects (Gielow *et al.*, 1995; Papaefthimiou and Theophilidis, 2001). The other aim is to advance research implicating the critical involvement of a voltage-gated calcium channel in pacemaking by determining whether a *cac* encoded ion channel α_1 subunit is involved (Johnson *et al.*, 1997). Although preliminary research in this lab excluded the involvement of Dmca1A in pacemaking (Johnson *et al.*, 1997), more intense study suggests the opposite (Johnson, unpublished observations).

A continuation of the goal of researching *cac* mutants' effects on pacemaking is to determine whether a homologous human calcium channel may be implicated in heart disease. The numerous similarities between human and *Drosophila* hearts suggest that information on the participation of *cac* in pacemaking may be extrapolated between the two organisms (Kim and Nirenberg, 1989; Amichot *et al.*, 1993; Strong *et al.*, 1993; Bodmer, 1993; Guyton and Hall, 1996; Johnson *et al.*, 1998; Schott *et al*, 1998; Gilbert, 2000; Littleton and Ganetzky, 2000; Ashcroft, 2000; Hille, 2001; Kardong, 2002). The high evolutionary conservation of calcium channel genomic structure (Peixoto *et al.*, 1997) ensures that information concerning Dmca1A's impact on pacemaking would be useful in identifying the human counterpart of this gene. In support of this rationale, similar genes to *cac* (U55776) have been identified not only in *Homo sapiens*, but also in organisms phylogenetically intermediate between the two like *Rattus norvegicus* (α1A - M64373 (Smith *et al.*, 1996), and α1B - M92905 (Kawasaki *et al.*, 2000)). The gene identified in humans parallels *cac* in protein function as well as sequence, encoding the α_1 subunit of a voltage-dependent calcium channel (α_{1A} - U79666) (Kawasaki *et al.*, 2000). Because genes similar to *cac* have also been found in *Mus musculus* (U76716, and α_{1A} – NM007578 (Brooks *et al.*, 2003)), *Caenorhabditis elegans* (U55374, and unc-2 - U25119 (Brooks *et al.*, 2003)) and *Loligo bleekeri* (D86600) (FlyBase Report: http://flybase.bio.indiana.edu/.bin/fbidq.html?content=full-report&FBgn0005563), it appears that this gene is indeed evolutionarily conserved, which gives strength to the argument for extrapolating information relevant to it from *Drosophila* to other organisms.

Additional endorsements for this line of research come from other *Drosophila* genome resources, like the National Center for Biotechnology Information (NCBI)

(http://ncbi.nlm.nih.gov/). A NCBI Homologene search (http://ncbi.nlm.nih.gov/HomoloGene/homol.cgi?HID=6164) shows 72.5% sequence identity between aligned regions of *Drosophila cac* and human CACNA1B (000718) DNA. Voltage-gated calcium channel proteins are also similar between the two species. There is 47% identity between aligned regions of Dmca1A (P91645) and a human α_{1D} subunit protein (JH0564) (NCBI Unigene search: http://ncbi.nlm.nih.gov/UniGene/clust.cgi?ORG=Dm&CID=2395).

The following work is concerned with the contribution of a Dmca1A calcium channel to cardiac pacemaking. Aberrant heartbeats of separately isolated cac^{s} and cac^{ts2} mutants support that Dmca1A is involved in heart function, potentially by affecting pacemaking. Cardiac activities of the temperature-dependent cac^{s} and the temperature-independent cac^{ts2} mutants are described herein, contributing another phenotypic association to the *cac* locus in an effort to unravel the biological significance of this calcium channel gene.

MATERIALS AND METHODS

Fly Culture and Experimental Strains

Flies were cultured in uncrowded conditions in 250 ml glass bottles on a standard malt-cornmeal-molasses-yeast-agar medium, with propionic acid added to control the growth of mold. Animals were housed in incubators at 25°C on a cycle of 12:12 h of light and dark.

Two separate, unmarked, homozygous mutant lots of each *cacophony* [*cac*] mutant, cac^{s} and cac^{ts2}, were used for heartbeat recordings. Another strain of cac^{s} marked with *yellow* [*y*] and *chocolate* [*cho*] was used for a control mating with cac^{ts2}. Dr. J.C. Hall kindly donated three strains of *cac* mutants (cac^{s}, cac^{ts2}, and *y cho* cac^{s}). The other cohorts of cac^{s} and cac^{ts2} came from Jeff Hall's lab as well, but in a separate shipment at a much earlier date. To map aberrant heartbeat phenotypes to the *cac* locus, heartbeat was recorded from a strain of cac^{s} mutants over a deficiency that deletes the locus (Kulkarni and Hall, 1987). The deficiency line, Df(1)N105 (here 'Df'), was obtained from the Bloomington Stock Center (Indiana University, Bloomington, IN). Canton-S was used as the wild-type strain for comparative purposes and in genetic manipulation.

Control Strains

The cac^{s} strain marked with *y* and *cho* was used to facilitate selecting female larvae during production of a test strain heteroallelic for cac^{ts2}. Despite neurological effects, *y* has no effect on heartbeat (E. Johnson, personal communication). This result was confirmed because heartbeat recordings from an unmarked heteroallelic cac^{s}/cac^{ts2} strain showed no significant difference from the strain marked with *y*. Heartbeat was recorded from heteroallelic *y cho* cac^{s}/cac^{ts2} females to determine if the two alleles complement (Kawasaki *et al.*, 2000) for effect on heartbeat.

To determine whether the effect of cac^{s} and cac^{ts2} on heartbeat is recessive, homozygous *cac* mutants were mated with wild-type and heartbeat was recorded from heterozygous *cac*/+ females. The cac^{s} strain marked with *y* and *cho* was used to produce

some heterozygotes, and heartbeat recordings were compared to those from an unmarked strain to confirm that the background of the mutant chromosome was not affecting the heart phenotype.

Heartbeat Recordings and Temperature Step Protocols

Heartbeat was recorded from individual translucent "white", P1 pupae (Ashburner, 1989), soon after they became immobile and everted their spiracles upon transition from third instar larvae. Because the pupal case of early P1 pupae is untanned, and because the heart lies dorsally and medially, it is easy to view beating in intact pupae at this stage of development (Johnson *et al.*, 1997). A pupa was removed from the side of the culture bottle, placed dorsal side up on a slide, and submerged in a small drop of distilled water. The water increased light concentration through the pupa and facilitated heat transfer from the temperature-controlled slide during heartbeat recordings. This preparation was non-invasive and minimized trauma to the pupae so that they could be allowed to recover from the treatment if necessary, unlike alternative methodologies (McCann, 1969).

The dorsal vessel was brought into focus on an Olympus BH2 microscope (Olympus Optical, Melville, N.Y., USA), at a magnification of 400X. The light for the microscope came from a DC source to eliminate AC 60 Hz variation. As the heart beat it moved surrounding organs, causing varying intensities of light to pass. To record light transmittance, one eyepiece was modified with a phototransistor centered in the exit pupil. Voltage changes were pre-amplified using a 741C operational amplifier (Radio Shack, Fort Worth, T.X., USA), and conditioned with a low-pass electronic filter (World

Precision Instruments, LPF-30; 200 Hz cutoff) and a Grass 79D Polygraph (Grass, Warwick, R.I., USA) (Dowse *et al.*, 1995). The signal was digitized at 100 Hz with a DAS-8 Analog to Digital (AD) card (Metrabyte, Taunton, M.A., USA) and recorded by a desktop computer (White *et al.*, 1992). Data were then analyzed digitally using our own software (Dowse *et al.*, 1995).

A Sensor-Tek TS-4 unit (Sensortek, Clifton, N.J., USA) controlled and monitored temperature during heartbeat recordings. Heartbeat from at least 10 pupae of each strain was recorded once the temperature became fixed at each increment of the protocol (Gibbs, 1981). Before recording heartbeat, pupae were subjected to a brief initial set-up period at the first temperature of the protocol (20°C). Each pupa underwent an intermediate temperature step protocol of 20°C, 25°C, 30°C, 35°C, and 37°C, followed immediately by a high temperature protocol of 37°C, 39°C, 40°C, 41°C, and 42°C. To determine if low temperatures had any effect, five of the ten pupae were first tested at low temperatures (20°C, 18°C, 16°C, 14°C, and 12°C) before being subjected to the two standard (medium and high) temperature protocols (Dowse *et al.*, 1995). After pupae were exposed to the low temperature protocol they were acclimated to 20°C for at least 2 min to ensure that heartbeat had returned to normal before starting the medium temperature step protocol (Dowse *et al.*, 1995).

A heartbeat recording step consisted of an acclimation period of 90 s at a given temperature, followed by a 30-s recording period. Immediately following the recording period the temperature was changed to the next temperature in the protocol and the equilibration and recording period sequence was repeated. This pattern continued until the temperature protocol was complete. Keeping the recording periods consistent

eliminated bias due to sample selection (Dowse *et al.*, 1995). The accuracy of the temperature of the apparatus was confirmed earlier by replicating all temperature protocols with a probe substituted for a pupa (Dowse *et al.*, 1995).

After heartbeat was recorded, all flies were reared in separate vials to ensure that they had not been harmed by the procedure. The flies were scored for sex and genetic markers after eclosion to ascertain genotype.

Data Analysis

Raw data from the 30-s recordings at each temperature were plotted. Data were subjected to two digital signal analysis techniques - Maximum Entropy Spectral Analysis (MESA) and Autocorrelation (Ulrych and Bishop, 1975; Chatfield, 1980). MESA was used to estimate the frequency of heartbeat (i.e. heart rate - FR) in conjunction with plots of raw data (Ulrych and Bishop, 1975; Dowse and Ringo, 1989). To determine heartbeat regularity, data were subjected to Autocorrelation analysis (Chatfield, 1980; Johnson *et al.*, 1997). The data from a 30-s recording were "lagged" through 250 data points (100 Hz x 2.5 s, equivalent to two complete cycles) and the height of the resulting third peak of autocorrelation was expressed as a fraction of the height of the first peak. Correlation coefficients are normally distributed, facilitating statistical analysis of rhythmicity because the first peak always has a fractional value of one to exemplify perfect rhythmicity (For a thorough explanation see Dowse *et al.*, 1995; Johnson *et al.*, 1997). The fraction comparing the third peak (see Fig. 1c, asterisk) to the first is the correlation coefficient for a data set, and is an objective measure of heartbeat regularity that is expressed as a rhythmicity index (RI) score ranging from zero to one. Therefore, the

autocorrelation reflects periodicity in heart rate directly; the more arrhythmic the heartbeat, the more rapid the decay in autocorrelation, and the lower the correlation coefficient (Chatfield, 1980; Dowse and Ringo, 1989).

Raw data records were plotted to confirm validity of spectral analyses derived from MESA and autocorrelation analyses (Levine *et al.*, 2002). Data from low temperatures were excluded from statistical tests and results because most flies' hearts became arrhythmic at these temperatures, making it inadvisable to draw conclusions based on their analyses. Data from the two separate cohorts of each mutant, cac^{s} and cac^{ts2}, were pooled for all analyses because they were not significantly different. Initially, heart rate and rhythmicity indices of fly strains were compared across temperature by analysis of variance (ANOVA), and this was followed by Ryan-Einot-Gabriel-Welsch multiple F tests (REGWF, Einot and Gabriel, 1975) ($\alpha = 0.05$) that grouped means with significant differences. Normalized dominance values were determined from overall means across temperature using the formula:

$$\text{dominance} = \frac{\text{heterozygote} - \text{mean}}{|\,\text{homozygote} - \text{mean}\,|}$$

To allow for more detailed data analysis, mean heart rates and rhythmicity indices of all pupae of a given genotype were computed at each temperature, and the means were plotted for certain key genotypes (see results sections, Figs. 7, 8, 11, 16). Means of critical genotypes were compared at individual temperatures using analysis of variance

(ANOVA). Heart rates and rhythmicity indices of critical genotypes were regressed on temperature and the results were plotted to reveal relationships between the data (see results sections). Homogeneity of slopes tests were performed for critical genotypes to determine if there were temperature effects, genotype effects, and/or interactions between genotype and temperature for the two heartbeat variables.

RESULTS

Wild-type Heart Rate Phenotype

The frequency of wild-type *Drosophila* heartbeat increases steadily with temperature until temperatures that it would not encounter in its natural habitat are encountered (> 41°C) (Table 1, Figs. 1a, 1b, 2a, 2b, 7). When such temperatures are reached heart rate begins to fall owing to the excessive amount of stress imposed on the system (Table 1, Figs. 2a, 2b, 7).

Effect of cac^s on Heartbeat Frequency

Heartbeat frequency is significantly higher in cac^s homozygotes than in wild-type at temperatures ≥37°C (37°C: $F = 5.08$, $P = 0.0286$; 39°C: $F = 6.79$, $P = 0.0158$; 40°C: $F = 6.47$, $P = 0.0181$; 41°C: $F = 4.81$, $P = 0.0386$; 42°C: $F = 6.27$, $P = 0.0198$) (Table 1; Fig. 7). However, raw data and MESA plots at 25°C and at 40°C show that heart rate in cac^s mutants is higher than wild-type across temperature (Figs. 1ab, 2ab, 3ab, 4ab). These results are fairly consistent with earlier work on cac^s, where over the temperature

range tested (20°C to 37°C) the mutant's heart rate was not significantly different from wild-type (Johnson *et al.*, 1998). However, the slight decrease in heart rate of cac^s flies noted in the prior study was probably an error due to low sample size.

Of particular interest is the divergence of heart rate in cac^s pupae from wild-type pupae around the critical temperature (37°C) that is clearly depicted in Figure 7. At temperatures above 37°C wild-type pupae have heart rates that continue to decrease (Table 1). In contrast, cac^s pupae have heartbeat frequencies that dramatically increase at temperatures over 35°C (Table 1). Therefore, as heart rates of wild-type pupae are declining, those of cac^s pupae are noticeably increasing. When heart rates of cac^s pupae begin increasing at 35°C, they soon become similar to those of cac^{ts2}. Actually, cac^{ts2} and cac^s pupae have heart rates that are not significantly different at temperatures ≥39°C (39°C: $F = 2.61$, $P = 0.1157$; 40°C: $F = 0.73$, $P = 0.4004$; 41°C: $F = 1.94$, $P = 0.1730$; 42°C: $F = 0.77$, $P = 0.3855$) (Table 1; Fig. 7). This trend ends at 41°C, at which temperature cac^s pupal heart rates begin decreasing in parallel to those of wild-type (Table 1, Fig. 7).

cac^s affects heart rate in a dominant fashion, as there is no significant difference between cac^s homozygotes and $cac^s/+$ heterozygotes at any temperature (20°C: $F = 0.39$, $P = 0.5375$; 25°C: $F = 0.00$, $P = 0.9948$; 30°C: $F = 0.24$, $P = 0.6263$; 35°C: $F = 0.43$, $P = 0.5162$; 37°C: $F = 0.10$, $P = 0.7546$; 39°C: $F = 0.09$, $P = 0.7633$; 40°C: $F = 0.25$, $P = 0.6178$; 41°C: $F = 0.30$, $P = 0.5866$; 42°C: $F = 0.00$, $P = 0.9769$ (Table 1; Fig. 7). In support of this assessment, the normalized heartbeat frequency dominance value of homozygous cac^s over wild-type is 1.03.

cac^{s} is dominant over *cac*^{ts2} for the heart rate phenotype because heteroallelic (*cac*^{s}/*cac*^{ts2}) pupae do not have significantly different heartbeat frequencies from *cac*^{s} homo- and heterozygotes at any temperature (20°C: F = 0.22, P = 0.8026; 25°C: F = 0.03, P = 0.9746; 30°C: F = 0.23, P = 0.7938; 35°C: F = 0.20, P = 0.8158; 37°C: F = 0.12, P = 0.8848; 39°C: F = 0.07, P = 0.9324; 40°C: F = 0.16, P = 0.8552; 41°C: F = 0.19, P = 0.8269; 42°C: F = 0.02, P = 0.9831) (Table 1; Fig. 7). The dominance value of *cac*^{s} over *cac*^{ts2} is 1.02.

cac^{s}/Df(1)N105 (from here on called '*cac*^{s}/Df') is not significantly different from *cac*^{s} for heart rate at all temperatures (20°C: F = 1.41, P = 0.2425; 25°C: F = 0.18, P = 0.6734; 30°C: F = 0.41, P = 0.5275; 35°C: F = 0.03, P = 0.8720; 37°C: F = 1.63, P = 0.2071; 39°C: F = 1.12, P = 0.3014; 40°C: F = 0.88, P = 0.3580; 41°C: F = 1.06, P = 0.3145; 42°C: F = 0.22, P = 0.6447). This deletion has breakpoints in 10F7; 11D1 and was used to uncover the abnormal song phenotype of *cac*^{s} (Kulkarni and Hall, 1987). Because *cac*^{s} appears to be dominant for the aberrant heart phenotype, it is not possible to map the phenotype to the locus in this manner.

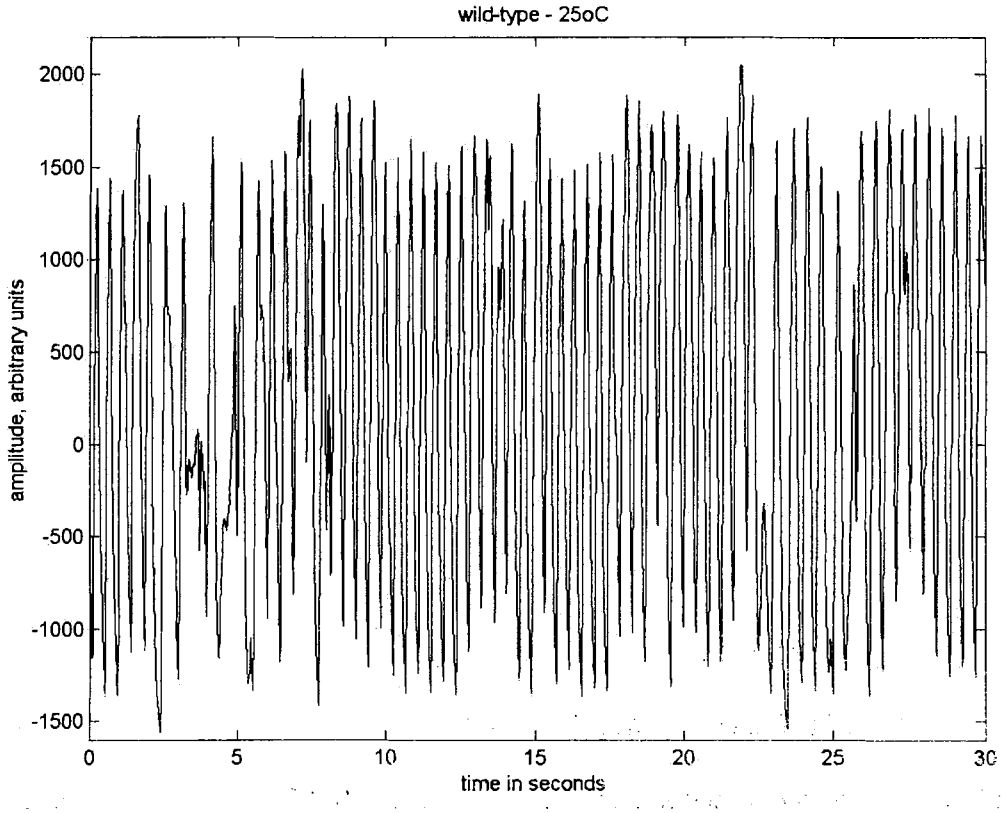

Figure 1. Example of the complete set of analyses performed on heartbeat data from a single wild-type pupa at 25°C. The same analyses were performed for every pupa of all genotypes at every temperature tested.

a) Output of the optical recording device (raw data) for heartbeat of typical wild-type *Drosophila melanogaster* at 25°C. The beat is fairly regular throughout the 30-s test period (Tables 1, 2; Figs. 7, 8).

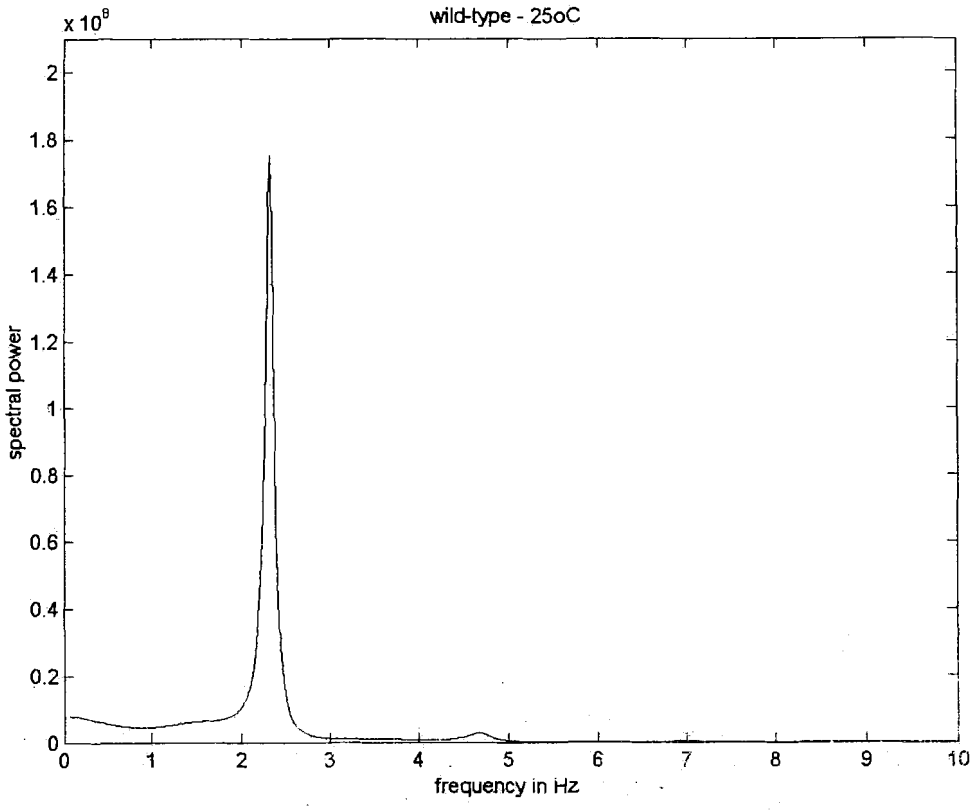

Figure 1. Continued.

b) Heartbeat of wild-type *Drosophila melanogaster* at 25°C. Power spectrum derived from Maximum Entropy Spectral Analysis (MESA) for the same wild-type pupa tested at 25°C, indicating the estimated frequency of the heartbeat. Any less pronounced additional peaks are reflections of irregularities (noise) in the raw data. Because there is a huge range of spectral power magnitudes among records, they are not all to the same scale (see ordinate scale at left of spectrum). The heartbeat frequency for this pupa is 2.33 Hz. The mean heart rate for wild-type pupae at 25°C is 2.18 Hz (Table 1).

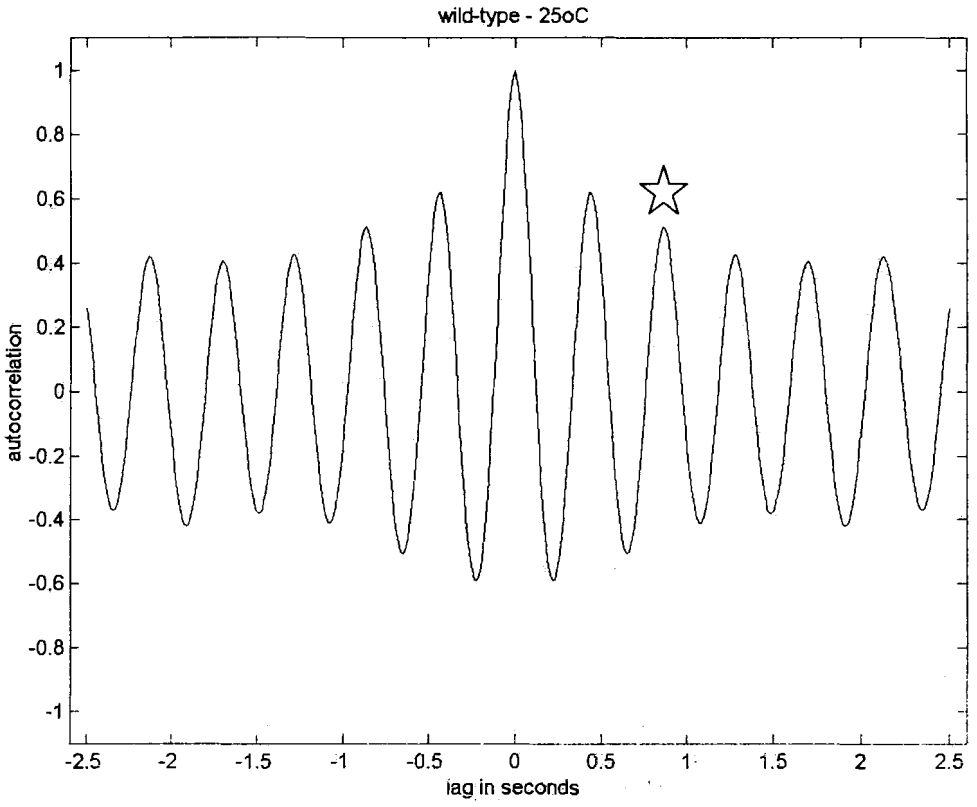

Figure 1. Continued.

c) Heartbeat of wild-type *Drosophila melanogaster* at 25°C. Autocorrelogram for the same wild-type pupa tested at 25°C. Decay of the autocorrelation function, in conjunction with results of the raw data plot and MESA spectrum, indicate heartbeat regularity. The height of the third peak (indicated by a star), expressed as a fraction of the height of the first peak, is a good measure of the rhythmicity index score. The rhythmicity index is 0.51 for this pupa. The average rhythmicity index score for wild-type pupae at 25°C is 0.39 (Table 2).

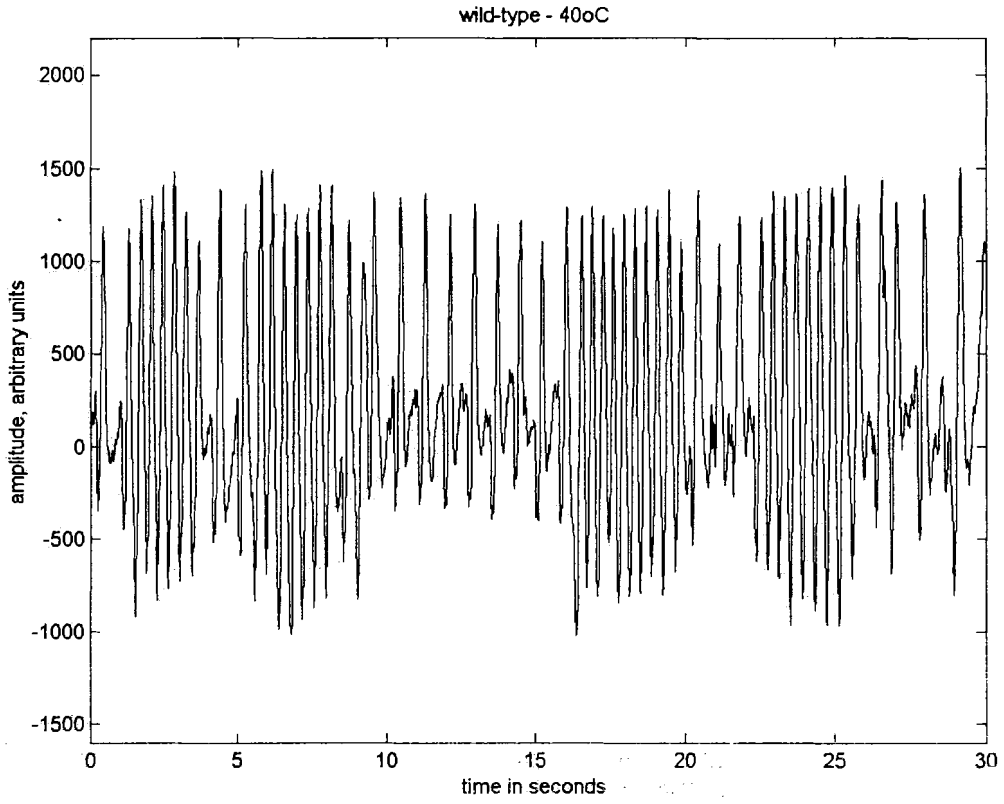

Figure 2. Example of the complete set of analyses performed on heartbeat data from a single wild-type pupa at 40°C.

a) Output of the optical recording device (raw data) for heartbeat of typical wild-type *Drosophila melanogaster* at 40°C. The beat is much less regular throughout the 30-s test period than it was at 25°C, but the rate has increased (Tables 1, 2; Figs. 1a, 7, 8).

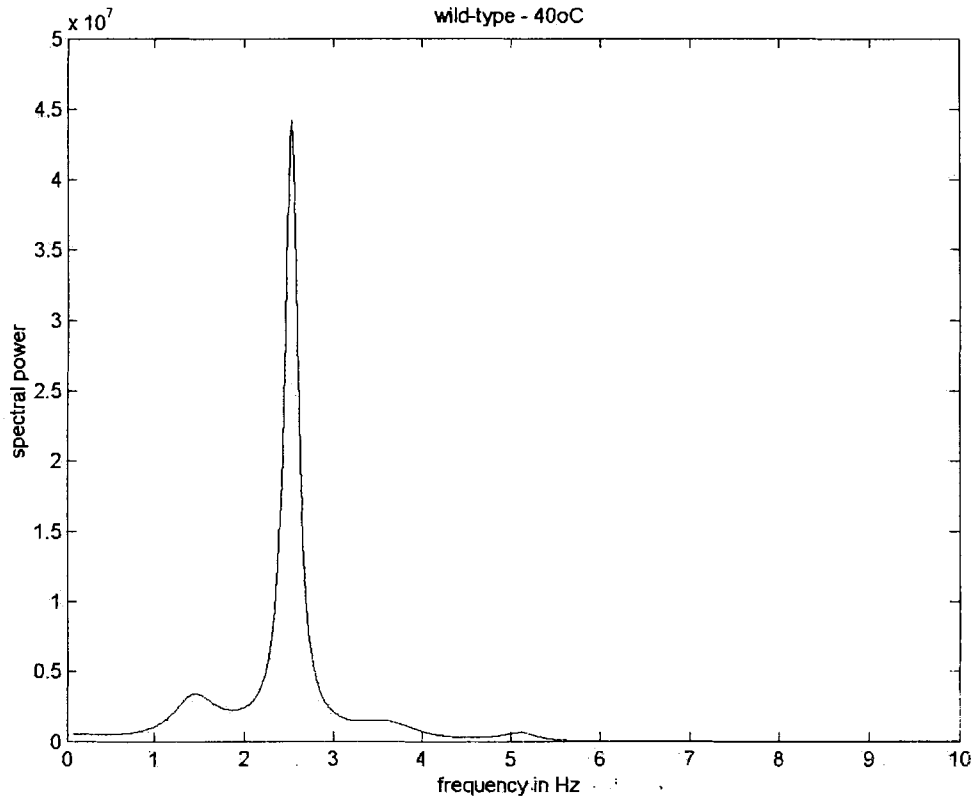

Figure 2. Continued.

b) Heartbeat of wild-type *Drosophila melanogaster* at 40°C. Power spectrum derived from MESA for the same wild-type pupa tested at 40°C, indicating the average frequency of the heartbeat, which is moderately increased from 25°C (Table 1; Fig. 1b). The frequency of heartbeat for this pupa is 2.53 Hz. The mean heart rate for wild-type pupae at 40°C is 2.38 Hz (Table 1).

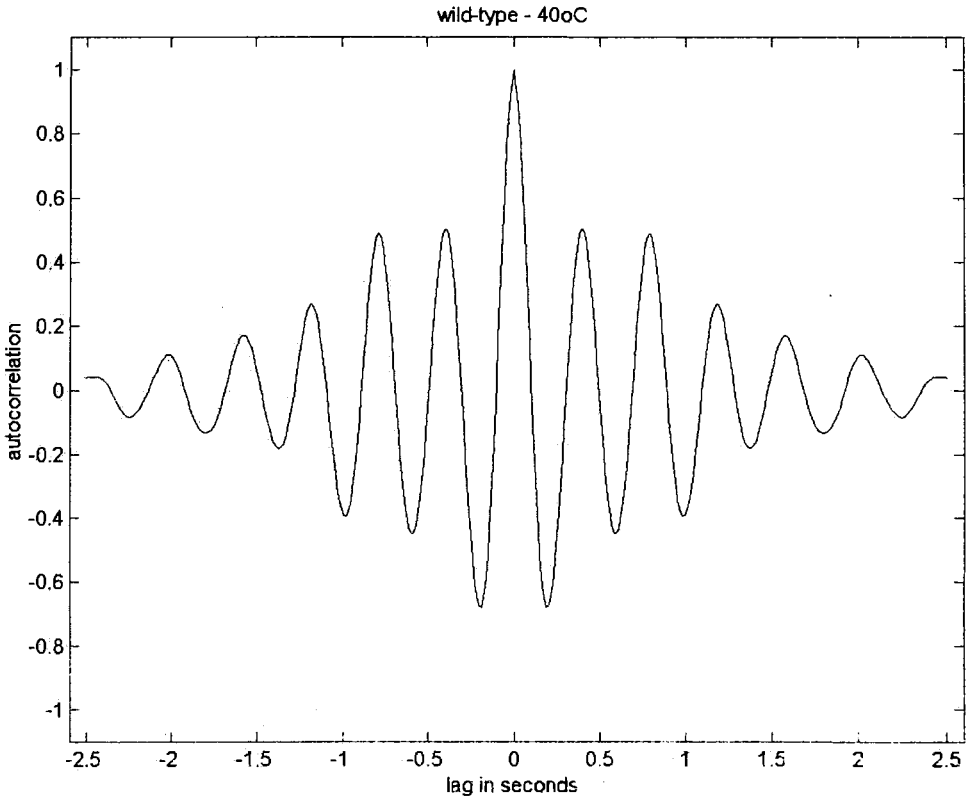

Figure 2. Continued.

c) Heartbeat of wild-type *Drosophila melanogaster* at 40°C. Autocorrelogram for the same wild-type pupa tested at 40°C. The decay of the autocorrelogram indicates that the heartbeat of this pupa is less rhythmic at high temperature than it was at 25°C (Table 2; Fig. 1c). At 40°C, the rhythmicity score 0.49 for this pupa. The average rhythmicity score for wild-type pupae at 40°C is 0.32 (Table 2).

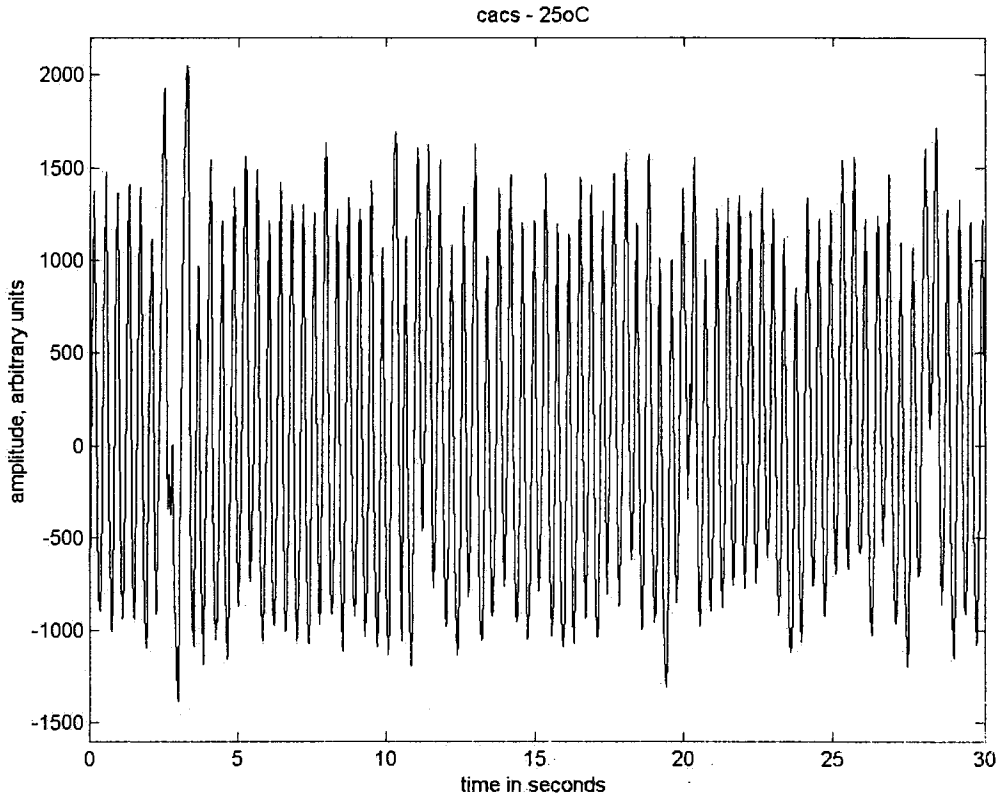

Figure 3. Example of the complete set of analyses performed on heartbeat data from a single *cac*^{s} pupa at 25°C.

a) Output of the optical recording device (raw data) for heartbeat of typical *cac*^{s} *Drosophila melanogaster* at 25°C. The beat is very regular and slightly faster throughout the 30-s test period compared to wild-type pupae at the same temperature (Tables 1, 2; Figs. 1a, 7, 8).

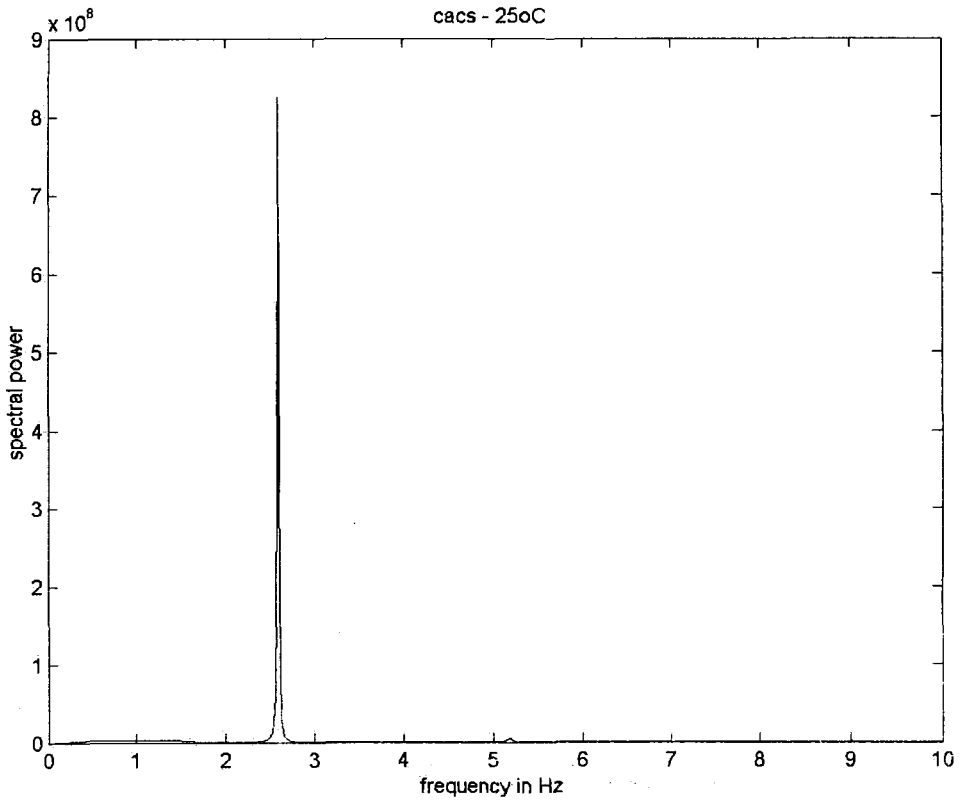

Figure 3. Continued.

b) Heartbeat of *cac*^{s} *Drosophila melanogaster* at 25°C. Power spectrum derived from MESA for the same *cac*^{s} pupa tested at 25°C, indicating the average frequency of the heartbeat, which is 2.60 Hz. The mean heart rate for *cac*^{s} pupae at 25°C is 2.29 Hz (Table 1). The heartbeat frequency is higher than for wild-type pupae at the same temperature (Table 1; Fig. 1b).

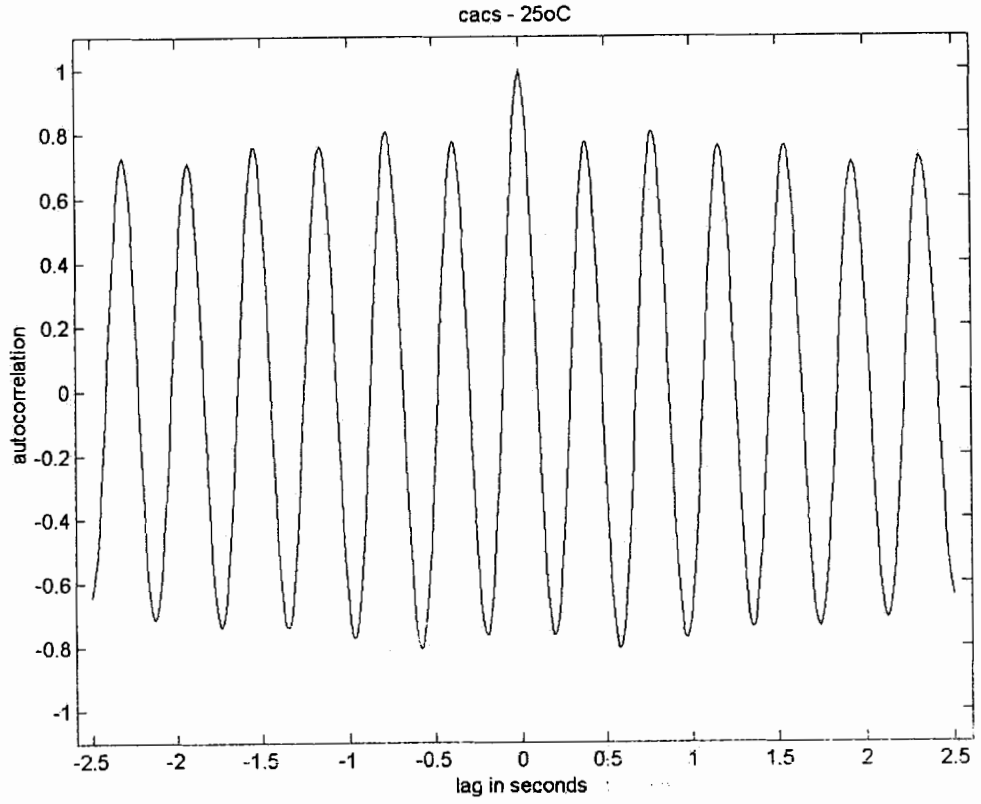

Figure 3. Continued.

c) Heartbeat of *cac*^{s} *Drosophila melanogaster* at 25°C. Autocorrelogram for the same *cac*^{s} pupa tested at 25°C. The rhythmicity index score is 0.81 for this pupa. The average rhythmicity score for *cac*^{s} pupae at 25°C is 0.63, which is considerably more rhythmic than for wild-type pupae at 25°C (Table 2; Fig. 1c).

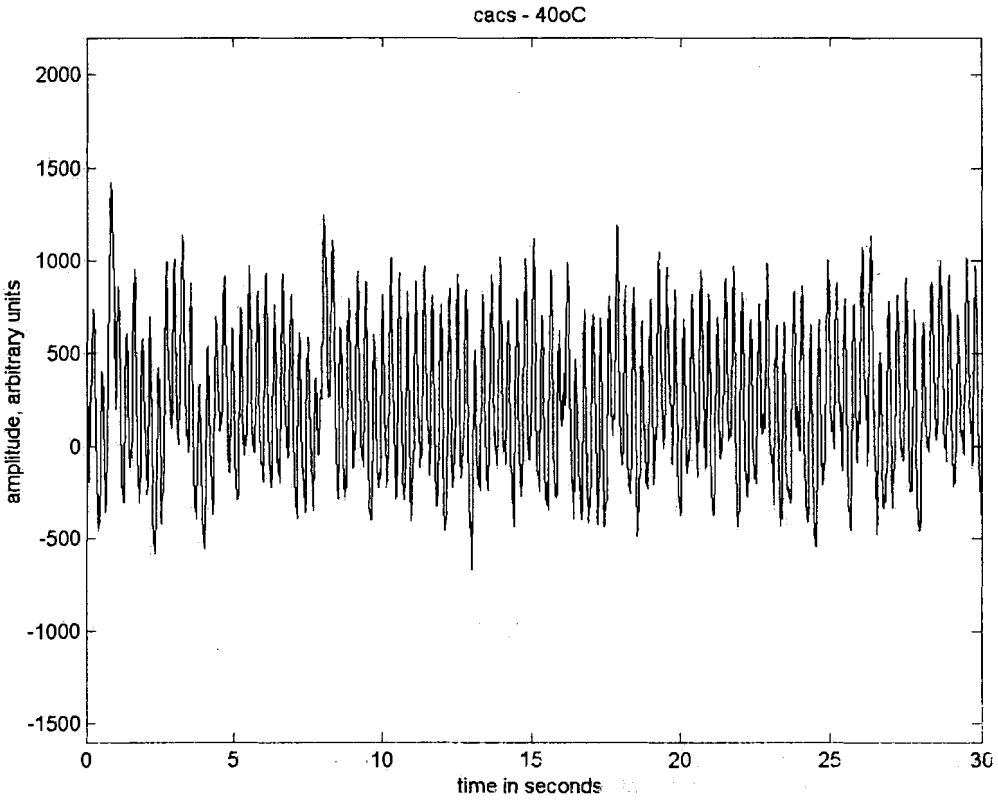

Figure 4. Example of the complete set of analyses performed on heartbeat data from a single cac^s pupa at 40°C.

a) Output of the optical recording device (raw data) for heartbeat of typical cac^s *Drosophila melanogaster* at 40°C. Heartbeat is fast and regular throughout the 30-s test period compared to wild-type pupae at the same temperature (Tables 1, 2; Figs. 2a, 7), although it is not as consistent as it was at 25°C (Figs. 3a, 8).

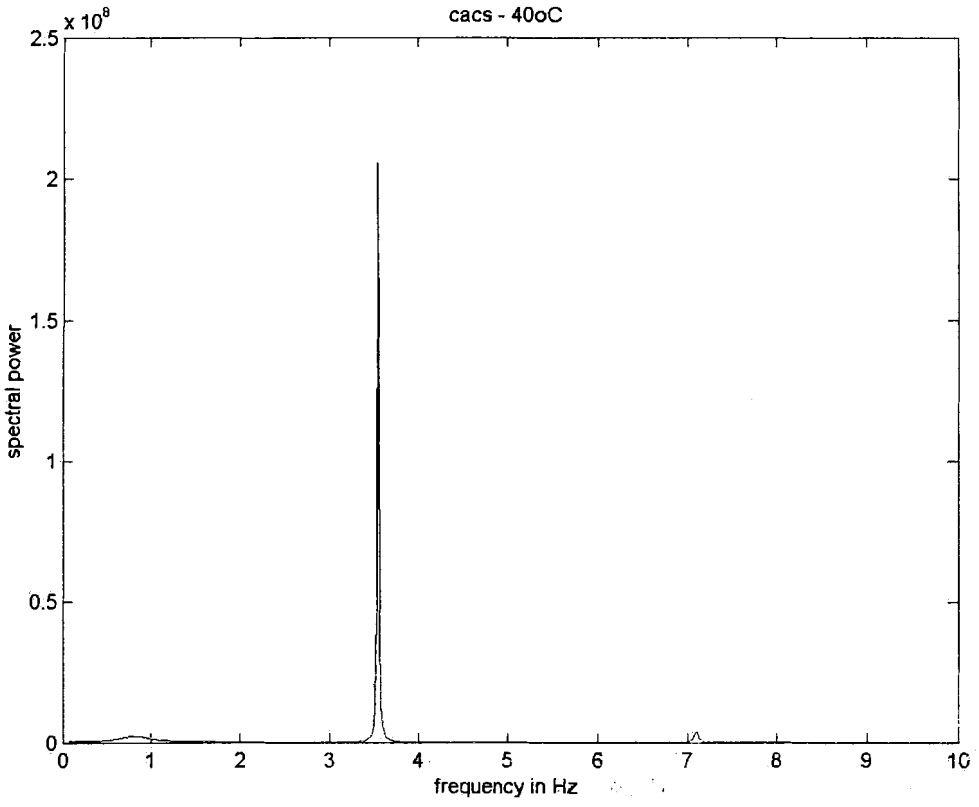

Figure 4. Continued.

b) Heartbeat of *cac*^{s} *Drosophila melanogaster* at 40°C. Power spectrum derived from MESA for the same *cac*^{s} pupa tested at 40°C, indicating the average frequency of the heartbeat. The heartbeat frequency for this pupa is 3.55 Hz. The mean heart rate for *cac*^{s} pupae at 40°C is 3.31 Hz, indicating that the heart is beating much more quickly than those of wild-type pupae at the same temperature (Table 1; Fig. 2b).

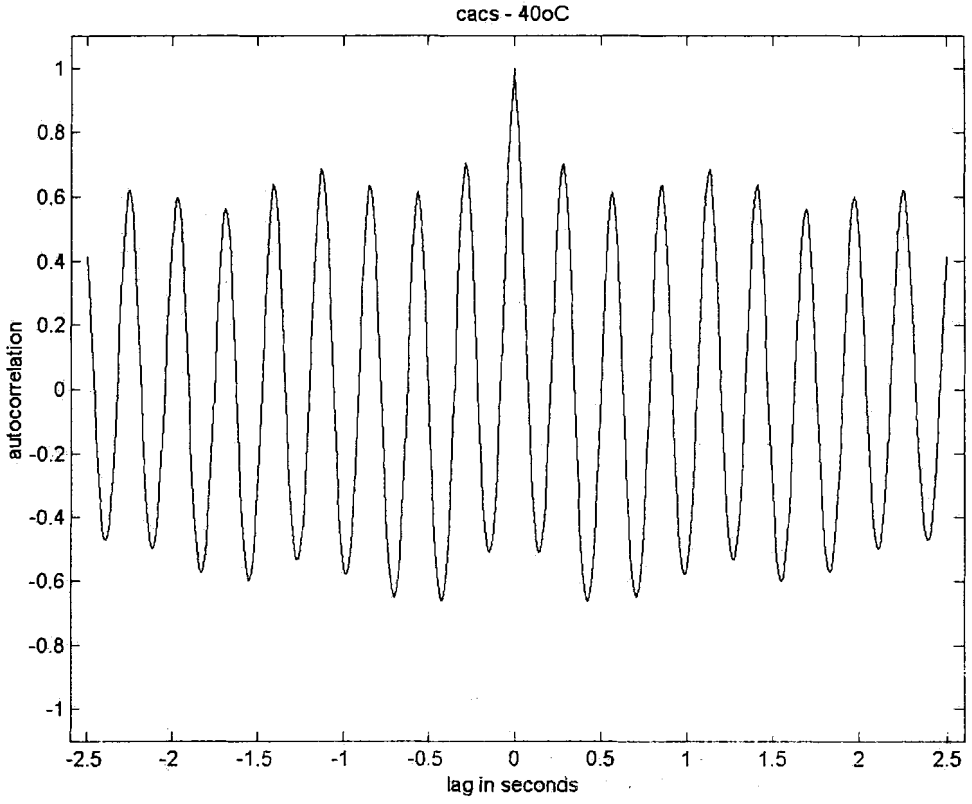

Figure 4. Continued.

c) Heartbeat of *cac*^{s} *Drosophila melanogaster* at 40°C. Autocorrelogram for the same *cac*^{s} pupa tested at 40°C. The rhythmicity index score for this pupa is 0.62, which is much lower than the same pupa at 25°C (Fig. 3c). The average rhythmicity score for *cac*^{s} pupae at 40°C is 0.44, which is still higher than wild-type, even at low temperature (Table 2; Figs. 1c, 2c).

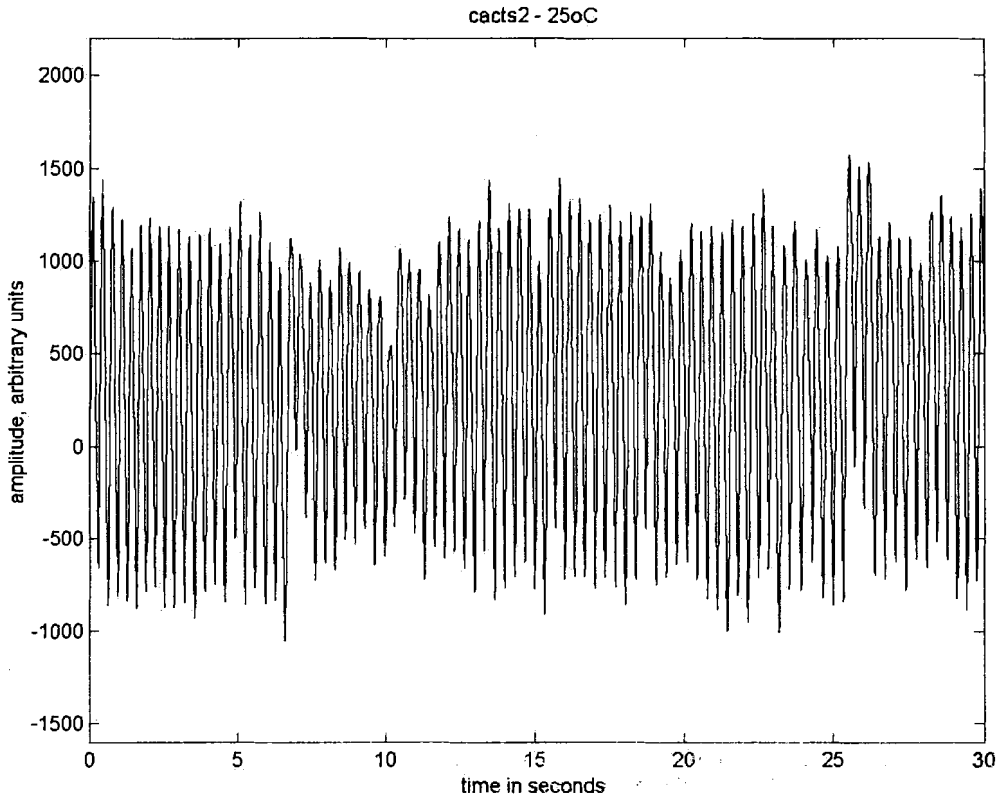

Figure 5. Example of the complete set of analyses performed on heartbeat data from a single cac^{ts2} pupa at 25°C.

a) Output of the optical recording device (raw data) for heartbeat of typical cac^{ts2} *Drosophila melanogaster* at 25°C. The beat is very fast and highly regular throughout the 30-s test period, especially when compared to wild-type pupae at the same temperature (Tables 1, 2; Figs. 1a, 7, 8).

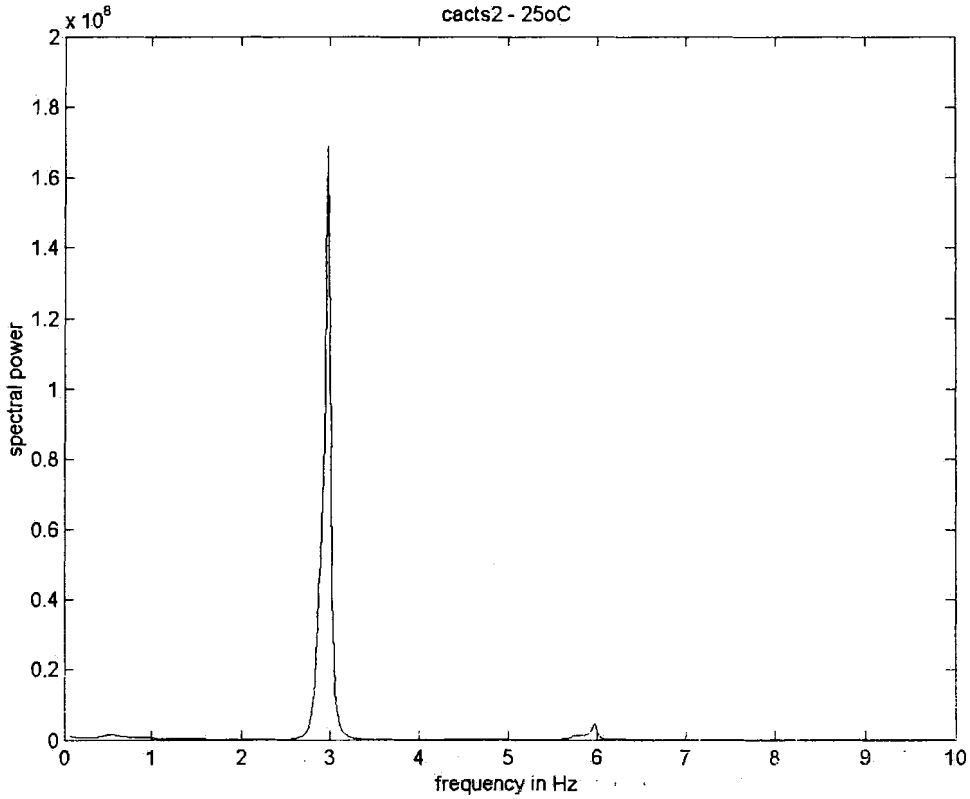

Figure 5. Continued.

b) Heartbeat of *cac*^{ts2} *Drosophila melanogaster* at 25°C. Power spectrum derived from MESA for the same *cac*^{ts2} pupa tested at 25°C, indicating the average frequency of the heartbeat. The heartbeat frequency for this pupa is 2.98 Hz. The mean heart rate for *cac*^{ts2} pupae at 25°C is 2.84 Hz (Table 1). Heart rate is very high in comparison to *cac*^{s} (Fig. 3b), and especially to wild-type (Fig. 1b) pupae at the same temperature (Table 1).

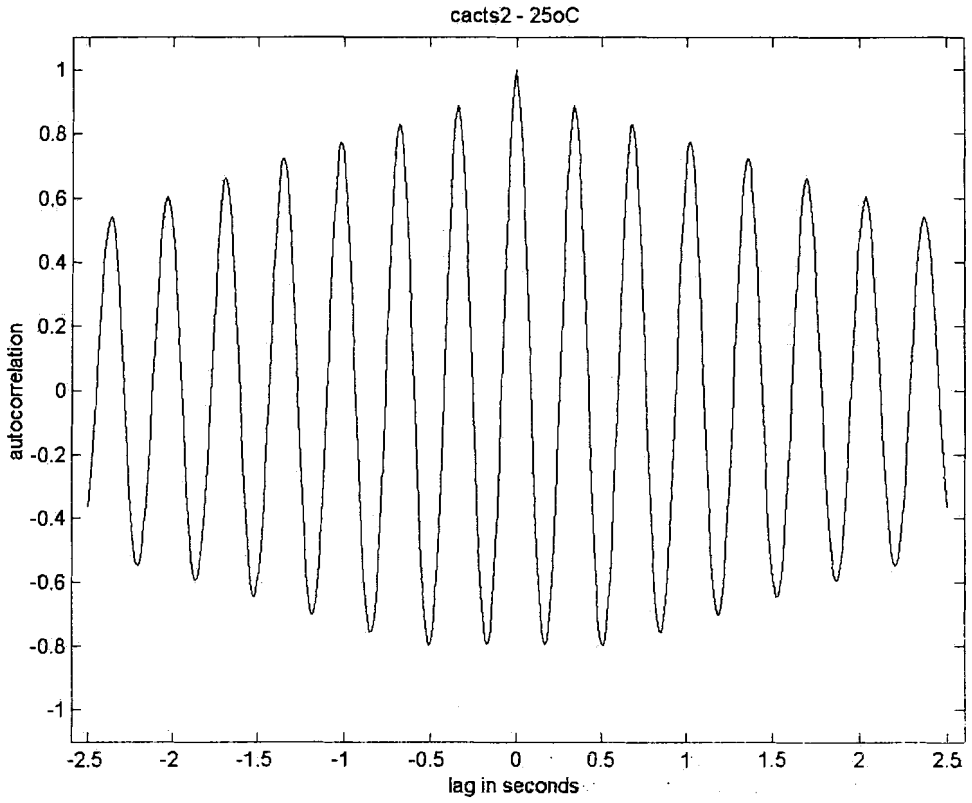

Figure 5. Continued.

c) Heartbeat of *cac*^{ts2} *Drosophila melanogaster* at 25°C. Autocorrelogram for the same *cac*^{ts2} pupa tested at 25°C. The rhythmicity index score for this pupa is 0.83. The average rhythmicity score for *cac*^{ts2} pupae at 25°C is 0.64, which is slightly higher than wild-type (Fig. 1c) but almost the identical to *cac*^{s} (Fig. 3c) pupae at the same temperature (Table 2).

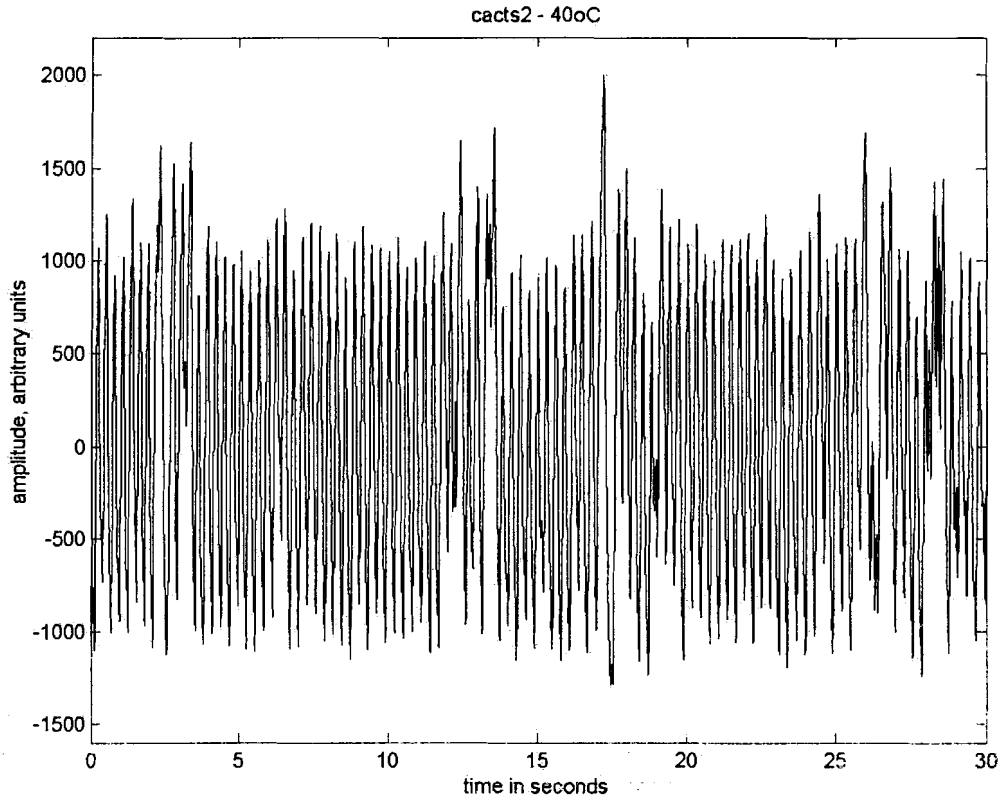

Figure 6. Example of the complete set of analyses performed on heartbeat data from a single cac^{ts2} pupa at 40°C.

a) Output of the optical recording device (raw data) for heartbeat of typical cac^{ts2} *Drosophila melanogaster* at 40°C. The beat is quite regular throughout the 30-s test period and much faster than at 25°C (Tables 1, 2; Figs. 5a, 7). The increased speed and regularity of the heartbeat is made more evident by comparison to wild-type pupae at the same temperature (Tables 1, 2; Figs. 2a, 7, 8).

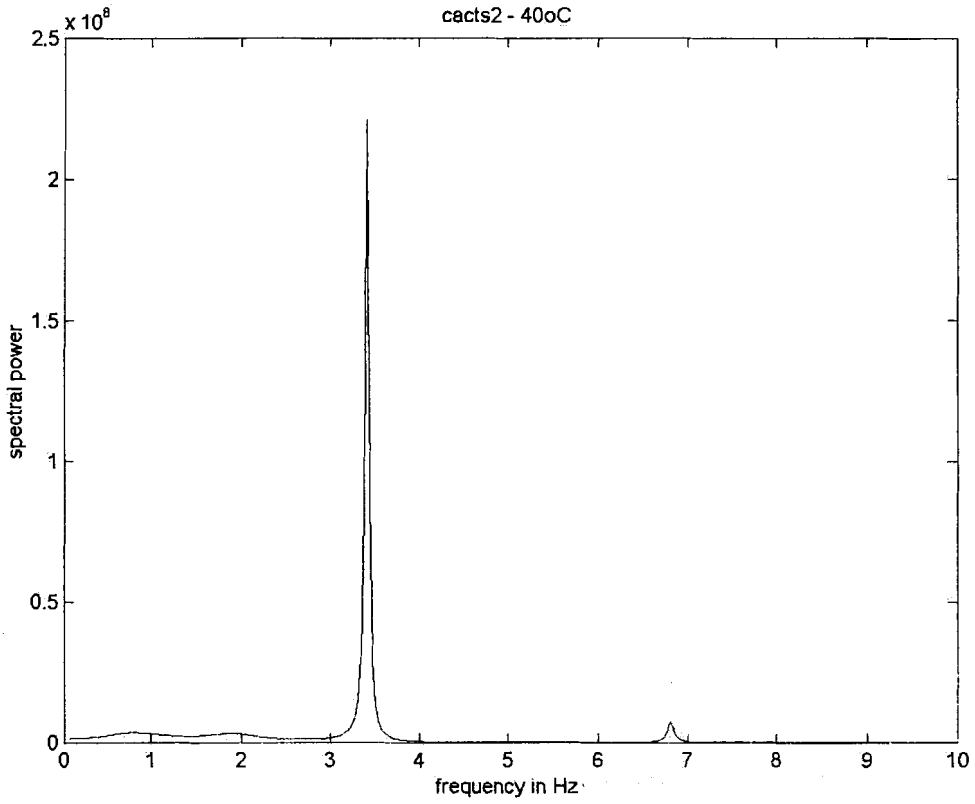

Figure 6. Continued.

b) Heartbeat of *cac*^{ts2} *Drosophila melanogaster* at 40°C. Power spectrum derived from MESA for the same *cac*^{ts2} pupa tested at 40°C, indicating the average frequency of the heartbeat. The heartbeat frequency for this pupa is 3.41 Hz. The mean heart rate for *cac*^{ts2} pupae at 40°C is 3.60 Hz, which is drastically faster than wild-type pupae (Fig. 2b) but only slightly faster than *cac*^{s} pupae (Fig. 4b) at the same temperature (Table 1).

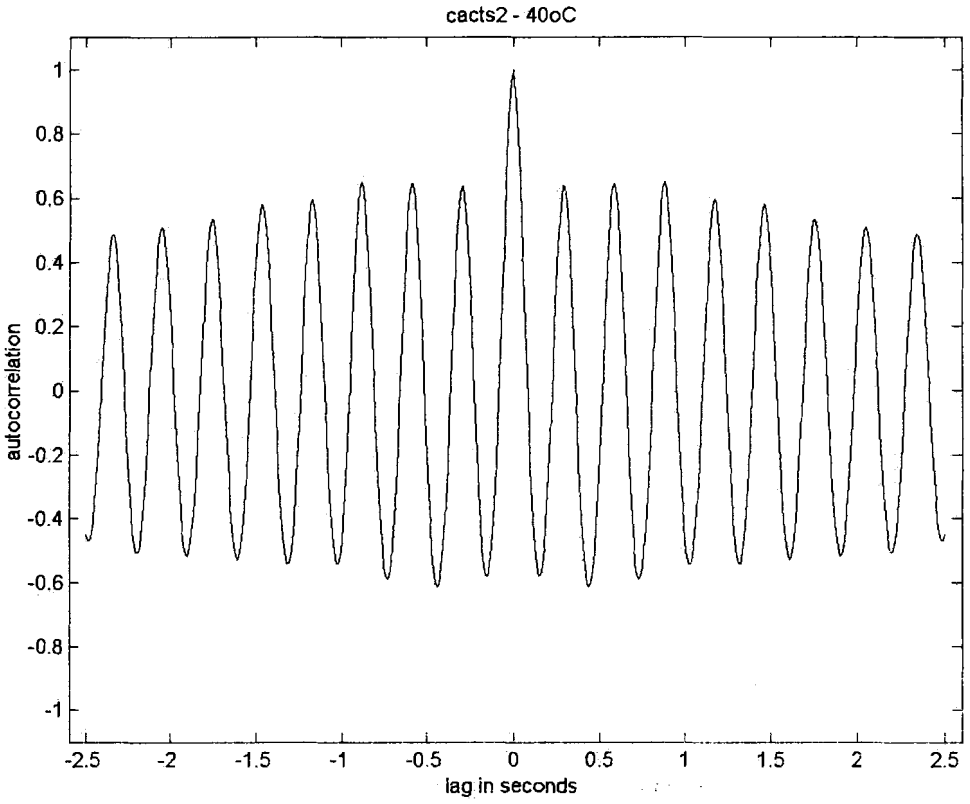

Figure 6. Continued.

c) Heartbeat of *cac*^{ts2} *Drosophila melanogaster* at 40°C. Autocorrelogram for the same *cac*^{ts2} pupa tested at 40°C. The rhythmicity index score for this pupa is 0.64. The average rhythmicity score for *cac*^{ts2} pupae at 40°C is 0.52, which is very similar to that of *cac*^{s} pupae (Fig. 4c) and not far from that of wild-type pupae (Fig. 2c) at the same temperature (Table 2).

Table 1. Mean heartbeat frequency of *cac* strains and wild-type. Mean heartbeat frequency ± standard error of the mean (SEM) at medium and high temperatures, determined by univariate analyses. Heartbeat frequencies measured at low temperatures are not reported because hearts of most pupae were arrhythmic at these temperatures. Strains are ordered according to their overall heart rate values across temperatures (column at right).

Heartbeat frequencies of strains were initially compared across temperature by ANOVA and then grouped by Ryan-Einot-Gabriel-Welsch multiple F test (REGWF, Einot and Gabriel, 1975) ($\alpha = 0.05$). There is a significant difference between genotypes ($F = 21.11$, $P = 0.0001$), and groupings are indicated by letter superscript (A, B, or C) in the overall frequency column. Means that share a superscript are not significantly different. SEM = standard error of the mean, N = number of pupae tested and analyzed for given strain at each temperature.

FR Genotype	Temperature 20	25	30	35	37	39	40	41	42	Over-all FR across temp
wild-type	1.80	2.18	2.44	2.63	2.73	2.39	2.38	2.36	1.84	2.32[A]
+/- SEM	0.10	0.19	0.19	0.20	0.09	0.24	0.25	0.30	0.36	
N	14	9	9	9	18	9	9	9	9	
cac^{s}/Df	2.13	2.40	2.32	2.78	2.89	2.90	2.99	2.87	2.84	2.66[B]
	0.11	0.19	0.32	0.20	0.16	0.28	0.18	0.21	0.22	
	15	9	9	9	18	9	9	9	9	
cac^{s}	1.93	2.29	2.53	2.72	3.16	3.29	3.31	3.25	3.04	2.79[B]
	0.11	0.15	0.18	0.21	0.13	0.22	0.23	0.25	0.30	
	29	19	19	19	37	16	16	16	16	
cac^{s}/*cac*^{ts2}	2.01	2.25	2.49	2.79	3.07	3.29	3.30	3.28	2.97	2.79[B]
	0.13	0.16	0.18	0.23	0.13	0.16	0.18	0.28	0.38	
	23	16	16	16	30	14	14	14	14	
cac^{s}/+	2.01	2.29	2.64	2.90	3.10	3.21	3.18	3.09	3.03	2.80[B]
	0.07	0.11	0.13	0.16	0.10	0.11	0.10	0.12	0.12	
	28	17	17	17	33	16	16	16	16	
cac^{ts2}/+	2.28	2.64	3.00	3.32	3.47	3.59	3.59	3.18	2.97	3.10[C]
	0.04	0.07	0.10	0.09	0.07	0.07	0.09	0.24	0.30	
	30	19	19	19	38	19	19	19	19	
cac^{ts2}	2.55	2.84	3.00	3.50	3.59	3.73	3.60	3.68	3.40	3.31[C]
	0.08	0.14	0.19	0.17	0.14	0.17	0.24	0.19	0.28	
	30	20	20	20	40	20	20	20	20	

Figure 7. Comparison of the relationship between rate of pupal heartbeat and temperature. Heart rates of wild-type (solid line), cac^{s} (line with circles), cac^{s}/+ (line with stars), cac^{ts2} (line with asterisks), cac^{ts2}/+ (line with squares), and cac^{s}/cac^{ts2} (line with diamonds) pupae. Mean heart rates at each temperature were determined by univariate anlyses and are listed in Table 1 (GLM procedure, SAS). Bars representing standard error of the mean were omitted for clarity, but values are listed in Table 1.

Regression of heartbeat frequencies on temperature performed for wild-type, cac^{s}, and cac^{ts2} pupae yielded slopes of 0.0201, 0.0628, and 0.0522, respectively. This indicates that there are positive relationships between heartbeat frequencies and temperature for these strains. After comparing the regression plot to that derived from univariate analyses (Fig. 7) it is evident that the regression lines do not accurately describe the data at all temperatures because they eliminate important variation between genotypes at individual temperatures. This is especially true for cac^{s}, where the relationship between heart rate and temperature is clearly non-linear (Table 1; Fig. 7).

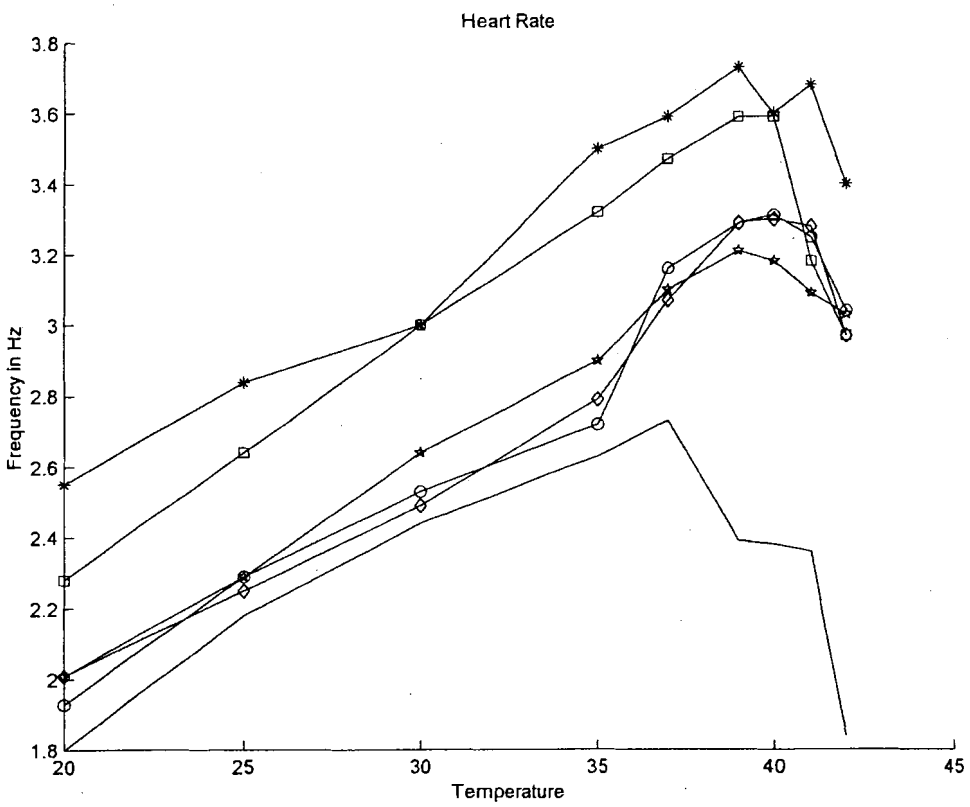
Heart Rate
Frequency in Hz
Temperature
3.8
3.6
3.4
3.2
3
2.8
2.6
2.4
2.2
2
1.8
20
25
30
35
40
45

Effect of cac^{ts2} on Heartbeat Frequency

cac^{ts2} affects heartbeat frequency in the same direction as cac^{s}, but more severely. Mutants have significantly higher heart rates compared to wild-type at all temperatures except 30°C (20°C: F = 28.70, P = 0.0001; 25°C: F = 6.94, P = 0.0138; 30°C: F = 3.23, P = 0.0834; 35°C: F = 9.39, P = 0.0049; 37°C: F = 15.11, P = 0.0003; 39°C: F = 19.82, P = 0.0001; 40°C: F = 9.33, P = 0.0050; 41°C: F = 14.28, P = 0.0008; 42°C: F = 10.56, P = 0.0031) (Table 1; Fig. 7). Raw data and MESA plots at 25°C and 40°C clearly demonstrate that cac^{ts2} causes increased heart rate across temperature (Figs. 1ab, 2ab, 5ab, 6ab). cac^{ts2} pupae do not exhibit the dramatic increase in heart rate at 37°C seen in cac^{s} pupae but instead heartbeat frequency continues to increase steadily (Fig. 7). cac^{ts2} heart rates begin to decline like wild-type at temperatures ≥41°C (Fig. 7).

cac^{ts2} is fully penetrant for the heart rate phenotype because there is no significant difference between cac^{ts2} homo- and heterozygotes at all temperatures ≥25°C (25°C: F = 1.41, P = 0.2432; 30°C: F = 0.00, P = 0.9871; 35°C: F = 0.91, P = 0.3456; 37°C: F = 0.53, P = 0.4707; 39°C: F = 0.58, P = 0.4495; 40°C: F = 0.00, P = 0.9547; 41°C: F = 2.68, P = 0.1099; 42°C: F = 1.10, P = 0.3011) (Table 1; Fig. 7). In further support of this statement, the normalized heartbeat frequency dominance value of homozygous cac^{ts2} over wild-type is 0.58.

Recordings of heartbeat were not performed for cac^{ts2}/Df because cac^{ts2} is dominant for the altered heartbeat phenotype, and so deleting the *cac* locus on one chromosome would likely not yield informative results. Heartbeat recordings of cac^{s} heterozygous with a *cac* deletion (Df(1)N105) were performed, as mentioned earlier, but they were statistically indistinguishable from those of cac^{s} homozygotes, and also from cac^{s} heterozygotes. Therefore, cac^{ts2}/Df heartbeat records would look like those of cac^{ts2}

homo- and heterozygotes, which does not help isolate the genetic origin of the cac^{ts2} mutant heartbeat phenotype.

Wild-type Rhythmicity Index Phenotype

The rhythmicity index of wild-type *Drosophila* heartbeat decreases in a non-linear fashion with increasing temperature (Table 2; Figs. 1a, 1c, 2a, 2c, 8). Therefore, in response to elevating temperature, heartbeat rhythmicity decreases while heart rate concomitantly increases.

Table 2. Mean heartbeat rhythmicity indices of *cac* strains and wild-type. Mean rhythmicity indices ± standard error of the mean (SEM) at medium and high temperatures, determined by univariate analyses for all genotypes tested. Strains are ordered according to their overall rhythmicity index values across temperature (column at right).

Rhythmicity indices of strains were initially compared across temperature by ANOVA ($F = 22.26$, $P = 0.0001$) and then grouped by REGWF test ($\alpha = 0.05$) (Einot and Gabriel, 1975). There is a significant difference between genotypes ($F = 22.26$, $P = 0.0001$), and groupings are indicated by letter superscript (A, B, C, or D) in the overall rhythmicity column. Means that share a superscript are not significantly different. SEM = standard error of the mean, N = number of pupae tested and analyzed for given strain at each temperature.

RI	Temperature									Over-all RI across temp
Genotype	20	25	30	35	37	39	40	41	42	
wild-type	0.52	0.39	0.42	0.36	0.29	0.33	0.32	0.35	0.30	0.37[A]
+/- SEM	0.08	0.08	0.07	0.09	0.04	0.08	0.05	0.08	0.05	
N	14	9	9	8	18	9	8	8	6	
cac^{s}/cac^{ts2}	0.48	0.61	0.51	0.45	0.43	0.46	0.42	0.41	0.32	0.46[B]
	0.04	0.05	0.06	0.05	0.04	0.07	0.08	0.06	0.06	
	20	15	16	14	29	14	14	13	11	
cac^{s}	0.55	0.63	0.63	0.51	0.54	0.40	0.44	0.49	0.43	0.53[B, D]
	0.05	0.06	0.06	0.06	0.04	0.06	0.05	0.06	0.06	
	28	19	19	19	34	15	15	15	14	
$cac^{s}/+$	0.63	0.60	0.58	0.60	0.56	0.53	0.46	0.43	0.46	
	0.05	0.07	0.06	0.06	0.04	0.06	0.06	0.05	0.06	0.55[C, D]
	28	17	16	16	33	16	16	16	16	
cac^{ts2}	0.67	0.64	0.64	0.61	0.60	0.51	0.52	0.51	0.51	
	0.05	0.06	0.07	0.06	0.04	0.06	0.06	0.06	0.05	
	29	20	19	20	39	20	19	20	17	0.59[C, D]
cac^{s}/Df	0.69	0.69	0.57	0.56	0.59	0.67	0.56	0.46	0.46	
	0.05	0.05	0.11	0.07	0.05	0.07	0.09	0.10	0.07	
	14	9	9	9	17	8	9	8	9	
										0.59[C, D]
$cac^{ts2}/+$	0.67	0.67	0.68	0.65	0.60	0.58	0.62	0.55	0.62	
	0.04	0.06	0.05	0.05	0.04	0.05	0.05	0.07	0.06	
	30	19	19	19	38	19	19	17	16	
										0.63[C]

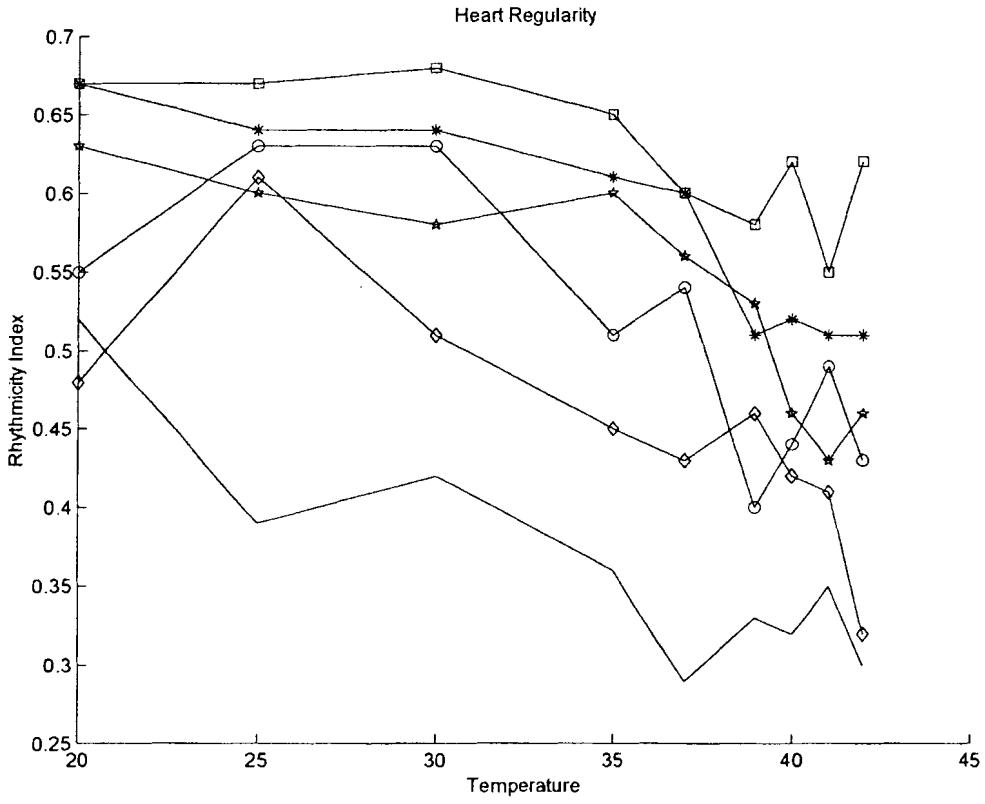

Figure 8. Comparison of the relationship between rhythmicity index of pupal heartbeat and temperature. Rhythmicity indices of wild-type (solid line), cac^{s} (line with circles), cac^{s}/+ (line with stars), cac^{ts2} (line with asterisks), cac^{ts2}/+ (line with squares), and cac^{s}/cac^{ts2} (line with diamonds) pupae. Mean rhythmicity indices and SEM are listed in Table 2.

Regressions of rhythmicity of heartbeat on temperature in wild-type, cac^{s}, and cac^{ts2} pupae were performed and yielded slopes of -0.0091, -0.0065, and -0.0075 and intercepts of 0.6750, 0.7418, and 0.8396, respectively, although relationships are not strictly linear. Prior heartbeat studies by this lab have consistently shown that rhythmicity index variation in relation to temperature is inconsistent (Dowse *et al.*, 1995; Johnson *et al.*, 1997; Johnson *et al.*, 1998; Johnson *et al.*, 2001).

Effect of *cac* Mutations on Heartbeat Rhythmicity Index

The effect of mutations in *cac* on heartbeat rhythmicity parallels their impact on heart rate. Raw data and autocorrelation plots at 25°C and 40°C demonstrate that *cac* mutants have increased rhythmicities in comparison to wild-type across temperature (Figs. 1ac, 2ac, 3ac, 4ac, 5ac, 6ac), but only significantly so at two temperatures (25°C: F = 3.32, P = 0.0452, 37°C: F = 9.62, P = 0.0002) (Table 2; Fig. 8). cac^{s} and cac^{ts2} pupae are grouped together for rhythmicity analyses because there is no significant difference between them at any temperature (20°C: F = 2.56, P = 0.1156; 25°C: F = 0.03, P = 0.8630; 30°C: F = 0.02, P = 0.8799; 35°C: F = 1.39, P = 0.2467; 37°C: F = 0.79, P = 0.3759; 39°C: F = 1.53, P = 0.2244; 40°C: F = 0.85, P = 0.3648; 41°C: F = 0.03, P = 0.8618; 42°C: F = 0.99, P = 0.3274) (Table 2; Fig. 8). Both cac^{s} and cac^{ts2} are dominant for the rhythmicity phenotype, as there is no significant difference between homo- or heterozygous strains of either mutant (cac^{s} - 20°C: F = 1.31, P = 0.2572; 25°C: F = 0.10, P = 0.7509; 30°C: F = 0.32, P = 0.5757; 35°C: F = 1.12, P = 0.2983; 37°C: F = 0.11, P = 0.7465; 39°C: F = 2.18, P = 0.1506; 40°C: F = 0.05, P = 0.8233; 41°C: F = 0.61, P = 0.4396; 42°C: F = 0.14, P = 0.7108; cac^{ts2} - 20°C: F = 0.00, P = 0.9849; 25°C: F = 0.08, P = 0.7747; 30°C: F = 0.20, P = 0.6595; 35°C: F = 0.23, P = 0.6334; 37°C: F = 0.01, P = 0.9255; 39°C: F = 0.60, P = 0.4420; 40°C: F = 1.76, P = 0.1931; 41°C: F = 0.25, P = 0.6209; 42°C: F = 2.43, P = 0.1295) (Table 2; Fig. 8). Furthermore, the normalized heartbeat rhythmicity dominance values of homozygous cac^{s} and cac^{ts2} over wild-type are 1.29 and 1.39, respectively. Although there are statistical differences between genotypes, the only distinctive trend depicted in Figure 8 is that for all strains tested rhythmicities decrease with temperature.

Just as it is for heart rate, cac^{s} is dominant to wild-type and cac^{ts2} for the heartbeat rhythmicity phenotype; there is no significant difference in this character between homo- or heterozygotic cac^{s}, or heteroallelic (cac^{s}/cac^{ts2}) pupae at any temperature (20°C: F = 2.29, P = 0.1082; 25°C: F = 0.06, P = 0.9393; 30°C: F = 0.94, P = 0.3964; 35°C: F = 1.72, P = 0.1909; 37°C: F = 2.62, P = 0.0781; 39°C: F = 1.08, P = 0.3499; 40°C: F = 0.13, P = 0.8760; 41°C: F = 0.59, P = 0.5601; 42°C: F = 1.43, P = 0.2514) (Table 2; Fig. 8). The normalized dominance value of cac^{s} over cac^{ts2} for heartbeat rhythmicity is 3.3. In contrast, cac^{ts2} is significantly different from cac^{s}/cac^{ts2} heteroallelic pupae at several temperatures (20°C, P = 0.0129; 37°C, P = 0.0079; 42°C, P = 0.0196) (Table2, Fig. 8).

Comparisons of cac^{s} rhythmicity indices to those of cac^{s}/Df yield analogous results to those for heart rates of these strains. Heart rates of cac^{s}/Df pupae are not significantly different from those of cac^{s} homozygotes, and by extension heterozygotes, at all temperatures (20°C: F = 2.74, P = 0.1057; 25°C: F = 0.49, P = 0.4895; 30°C: F = 0.30, P = 0.5856; 35°C: F = 0.23, P = 0.6380; 37°C: F = 0.51, P = 0.4766; 39°C: F = 6.98, P = 0.0153; 40°C: F = 1.38, P = 0.2526; 41°C: F = 0.10, P = 0.7523; 42°C: F = 0.14, P = 0.7159) (Table 2; Fig. 8). Because cac^{s} is dominant for the altered heartbeat rhythmicity phenotype as well as for aberrant heart rate, recordings from pupae deficient for the *cac* gene on one chromosome yield uninformative results. For this reason parallel recordings of cac^{ts2}/Df were not performed.

DISCUSSION

The *cac* Gene's Participation in Heartbeat Pacemaking

I have analyzed heartbeat of flies bearing mutations in the *cac* gene. *cac* encodes the α_1 subunit of a calcium ion channel putatively involved in cardiac pacemaking in *Drosophila*. The two mutant alleles, cac^{s} and cac^{ts2}, increase heartbeat frequency above wild-type levels in a dominant fashion; furthermore, normalized dominance values support this conclusion (Table 1; Fig. 7). Molecular data from previous studies (Smith *et al.*, 1996; Smith *et al.*, 1998; Chan *et al.*, 2002; Kawasaki *et al.*, 2002), suggests that these two lesions alter calcium channel inactivation. I hypothesize that such altered channel inactivation accounts for the cardiac effects.

It is highly unlikely that Dmca1A affects heartbeat indirectly via the nervous system because *Drosophila* heartbeat is not neurogenically generated. Initial evidence of this comes from studies where isolated hearts continued to beat for several hours after extraction from the body (Rizki, 1978). Further support for a myogenic origin of impulses comes from an *in situ* hybridization assay where *paralytic* (*para*) channels, which are the primarily expressed sodium channel subunit in *Drosophila* (Loughney *et al.*, 1989), were not detected in any type of muscle or in the abdomen, which makes the possibility of their involvement in heart function remote (Amichot *et al.*, 1993). The $paralytic^{temperature\text{-}sensitive}$ ($para^{ts}$) mutation has no effect on heartbeat (Suzuki *et al.*, 1971; Dowse *et al.*, 1995) even at temperatures that eliminate Na^{+}-dependent action potentials (Suzuki *et al.*, 1971; Wu *et al.*, 1978; Jackson *et al.*, 1984; Ganetzky, 1984). Furthermore, tetrodotoxin (TTX), which selectively blocks sodium channels in fast

response fibers (Wu *et al.*, 1978; Fozzard and Arnsdorf, 1992; Hille, 2001), has no effect on heart rate even at high doses (Dowse *et al.*, 1995; Gu and Singh, 1995; Johnson *et al.*, 1998; Markou and Theophilidis, 2000). Thus an aberrant nervous system owing to a *cac* defect would seem unable to have any more affect than these more drastic treatments.

The *cac*-encoded channel has been postulated to act at the level of the synapse, modulating neurotransmitter release (Kawasaki *et al.*, 2000; Dellinger *et al.*, 2000; Kawasaki *et al.*, 2002); however, *cac* is likely not affecting heart function through synaptic effects. There are no significant heartbeat abnormalities in flies bearing mutant *comatose* (*comt*), which encodes the synaptic vesicle fusion priming protein NSF1 (N-ethylmaleimide-sensitive fusion protein) (Johnson *et al.*, 1997; Dellinger *et al.*, 2000). *comt* interacts with both *cac* alleles to further decrease synaptic activity (Dellinger *et al.*, 2000). Thus if *cac* were mediating heart function via altered synaptic function, then *comt* mutants would have alterations in heartbeat similar to those of *cac* mutants. Instead, *comt* mutants have marginally decreased heart rates at only a few temperatures (20°C, 30°C, and 37°C) (Johnson *et al.*, 1997). This phenotype is not only much less pronounced than that of either *cac* allele, but it also affects heart rate in the opposite direction.

Because of Dmca1A's synaptic involvement (Kawasaki *et al.*, 2000; Dellinger *et al.*, 2000), however, and since it is not possible to completely isolate the heart from connective tissue strands that may be innervated (Dowse *et al.*, 1995; Curtis *et al.*, 1999), it would be necessary to test heartbeat of *cac*; *para* double mutants, perhaps combined with TTX injection, to rule out the possibility that *cac* heartbeat alterations are neural in origin. If double mutants retain heartbeat abnormalities at the same level as those seen in

cac single mutants, then Dmca1A could be conclusively considered a participant in heartbeat pacemaking. Furthermore, studies of *cac* expression are currently being performed in this lab, and they will contribute to understanding the heartbeat effects of this gene.

Aberrant Calcium Channel Inactivation in *cac* Mutants

The phenotypes of the two mutants are similar to each other, especially at high temperatures ($\geq$39°C). In all probability both *cac* alleles affect channel inactivation of a voltage-gated calcium channel in which Dmca1A participates; cac^{s} has altered voltage-dependent inactivation (Hering *et al.*, 1996; Smith *et al.*, 1996; Smith *et al.*, 1998; Chan *et al.*, 2002) and cac^{ts2} has aberrant calcium-dependent inactivation (Zhou *et al.*, 1997; Dellinger *et al.*, 2000; Kawasaki *et al.*, 2000; Chan *et al.*, 2002; Kawasaki *et al.*, 2002). Based on the likelihood that Dmca1A is involved in heartbeat pacemaking, *cac* mutants' altered channel inactivation is predicted to affect channel interactions underlying these oscillations. Presumably, Ca^{2+} current depolarizes pacemaker cells, leading them into the heartbeat-triggering action potential (Fozzard and Arnsdorf, 1992; Irisawa *et al.*, 1993). Therefore, if inactivation were disrupted, as it theoretically is in *cac* mutants, the normal automaticity of the oscillatory mechanism would be impacted. Aberrant Ca^{2+} influx would trigger pacemaker action potentials prematurely by causing either early afterdepolarizations (EADs) or delayed afterdepolarizations (DADs), creating prolonged altered impulse formation (Fozzard and Arnsdorf, 1992).

Based on Dmca1A's classification as a type of non-L-type HVA channel (Smith *et al.*, 1996; Peixoto *et al.*, 1997; Littleton and Ganetzky, 2000; Jeziorski *et al.*, 2000;

MacPherson *et al.*, 2001; Kawasaki *et al.*, 2002), under wild-type circumstances it would partially and fairly slowly inactivate and remain that way at membrane potentials above –30 mV (Hille, 2001). However, if calcium channels inactivate in a delayed manner or not at all, then they would allow an increased amount of Ca^{2+} to enter pacemaker cells at depolarizing membrane potentials below the reversal potential for Ca^{2+} (E_{Ca} = 128 mV theoretically, or ~50 mV experimentally) (Hille, 2001). Although some Dmca1A channels would close based on open duration or membrane repolarization below –20mV, others would remain open, allowing a greater overall Ca^{2+} current to enter pacemaker cells. This hypothesis could explain high heartbeat frequencies and rhythmicities of *cac* mutants, because intracellular calcium plays a fundamental role in the regulation of pacemaker rate (Rigg and Terrar, 1996; Terrar and Rigg, 2000; Hüser *et al.*, 2000; Rigg *et al.*, 2000; Lipsius *et al.*, 2001). Defectively inactivating calcium channels would increase the rate of action potentials by eliminating the Ca^{2+} current delay due to triggering channel activation and awaiting the arrival of the calcium current that stimulates *slo* potassium channels to repolarize the membrane (Johnson *et al.*, 1998; Hüser *et al.*, 2000). Intracellular Ca^{2+} may interact with other putative pacemaker channels (I_h, I_K-*eag*) as well, affecting their contributions to the oscillating system (Rigg and Terrar, 1996; Terrar and Rigg, 2000; Rigg *et al.*, 2000; Rigg *et al.*, 2003). Also, intracellular Ca^{2+} is a signaling ion for second messenger pathways, which also stimulate certain pacemaker channels (Johnson *et al.*, 2002). The effect of aberrant inactivation of mutant *cac* channels would be exacerbated under the stress of increased temperature, as is clearly shown by the results of this study (Table 1; Fig. 7).

In addition to its direct action on pacemaker ion channels and second messenger pathways, increased intracellular calcium would stimulate ryanodine receptor channels in the sarcoplasmic reticulum (SR) to release intracellularly stored Ca^{2+} (Rigg and Terrar, 1996; Hüser *et al.*, 2000; Terrar and Rigg, 2000; Rigg *et al.*, 2000; Lipsius *et al.*, 2001). The resulting subsarcolemmal Ca^{2+} 'sparks' have been shown to influence heart rate in several vertebrate sinoatrial (SA) node cells (Rigg and Terrar, 1996; Terrar and Rigg, 2000; Lipsius *et al.*, 2001), and may similarly affect pacemaking in *Drosophila*. The putative action of Ca^{2+} sparks is to bring the pacemaker potential to threshold in the late phase of diastolic depolarization by stimulating an inward electrogenic Na^{+}-Ca^{2+} exchange current ($I_{Na\text{-}Ca}$) that depolarizes the membrane (Hüser *et al.*, 2000; Terrar and Rigg, 2000; Lipsius *et al.*, 2001). Membrane depolarization also acts as a positive feedback amplifier to further activate voltage-sensitive calcium channels (Lipsius *et al.*, 2001). It has been hypothesized by Lipsius *et al.* (2001) that disturbances altering content or release of SR Ca^{2+} impact pacemaking in the heart (Rigg and Terrar, 1996; Rigg *et al.*, 2000). Greater overall Ca^{2+} current entering through mutant Dmca1A channels would cause greater release of intracellular Ca^{2+} stores, and simultaneously provide an abundant source for greater future storage of these ions in the SR (Hüser *et al.*, 2000; Rigg *et al.*, 2000). The cumulative effect of these processes would be an elevated number of Ca^{2+} sparks increasing the rate of rise of the diastolic potential to drive the pacemaker into action potential more rapidly, thereby increasing heart rate (Hüser *et al.*, 2000; Rigg *et al.*, 2000). Overloading of the SR with Ca^{2+} would exacerbate this heartbeat effect by eliciting more spontaneous Ca^{2+} sparks that trigger abnormal pacemaker action potentials through Na^{+}/Ca^{2+} exchange (Lipsius *et al.*, 2001). However,

the mechanism of the additional hypothetical pacemaker effect described here depends on the presence of Ca^{2+} stores in the SR, and of Na^{+}-Ca^{2+} exchange pumps in membranes of *Drosophila* pacemaker cells, which to my knowledge have yet to be reported.

The increased overall inward Ca^{2+} current in *cac* mutants would also increase heartbeat strength (Johnson *et al.*, 1997), but perhaps not greatly, because all of the channel components of the oscillator are intact and contribute their required ionic currents in the normal order. This is in accordance with my results that heartbeat rhythmicities of *cac* mutants are higher than those of wild-type but only significantly so at a few temperatures. This contrasts with their prior classification as loss-of-function mutations (Littleton and Ganetzky, 2000); cac^{s} and cac^{ts2} alleles may be gain-of-function mutations of the *cac* gene, at least in terms of their contribution to pacemaking in the heart.

It is somewhat surprising that both *cac* alleles are dominant for heartbeat phenotypes because they are recessive for adult behavioral phenotypes for which this control has been reported. However, this is perhaps due to the nature of the two *cac* alleles studied here. Channel inactivation failure could explain dominance of the heartbeat phenotype because the possession of even a few calcium channels that allow more Ca^{2+} to enter cells would cause tachycardia according to our model of the *Drosophila* heart pacemaker.

Support for the theory that *cac* mutants have overactive calcium channels comes from many sources. One study by this lab raises the possibility that direct inhibition of calcium channels involved in pacemaking by a class of pertussis-sensitive G-proteins (Johnson *et al.*, 1997; Ashcroft, 2000) may be necessary to modulate heart rate,

preventing it from being constitutively elevated (Johnson *et al.*, 2002). To further rationalize how *cac* alleles with altered inactivation may impact pacemaking it is informative to draw a comparison to a study of the cardioacceleratory effect of cGMP on the heart (Johnson *et al.*, 2002). cGMP's effect on the heart is separate from the aforementioned inhibitory effect of a pertussis-sensitive G-protein class (Johnson *et al.*, 2002) because guanylyl cyclase receptors lack the topology of G-protein-coupled receptors, indicating that they are activated by direct interaction with primary messengers (hormones, neurotransmitters, etc) (Hille, 2001; Johnson *et al.*, 2002). cGMP may have multiple indirect and direct mechanisms for causing heartbeat acceleration (Johnson *et al.*, 2002). cGMP's indirect action is to release free Ca^{2+} from intracellular stores, putatively increasing its availability to the heart's contractile machinery (Ashcroft, 2000; Johnson *et al.*, 2002) and allowing it to interact with pacemaker components (Hüser *et al.*, 2000; Terrar and Rigg, 2000), and a calcium-calmodulin dependent protein kinase II (CaMKII) signaling pathway that also modulates putative pacemaker channels like calcium and potassium channels (Johnson *et al.*, 2002; Rigg *et al.*, 2003). Simultaneously, cGMP directly activates some of these putative pacemaker ion channels like *eag* potassium channels (Brüggeman *et al.*, 1993; Johnson *et al.*, 1998), and it may have the same stimulatory effect on *cac* calcium channels (Johnson *et al.*, 2002). If cGMP activates calcium channels the resulting increased intracellular Ca^{2+} would intensify the stimulatory effects on other susceptible pacemaker ion channels (ex. *slo*) and on the heart's contractile machinery (Johnson *et al.*, 2002). The phenotypic similarity of heartbeat in *cac* mutants to those injected with cGMP reinforces the

hypothesis that increased heart rate is due to elevated intracellular calcium, which in the former case is due to altered calcium channel inactivation.

The heartbeat phenotype of cac^{s} and cac^{ts2} mutations - tachycardia without the loss of rhythmicity - is much like the chronotropic effect of β-adrenergic neurotransmitters norepinephrine, dopamine, and serotonin on the heart (Fozzard and Arnsdorf, 1992; Johnson *et al.*, 1997; Rigg *et al.*, 2000; Johnson *et al.*, 2001; Papaefthimiou and Theophilidis, 2001). Ambient levels of these neurotransmitters are necessary for regulating normal heart rate in *Drosophila* pupae (Johnson *et al.*, 1997; Johnson *et al.*, 1991). Studies of the effects of injected neurotransmitters were performed at 25°C (Johnson *et al.*, 1997), and the resulting heart rate increases (~40%) are most similar to those seen at much higher temperatures (≥37°C) in *cac* mutants, compared to wild-type (Table1). This is especially obvious for cac^{s} mutants that have much more temperature-dependent heartbeat aberrances than cac^{ts2} mutants. The distinction of temperature dependence between the heartbeat effects of mutations in *cac* and neurotransmitter injections is probably due to elevated temperature being necessary to impose on these mutants a comparable stress to that of increasing the amount of neurotransmitter, even at low temperature.

The fast heartbeat and strong rhythmicity of *cac* mutants at high temperature and pupae injected with neurotransmitters are similar, perhaps because the underlying cause of increased heart rate may be comparable. In both situations overactivity of pacemaker calcium channels may cause elevated Ca^{2+} currents (Fozzard and Arnsdorf, 1992). β2-adrenergic neurotransmitters modulate vertebrate heartbeat by increasing the inward Ca^{2+} current through cAMP directed phosphorylation of L-type calcium channels (Dascal *et*

al., 1986) by protein kinase A (PKA) (Rigg *et al.*, 2000), which increases the probability of their opening (Nunoki *et al.*, 1989; Koch *et al.*, 1990; Johnson *et al.*, 1997; Ashcroft, 2000; Hille, 2001). In nematodes calcium channels regulate adaptation to the neurotransmitters dopamine and serotonin, also potentially via a second messenger pathway (Eberl *et al.*, 1998). The elevated Ca^{2+} current directly, and in conjunction with greater triggered Ca^{2+} sparks, increases the pacemaker oscillation rate by enhancing the slope of the diastolic depolarization (Rigg *et al.*, 2000; Lipsius *et al.*, 2001). In addition to this effect, increased Ca^{2+} current results in overloading of the SR with Ca^{2+} (Rigg *et al.*, 2000), which as mentioned earlier causes spontaneous action potential-triggering Ca^{2+} sparks (Lipsius *et al.*, 2001). Pharmacological evidence suggests that L-type calcium channels (Dmca1D) are not part of the *Drosophila* pacemaker (Johnson *et al.*, 1998) and, along with studies of *dunce* (*dnc*) and *rutabaga* (*rut*) mutants, strongly indicate that the cAMP pathway is not involved in heartbeat modulation (Dowse *et al.*, 1995; Johnson *et al.*, 1997; Johnson *et al.*, 2002). The pathway of neurotransmitter action in *Drosophila* is probably via direct interactions of cGMP (Johnson *et al.*, 2002) or G-proteins (Johnson *et al.*, 1997; Ashcroft, 2000) with *cac* calcium channels. The impact of stimulating *cac* channels may be comparable to the pacemaking and SR loading effects reported to increase heart rate as a result of vertebrate L-type channel modulation by neurotransmitters (Lipsius *et al.*, 2001). No matter the pathway of neurotransmitter action, the end result of increased Ca^{2+} currents causing tachycardia supports the hypothesis that *cac* mutants have overactive calcium channels.

It is likely that disrupted inactivation of voltage-gated calcium channels in *cac* mutants causes them to be open for an increased time period. However, it is possible that

channel inactivation abnormalities of mutant *cac* alleles have a somewhat opposite effect by allowing channels to inactivate but to never leave this state. The result of calcium channels remaining inactive would be different from the effect observed in *cac* mutants, however. Because Ca^{2+} influx is necessary to trigger diastolic depolarizations, and hence pacemaker action potentials, if the activity of calcium channels were destroyed pacemaking would be obliterated. The phenotype of such an aberration would be a heart that does not beat and thereby results in death, not the accelerated heartbeat of *cac* mutants. However, electrophysiological studies of *Xenopus* oocytes (Dascal *et al.*, 1986) injected with *cac* transcript will be highly informative in determining Dmca1A calcium channel characteristics and how they are altered in mutants (Brooks *et al.*, 2003).

Alternate Explanation for *cac* Mutants' Heartbeat Phenotypes

The preceding discussion of neurotransmitter action on the heart raises a troubling alternative explanation for *cac* mutants' heartbeat phenotypes that could rule out Dmca1A's involvement in pacemaking. Although the possibility of *cac* mutants altering heart activity via neural interaction was previously downplayed in this discussion, it cannot be completely disregarded. It seems possible that increased neurotransmitter release in cac^{s} and cac^{ts2} flies could cause tachycardia, especially after extensively explaining how heartbeat is modulated by these proteins, and that *cac* channels play a crucial role in neurotransmission. Under this scenario, altered inactivation in *cac* mutants would cause increased or perhaps even continuous neurotransmitter release at cardiac neuromuscular synapses, resulting in increased stimulation of the heart. It was reported as early as in 1964 that an insect's heart rate and amplitude are under nervous control

(Metcalf *et al.*, 1964). Therefore, perhaps eliminating nervous stimulation via TTX or mutations in *para* has little to no effect on the heart but increasing neural excitation increases heart rate. If this is so then neural modulation is not required for normal heart function, contradicting an earlier hypothesis by Johnson *et al.* (1997), but it may cause increased heart rate without affecting rhythmicity. However, *comt* mutants with damaged synaptic transmission have slightly decreased heart rates, so perhaps the heart can be subtly downregulated by a lack of neural stimulation. This alternate explanation for cac^{s} and cac^{ts2} mutants' heartbeat phenotypes would further require pacemaking in these mutants to be intact, which could explain why rhythmicity is barely impacted. The lack of significant changes in heartbeat rhythmicity in *cac* mutants also parallels the result in hearts stimulated by neurotransmitters, in which rhythmicity is only slightly decreased (Johnson *et al.*, 1997). Further rationale for excluding *cac* calcium channels from pacemaking comes from comparing the pacemakers of *Drosophila* and vertebrates. Vertebrate sinoatrial cells employ T-type calcium channels to trigger the pacemaker potential (Fozzard and Arnsdorf, 1992; Irisawa *et al.*, 1993; Hüser *et al.*, 2000; Terrar and Rigg, 2000), and the putative existence of this channel type in *Drosophila* (Littleton and Ganetzky, 2000) raises the possibility of its presence and parallel function in pacemaker cells in this organism. The role of L-type calcium channels in excitation-contraction coupling in the hearts of both vertebrates (Nunoki *et al.*, 1989; Fozzard and Arnsdorf, 1992; Irisawa *et al.*, 1993) and *Drosophila* (Johnson *et al.*, 1997; Littleton and Ganetzky, 2000) sets a precedent for calcium channels having comparable functions in these organisms. However, a study by Johnson *et al.* (1998) makes the possibility of a T-type channel being involved in pacemaking remote because amiloride had no effect on the

heart. Despite this ambiguity as to the mechanism by which mutations in *cac* affect the heart, the rest of the discussion will be centered on Dmca1A's potential pacemaker effects because it is a more parsimonious explanation.

Differences in Calcium Channel Defects of *cac* Mutants

Despite that average heartbeat frequencies of *cac* mutants over all temperatures are similar, when analyzed at individual temperatures heartbeat frequency of cac^{s} mutants deviates from that of cac^{ts2}. Instead of increasing steadily with temperature as does the heart rate of cac^{ts2} flies, that of cac^{s} flies shows a drastic increase at 35°C, at which point it deviates from wild-type and aligns with cac^{ts2} flies. Based on this, it appears that calcium-dependence is a more crucial contributor to inactivation than voltage-dependence, or alternatively, that cac^{s} mutants retain a greater degree of channel inactivation function than do cac^{ts2} mutants. Determining the relative contribution of voltage-dependence and calcium-dependence to inactivation would require electrophysiological studies of Dmca1A channels manipulated to utterly obliterate either function while still maintaining all other channel activities. In all probability channel inactivation mechanisms are additive, if not somewhat redundant, although the underlying processes are mostly independent (de Leon *et al.*, 1995). It would be surprising if calcium-dependence sufficiently outweighed voltage-dependence in its contribution to inactivation to produce the results seen here.

The kinetics of the two types of inactivation differ. Studies of an L-type vertebrate channel show that voltage-dependent inactivation renders channels incapable of opening, whereas Ca^{2+}-mediated inactivation shifts the channel gating pattern from a

mode with rapidly activating, high frequency opening (mode 1) to a state with slowly activating, infrequent opening (mode Ca^{2+}) (de Leon *et al.*, 1995). Also, vertebrate studies indicate that non-L-type calcium channels exhibit primarily voltage-dependent inactivation (Ashcroft, 2000; DeMaria *et al.*, 2001). I would thus expect to see greater inactivating defects in cac^{s} mutants, which is opposite to our findings. This suggests that an alternative explanation for differences in cac^{s} and cac^{ts2} mutant phenotypes is necessary.

A more likely explanation for differences in heartbeat phenotypes of *cac* mutants is that channel inactivation in cac^{s} flies remains more functionally intact than in cac^{ts2} flies simply by chance. This hypothesis is based on cac^{s} flies having normal heart rates under natural conditions, only revealing the mutation's impact on heartbeat under increased temperatures that impose greater stress on the oscillatory system. In contrast, calcium-dependent inactivation in cac^{ts2} flies is altered even at low temperatures. This suggests that inactivation is more severely impacted by the C-terminal mutation of cac^{ts2} flies than the cac^{s} mutation in transmembrane domain IIIS6. Perhaps because all four S6 domains contribute to fast voltage-dependent inactivation, and only one of these is altered in cac^{s} flies, the inactivation mechanism is not as severely damaged as it is by the cac^{ts2} mutation in the sole region responsible for calcium-dependent inactivation. Also, it appears that the IS6 segment may be the most crucial determinant of voltage-dependent inactivation, and this segment is not affected by the cac^{s} mutation (Ashcroft, 2000). Furthermore, because voltage-dependent inactivation more completely inhibits Ca^{2+} current, any residual inactivation function in cac^{s} mutants would more effectively

inactivate channels than would residual Ca^{2+}-mediated inactivation function in cac^{ts2} mutants.

That inactivation is damaged more severely in cac^{ts2} mutants is supported by other behavioral studies of *cac* mutants. Reports on motor and synaptic defects show that cac^{s} calcium channels retain greater wild-type function than those of cac^{ts2} mutants. Specifically, cac^{s} mutants show motor defects at greater temperatures (46°C) than cac^{ts2} mutants (38°C) (Peixoto and Hall, 1998; Dellinger *et al.*, 2000; Chan *et al.*, 2002), and they show only activity-dependent synaptic defects whereas cac^{ts2} mutants' transmission reduction is temperature sensitive (Kawasaki *et al.*, 2000; Kawasaki *et al.*, 2002).

The striking similarity of cac^{s}/cac^{ts2} heteroallelic flies' heartbeat to that of cac^{s} homozygotes, demonstrating that cac^{s} is dominant over cac^{ts2} for heartbeat frequency, further supports the hypothesis that the cac^{ts2} mutation is more detrimental than its counterpart, cac^{s}, in altering inactivation. This result is reminiscent of a study of the synaptic interactions between these alleles where cac^{ts2} reportedly complemented the cac^{s} activity-dependent synaptic reduction at 20°C but not at high temperatures, under which conditions the cac^{s} phenotype dominated (Kawasaki *et al.*, 2000). In Kawasaki *et al.*'s (2000) study, the cac^{ts2} synaptic aberrance became evident when homozygous in a temperature-sensitive manner, and was not evident at the low temperatures at which it complemented cac^{s}. Therefore, at temperatures where both mutations had phenotypic effects ($\geq$36°C), cac^{s} dominated, and only at temperatures where cac^{ts2} behaved like wild-type (~20°C) was it able to complement the other allele. In the present study the cac^{s} phenotype dominates at all temperatures because at no temperature does cac^{ts2} behave like wild-type.

Ion Channels of the *Drosophila* Cardiac Pacemaker

Past research enabled the formulation of a putative *Drosophila* cardiac pacemaker model. However, revision of this model based on current ion channel information and the vertebrate pacemaker model is necessary (Guyton and Hall, 1996; Ashcroft, 2000; Hille, 2001). The former model implicated three ion channels specific to potassium and one other that allows a calcium current (Johnson *et al.*, 1998). The current *Drosophila* cardiac pacemaker model involves the actions of all of these channels but in different capacities than those previously described, plus an additional ion channel that may not be distinguishable (Johnson *et al.*, 1997; Johnson *et al.*, 1998).

A cyclic nucleotide-gated (CNG) hyperpolarization-dependent (I_h – otherwise known as I_f) cation channel (HCN) non-specific for monovalent cations opens to begin depolarizing the cell (Ashcroft, 2000; Littleton and Ganetzky, 2000; Hille, 2001; Rigg *et al.*, 2003). There is only one channel of this type in *Drosophila*, and the current it generates is difficult to identify because it passes both Na^+ (primarily) and K^+ (Irisawa *et al.*, 1993), and its blockage by Cs^+ may be vertebrate specific (Hille, 2001; Lipsius *et al.*, 2001). Its putative presence in *Drosophila* pacemaker cells is based on homologous vertebrate channels' contribution to pacemaker potentials of vertebrate sinoatrial nodal cells (Fozzard and Arnsdorf, 1992; Irisawa *et al.*, 1993; Ashcroft, 2000; Hüser *et al.*, 2000; Lipsius *et al.*, 2001; Hille, 2001). Opening of I_h channels causes a slight rise in membrane potential that results in opening of a fast, transient, voltage-gated potassium channel ($I_{K(A)}$) encoded by *Shaker* (*Sh*) (Kaplan and Trout, 1968; Timpe *et al.*, 1998). The efflux of potassium begins repolarizing the membrane, thereby delaying the action potential. The opposing interaction between I_h and $I_{K(A)}$ currents, along with the time-

dependent decay of the delayed rectifier K^+ current (*eag*, see below), and potentially subsarcolemmal Ca^{2+} sparks (Hüser *et al.*, 2000; Terrar and Rigg, 2000) and the depolarizing currents ($I_{Na\text{-}Ca}$) they trigger provide the characteristic rhythmicity and slow diastolic depolarization of pacemaker action potentials (McCann, 1969; Fozzard and Arnsdorf, 1992; Irisawa *et al.*, 1993; Hüser *et al.*, 2000; Terrar and Rigg, 2000; Lipsius *et al.*, 2001; Hille, 2001). The existence of a low background K^+ leak current is made possible by extrapolation from vertebrate models, and if so it would help bring the diastolic depolarization to threshold (Hüser *et al.*, 2000; Lipsius *et al.*, 2001).

Eventually the membrane depolarizes enough that $I_{K(A)}$ channels close. Because I_h channels do not inactivate the membrane continues to depolarize until a voltage-gated calcium channel (I_{Ca}) (Fozzard and Arnsdorf, 1992; Irisawa *et al.*, 1993; Hüser *et al.*, 2000; Terrar and Rigg, 2000), the α_1 subunit of which is encoded by *cacophony* (*cac*) (von Schilcher, 1976; Smith *et al.*, 1996; Smith *et al.*, 1998), opens to allow Ca^{2+} to enter the cell, thereby triggering the cardiac action potential (Fozzard and Arnsdorf, 1992; Irisawa *et al.*, 1993). Further studies are required to determine if the voltage-gated calcium channel encoded by *cac* is the sole calcium channel necessary to pass the Ca^{2+} current. The large depolarization created by the Ca^{2+} current (Fozzard and Arnsdorf, 1992; Irisawa *et al.*, 1993) causes I_h channels to close (Ashcroft, 2000). A delayed-rectifier potassium channel (I_K), an α subunit of which is encoded by *ether à go-go* (*eag*) (Brüggeman *et al.*, 1993), is activated in response to the membrane depolarizing further (Elkins *et al.*, 1986; Fozzard and Arnsdorf, 1992). Simultaneously, the influx of Ca^{2+} from *cac* channels (Brüggeman *et al.*, 1993) activates a calcium-activated potassium channel ($I_{K(Ca)}$) (Fozzard and Arnsdorf, 1992; Markou and Theophilidis, 2000) partially

encoded by *slowpoke* (*slo*) (Elkins *et al.*, 1986; Atkinson *et al.*, 1991). Support for *slo*'s involvement in heart pacemaking comes from a study showing that mutants have almost no heartbeat (Johnson *et al.*, 1998), and from a genetic study whereby it is implicated in a repolarizing capacity for production of courtship song (Peixoto and Hall, 1998). The efflux of potassium, along with the actions of ion exchange pumps, repolarize the membrane so that the process can recommence (Thompson, 1977; Elkins *et al.*, 1986; Fozzard and Arnsdorf, 1992; Irisawa *et al.*, 1993; Littleton and Ganetzky, 2000; Lipsius *et al.*, 2001). As mentioned, slow inactivation of *eag* channels causes a prolonged decay in outward K^+ current that will contribute to rate modulation of pacemaker depolarizations (Fozzard and Arnsdorf, 1992; Irisawa *et al.*, 1993).

A mathematical pacemaker model by S. Crook and H. Dowse (unpublished) implicating a hyperpolarization-dependent cation channel, a voltage-gated calcium channel, and a calcium-activated potassium channel in producing cardiac oscillations supports the model presented here. Although revisions of the hypothetical pacemaker model are useful for further investigations, more work is required to isolate the pacemaker from the rest of the heart so that its characterization is clearer. This work would involve molecularly isolating ion channel genes, and potentially their specific splice variants, that are expressed in the heart. Co-expressing these channels in *Xenopus* oocytes (Dascal *et al.*, 1986) could potentially reproduce the heart's oscillator, thereby clarifying the current ambiguity surrounding this system.

Chapter 2

EFFECT ON HEARTBEAT OF *Drosophila melanogaster* OF AN INTERACTION BETWEEN THE RNA HELICASE MUTANT *maleless*^{napts} AND THE VOLTAGE-GATED CALCIUM CHANNEL MUTANT *cacophony*

INTRODUCTION

The *maleless*^{napts} Mutant

No action potential$^{temperature\text{-}sensitive}$ (*nap*^{ts}) (Wu *et al.*, 1978) alleles are gain-of-function mutations of the X chromosome gene *maleless* (*mle*) (Kernan *et al.*, 1991), which codes for an ATP-dependent double-stranded RNA (dsRNA) helicase protein (Reenan *et al.*, 2000). *mle* is one of four autosomal genes required for dosage compensation in *Drosophila* so that mutations in this gene that destroy its role in upregulation of X chromosome transcription are male-specific recessive lethals (Kernan *et al.*, 1991; Reenan *et al.*, 2000). MLE also contributes to development of the male germline (Kernan *et al.*, 1991).

After ethyl mutagenesis (EMS), *mle*^{napts} (2-56.2, 42A2-7) was isolated as a rapid temperature-sensitive ($\geq$33°C), reversibly paralytic mutant (Wu *et al.*, 1978; Ganetzky, 1984; Kernan *et al.*, 1991). The mutant's paralytic phenotype is caused by disrupted nerve conduction in larval and adult flies (Wu *et al.*, 1978; Ganetzky, 1984). The cause of *mle*^{napts} flies' neural defect was originally suggested by an approximately 40% reduction in binding of ^{3}H-saxitoxin, which is a ligand specifically antagonistic to sodium

channels (Jackson *et al.*, 1984; Amichot *et al.*, 1993). Since then, it was confirmed that mutants suffer from a greater than 80% reduction in the number of sodium channels (Jackson *et al.*, 1984; Kernan *et al.*, 1991; Amichot *et al.*, 1993), which are crucial to organisms' movements because they participate in action potentials in fast-response excitable tissue (Wu *et al.*, 1978; Fozzard and Arnsdorf, 1992; Rubin *et al.*, 2000; Hille, 2001). Action potentials in mle^{napts} flies are normal at permissive temperatures but membrane excitability is diminished because of the reduced number of sodium channels (Ganetzky, 1984). Because the fraction of sodium channels required to propagate action potentials increases with rising temperature, a reduction in channel number causes paralysis when the recruitment threshold is exceeded (Loughney *et al.*, 1989). Mutants' recovery from paralysis is nearly instantaneous when the temperature drops below the restrictive temperature (Wu *et al.*, 1978; Ganetzky, 1984; Dowse *et al.*, 1995).

Mutations in *mle* that result in the mle^{napts} paralytic phenotype affect a non-sex-specific regulatory role of the MLE protein (Kernan *et al.*, 1991; Reenan *et al.*, 2000). Evidence for this conclusion comes from studies showing that mle^{napts} does not affect dosage compensation of male X-linked genes, including *para* (Kernan *et al.*, 1991). In addition, MLE is found in female cell nuclei as well as in males, although the protein is not primarily associated with the X chromosome in the former, as it is in the latter (Reenan *et al.*, 2000).

The causative mutation of the mle^{napts} phenotype is somewhat unresolved. All mle^{napts} mutant alleles that exhibit temperature-sensitive paralysis have a C to G transversion at base pair (bp) 1664 that results in a threonine (T) to serine (S) missense substitution at amino acid 415 (Kernan *et al.*, 1991). A second polymorphism 90 bp

upstream of the first mutation is present within introns of all *mle*^{napts} alleles (Kernan *et al.*, 1991). This polymorphism is due to an insertion: in the mutants, 6 bp replace the single bp of the wild-type sequence (Kernan *et al.*, 1991). The insert is not solely responsible for the *mle*^{napts} phenotype because a probe containing the alteration from cloned DNA retaining wild-type MLE function (Kernan *et al.*, 1991). Because both alterations are consistent in all studied *mle*^{napts} alleles it seems that they did not arise independently; however, this suggestion contradicts their origins in separate mutagenesis experiments (Kernan *et al.*, 1991).

Interaction between *mle*^{napts} and *para*

The marked similarity between the distinctive and quantifiable behavioral defects caused by *mle*^{napts} and X-linked sodium channel gene *paralytic* (*para*^{ts}) mutants (Suzuki *et al.*, 1971; Loughney *et al.*, 1989) suggested a functional relationship between the two (Wu *et al.*, 1978; Jackson *et al.*, 1984; Ganetzky, 1984; Reenan *et al.*, 2000). Mutations in both *mle*^{napts} and *para* genes affect sodium channels, with the *para* gene encoding the primary sodium channel transcript expressed in the *Drosophila* nervous system (Loughney *et al.*, 1989; Reenan *et al.*, 2000).

Initial support for the hypothesis of an interaction between *mle*^{napts} and *para* genes came from studies of hypomorphic mutant *para* alleles in a homozygous *mle*^{napts} background that result in unconditional and partially dominant lethality (Wu *et al.*, 1978; Ganetzky, 1984; Kernan *et al.*, 1991). Lethality is complete when mutant *para*^{ts} alleles are homozygous and increased by about 60% when *para*^{ts} mutations are heterozygous (Ganetzky, 1984). Also, homozygous lethal null mutant *para* alleles become

heterozygous lethals when crossed into an *mle*^{napts} background (Ganetzky, 1984; Kernan *et al.*, 1991). In Ganetzky's (1984) study it was primarily thought that *para* and *mle*^{napts} encode different sodium channel subunits, or alternatively that their gene products directly interact as enzyme and substrate during posttranslational modification of sodium channels (Jackson *et al.*, 1984). These mechanistic theories were founded on the genes' allele-specific interactions (Ganetzky, 1984). Others thought that because the *mle*^{napts} mutation did not appear to affect the structural integrity of sodium channels that it was indirectly reducing their expression (Jackson *et al.*, 1984), perhaps by uncoupling an activity affecting transcription (Kernan *et al.*, 1991). An additional possibility was that in *mle*^{napts} mutants the polypeptide encoded by this gene lost its role of directly boosting expression of *para*, and perhaps other genes, at the transcription or splicing level in both sexes (Kernan *et al.*, 1991). Although the mechanism by which *mle*^{napts} and *para*^{ts} interact was unknown at that time, the basis for models was the fact that in both mutants paralysis at restrictive temperatures (29°C – 37°C) (Suzuki *et al.*, 1971; Wu *et al.*, 1978) results from a reduction in the number or activity of sodium channels that is exacerbated when they are co-expressed (Jackson *et al.*, 1984; Kernan *et al.*, 1991; Amichot *et al.*, 1993). This theory was supported by immunocytochemical evidence that the amount of *para* sodium channels is reduced in *mle*^{napts} flies (Amichot *et al.*, 1993). Since then it has been shown that the *mle*^{napts}-encoded protein directly interacts with *para* transcripts by causing a "splicing catastrophe" that results in a reduced number of viable sodium channels (Jackson *et al.*, 1984; Loughney *et al.*, 1989; Reenan *et al.*, 2000). The effect of this interaction to is that originally attributed to isolated *mle*^{napts} and *para*^{ts} mutants; namely, a failure to produce action potentials in neurons homozygous for either *mle*^{napts}

or *para*^{ts} at elevated temperatures that becomes complete and unrestricted by temperature, resulting in death, when the mutations are combined (Ganetzky, 1984; Jackson *et al.*, 1984).

The mechanism by which the splicing problem occurs involves the helicase activity of MLE. *para* transcripts contain an evolutionarily conserved 12 nucleotide (nt) exonic region of six specific A-to-I RNA editing sites that have potential coding diversity consequences because 70% of para cDNAs show some extent of editing (Reenan *et al.*, 2000, Hanrahan *et al.*, 2000). Editing at three of these sites occurs at high frequency, two of which result in amino acid changes in the predicted protein product (Reenan *et al.*, 2000). Eleven para cDNAs produced by alternative editing generate four potential sodium channel isoforms (Reenan *et al.*, 2000).

For a site to be edited properly, an extensive dsRNA secondary structure must form around it. Via secondary structures (ex. hairpins, loops, bulges) of the intervening RNA region, the editing site is aligned with a conserved exonic complementary sequence (ECS) of the intron immediately downstream (Reenan *et al.*, 2000) so that a stable, base-paired, duplex RNA region can form between them (Hanrahan *et al.*, 2000; Palladino *et al.*, 2000). The dsRNA structure provides a target for the editing enzyme (dADAR) (Reenan *et al.*, 2000; Palladino *et al.*, 2000). After editing occurs the dsRNA structure must be unwound for splicing of the transcript to occur (Reenan *et al.*, 2000). It is during this step of the posttranscriptional process that MLE becomes crucial, as it is the primary helicase responsible for resolution of the dsRNA structure (Reenan *et al.*, 2000). Because this activity is mutated in *mle*^{napts} flies, the structure is not disassembled and aberrant splicing results. The MLE protein appears to be able to bind via its two amino-terminal

dsRNA binding motif (DSRBM) repeats but fails to disassemble the structure (Reenan *et al.*, 2000). This prevents the splicing machinery and other redundant RNA helicases from binding to resolve the dsRNA structure so that the *mle*^{napts} mutation has a more severe outcome than do null mutations (Reenan *et al.*, 2000). Specifically, the outcome of the *mle*^{napts} mutation is that exons are skipped in the splicing process because inappropriate splice donor sites upstream of the unresolved dsRNA structure are used (Reenan *et al.*, 2000). The end result is that more than 80% of *para* transcripts in an *mle*^{napts} background contain internal deletions (Reenan *et al.*, 2000).

Interaction between *cac* and *mle*^{napts}

The aberrant splicing consequence of the *mle*^{napts} mutation is a compelling subject for further study because defects affecting pre-mRNA splicing result in about 15% of genetic diseases (Horowitz and Krainer, 1994). Therefore, further exploration of genes with which this mutant interacts, such as the candidate *cac*, will provide critical information about these ailments.

mle^{napts} mutants recessively exhibit decreased heartbeat frequencies and rhythmicities compared to wild-type flies, and fail to respond to temperature increases with concomitant heart rate accelerations (Dowse *et al.*, 1995). In addition, electrocardiograms (EKGs) of *mle*^{napts} hearts have small, frequent, but irregular voltage spikes that do not succeed in eliciting a general depolarization (Johnson *et al.*, 2001). *mle*^{napts} mutants also do not respond to injections of the neurotransmitters norepinephrine and serotonin with increased heart rates, as do wild-type flies (Johnson *et al.*, 1997; Johnson *et al.*, 2001).

The cause of these heartbeat abnormalities in *mle*^{napts} flies has yet to be determined and preliminary studies suggest an epistatic effect of *mle*^{napts} on *cac* (Johnson, personal communication; Peixoto and Hall, 1998). Because the *cac* sequence, like *para*, undergoes RNA editing and contains many introns, it would similarly be sensitive to a reduction in splicing accuracy or efficiency (Loughney *et al.*, 1989; Kernan *et al.*, 1991).

The first hint of an interaction between *mle*^{napts} and *cac* came from work with a dynamin-encoding *shibire* (*shi*) mutant, *shi*^{ts} (Johnson *et al.*, 2001). Conclusions taken from this study rely on the theory, discussed in Chapter 1, that β2-adrenergic neurotransmitters may be necessary in ambient levels for normal heartbeat (Johnson *et al.*, 1997; Johnson *et al.*, 2001). *shi*^{ts} causes neurotransmitter insensitivity, probably owing to a failure to endocytose receptors for these messengers, thereby causing the bradycardia and arrhythmia heartbeat phenotypes of mutants (Johnson *et al.*, 2001). In *shi*^{ts} mutants, the inability of receptors to undergo downregulation after agonistic desensitization may result in chronic overstimulation of the heart that results in slowed and arrhythmic heartbeat (Johnson *et al.*, 2001; Hille, 2001). *shi*^{ts} ; *mle*^{napts} double mutants have a normal heartbeat, perhaps because of a physiological interaction between the two that also involves *cac* transcripts (Johnson *et al.*, 2001). Potentially, *mle*^{napts} interacts with *cac* transcripts in a similar manner to those of *para*, causing a splicing catastrophe that results in a reduction of Ca^{2+} channels (Johnson *et al.*, 2001). As previously explained, *cac* calcium channels contribute to fast coupling of neurotransmitter vesicles for synaptic release (Kawasaki *et al.*, 2000; Dellinger *et al.*, 2000; Kawasaki *et al.*, 2002). Therefore, a reduction in *cac* channels would cause understimulation of the heart, resulting in bradychardia. Because *shi*^{ts} mutations cause

heart neurotransmitter overstimulation, and *mle*^{napts} mutations cause inherent insensitivity due to a putative reduction in Ca^{2+} channels, the resulting interaction in double mutants is normal heartbeat (Johnson *et al.*, 2001).

Support from outside laboratories for the hypothetical interaction between *mle*^{napts} and *cac* comes from a study by Peixoto and Hall where *mle*^{napts} was shown to be epistatic for a *cac* mutant's (*cac*^{s}) defective song phenotype (1998). *cac*^{s} flies in a homozygous *mle*^{napts} background have enhanced song interpulse interval (IPI) defects but suppressed cycles-per-pulse (CPP) and song amplitude aberrances, even though homozygous *mle*^{napts} mutants' song parameters are all wild-type except for increased IPIs (Peixoto and Hall, 1998). Therefore, not only is *mle*^{napts} a courtship song mutant in its own right, but the song parameters of *cac*^{s} ; *mle*^{napts} double mutants are not like either single mutant, which suggests that the two genes interact (Peixoto and Hall, 1998). However, it is possible that *mle*^{napts} and *cac*^{s} have additive effects for IPI and that *mle*^{napts} rescues aberrances in CPP and amplitude of *cac*^{s} mutants.

It has already been established that *mle*^{napts} interacts with other ion channel genes that are implicated in coding for components of the heart pacemaker. *mle*^{napts} suppresses certain behavioral and neuromuscular phenotypes like abnormal flight muscle activity at rest and wings-down posture of potassium channel mutants with hyperexcitable membranes (Ganetzky, 1984), mutants such as *Shaker* (*Sh*) and *ether à-go-go* (*eag*) (Kernan *et al.*, 1991), which are both implicated in the heart pacemaker (Engel and Wu, 1992; Johnson *et al.*, 1998; Johnson *et al.*, 2001). Although *mle*^{napts} does not counteract basic process aberrances produced by *Sh* and *eag*, it does counteract novel phenotypes produced by *Sh eag* double mutants (Engel and Wu, 1992).

Johnson *et al.* (1998) reported that *cac* mutants have slightly lower heart rate and rhythmicity than wild-type (E. Johnson, unpublished data). Mutations in mle^{napts} mirror this effect but in a more pronounced manner (Dowse *et al.*, 1995). If the heartbeat phenotypes of *cac* and mle^{napts} mutants are qualitatively the same, then potentially mle^{napts} could be interacting with *cac* transcripts in a manner similar to *para* transcripts (Reenan *et al.*, 2000; Peixoto and Hall, 1998). Johnson *et al.* (1998) originated this hypothesis of a splicing interaction between mle^{napts} mutants and *cac* transcripts affecting the pacemaker directly. However, the findings on *cac* reported in chapter 1 contradict earlier reports on the heartbeat effects of *cac* mutants; still, the possibility remains that mle^{napts} interacts with *cac*. This study was designed to examine interactions between *cac* and mle^{napts}. By creating strains double mutant for *cac* and mle^{napts}, I hope to exacerbate the phenotypic effects of these mutations to determine whether they interact.

MATERIALS AND METHODS

Fly Culture, Experimental and Control Strains

Flies were cultured in the same conditions as *cac* strains (Materials and Methods, Chapter 1). Two separate unmarked, homozygous mutant strains of *cacophony* [*cac*], cac^{s} and cac^{ts2}, were used for control heartbeat recordings, as well as to produce homozygous *cac ; * mle^{napts} double mutants. The *no action potential* [mle^{napts}] allele of the *maleless* [*mle*] gene marked with *cinnabar* [*cn*] was used for heartbeat recordings, and generation of double mutants. A lz^{3}/C(1)DX, $y^{1}f^{1}$ stock (here 'attached X'), obtained

from the Bloomington Stock Center (Indiana University, Bloomington, IN), along with a stock (FM7a//FM7a ; *Cyo//Pin*) homozygous for FM7a, a first chromosome multiple balancer (y^{31d} sc^{8} w^{a} v^{Of} B^{1}), and heterozygous for *Curly Oster* (*Cyo*), a second chromosome balancer, and a chromosome marked with pin-like truncated bristles (*Pin*) were used in double mutant mating schemes. The same Canton-S heartbeat recordings used as wild-type in Chapter 1 for comparative purposes with both *cac* alleles were again used as controls for double mutant recordings.

Double Mutant Mating Schemes

Double mutants were produced according to two different mating schemes that are explained and diagrammed below. To determine whether *cac* ; mle^{napts} double mutants were eclosing in the expected segregation and sex ratios, progeny were evaluated by chi-square (X^2) analysis for goodness of fit and by Replicated Goodness-of-Fit tests (G_{pooled} (G_p), which gave essentially the same results (Sokal and Rohlf, 1995).

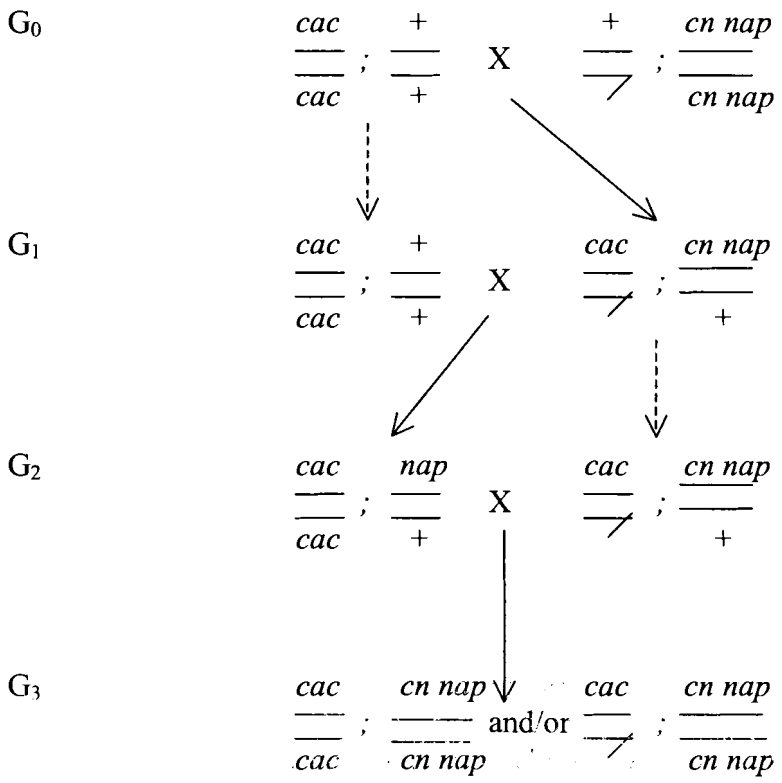

Heartbeat was recorded from *cac ; mle*^{napts} double mutants of both *cac* alleles soon after they were generated. Unfortunately, neither mating scheme yielded double mutant (*cac* ; *mle*^{napts}) progeny from which heartbeat recordings could be performed on both *cac* alleles. The reason for this was that the *cac*^{ts2} ; *mle*^{napts} stock produced according to the first mating scheme was contaminated before heartbeat recordings were performed and the *cac*^{s} ; *mle*^{ts} stock produced according to the second mating scheme died before recordings could be performed. Heartbeat was recorded from *cac*^{s} ; *mle*^{napts} double mutants produced according to the first mating scheme that employed an unmarked *cac*^{s} strain. In G_0, homozygous *cac*^{s} females (*cac*^{s}//*cac*^{s} ; +//+) were mated to homozygous *mle*^{napts} males (+//+ ; *mle*^{napts}//*mle*^{napts}). In G_1, male progeny (*cac*^{s} hemizygous, *mle*^{napts} heterozygous males – *cac*^{s}/Y ; *mle*^{napts}//+) were backcrossed to *cac*^{s} homozygous females from G_0. In G_2 the same males (*cac*^{s}/Y ; *mle*^{napts}//+) from G_1 were

mated to the female progeny of G_1, which were cac^s homozygous and either heterozygous for mle^{napts} ($cac^s//cac^s$; $mle^{napts}//+$) or homozygous wild-type ($cac^s//cac^s$; +//+). It was not possible to distinguish the two female progeny genotypes by their phenotypes so twenty pair matings were performed with the expectation that ten of these would be involve desired mle^{napts} heterozygous females ($cac^s//cac^s$; $mle^{napts}//+$). In G_3, 1/8 (12.5%) were expected to be cac^s ; mle^{napts} double mutants. At eclosion double mutants were scored for sex and phenotypic markers, and tested for the pass-out phenotype. Although parallel matings were performed using the cac^{ts2} strain from this lab to produce cac^{ts2} ; mle^{napts} double mutants, the resulting stock was contaminated before heartbeat recordings were performed, as priorly mentioned.

A second mating scheme was used to produce cac^{ts2} ; mle^{napts} double mutants for heartbeat recordings using cac^{ts2}, kindly donated by Dr. J.C. Hall.

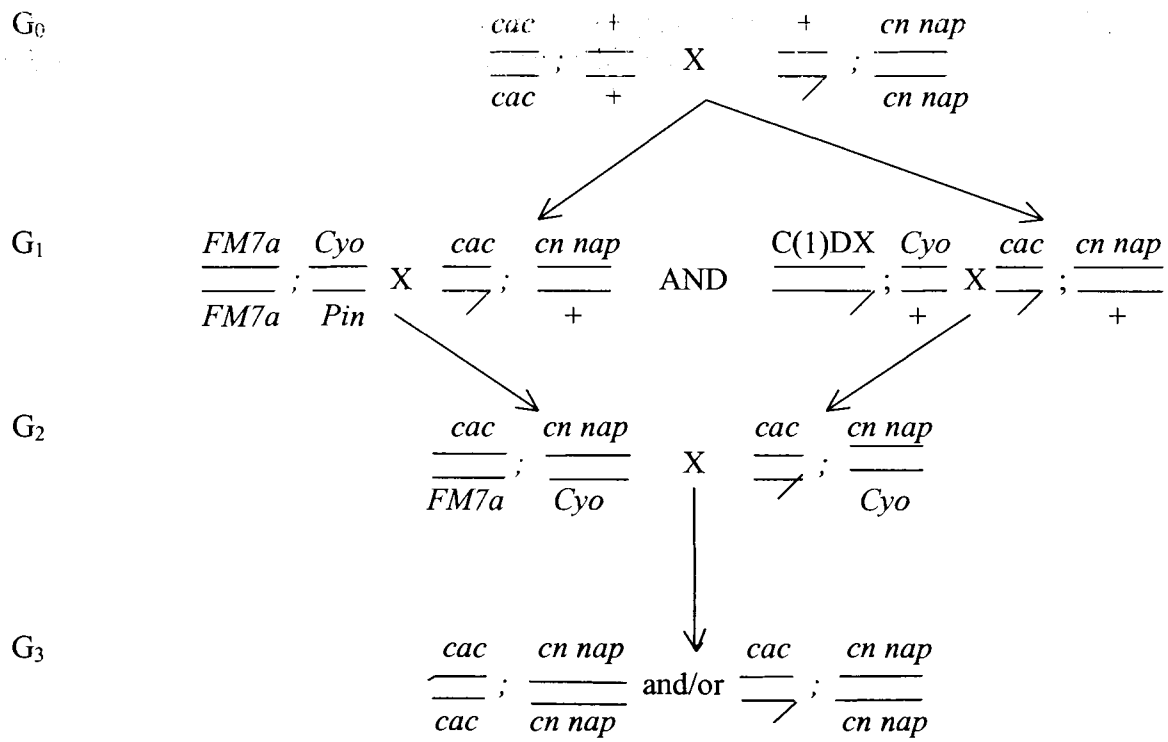

G_0 of this mating scheme was like that of the first scheme in that *cac*^{ts2} homozygous females (*cac*^{ts2}//*cac*^{ts2} ; +//+) and *mle*^{napts} homozygous males (+//+ ; *mle*^{napts}//*mle*^{napts}) were mated. In G_1 two separate crosses were performed to produce the parental flies for G_2. One mating involved attached X, heterozygous *Cyo* females (lz^3/C(1)DX, y^1f^1 ; *Cyo*//+) that were mated to homozygous *cac*^{ts2}, heterozygous *mle*^{napts} males (*cac*^{ts2}/Y; *mle*^{napts}//+) from G_0. The other cross involved the same males (*cac*^{ts2}/Y ; *mle*^{napts}//+) from G_0 mated to FM7a homozygous, *Cyo* and *Pin* heterozygous (FM7a//FM7a ; *Cyo*//*Pin*) females. In G_2, ten hemizygous *cac*^{ts2}, heterozygous *mle*^{napts} and *Cyo* males (*cac*^{ts2}/Y ; *mle*^{napts}//*Cyo*) from the first G_1 cross were mated in a pair-wise fashion to heterozygous *cac*^{ts2} and FM7a, heterozygous *mle*^{napts} and *Cyo* females (*cac*^{ts2}//FM7a ; *mle*^{napts}//*Cyo*) from the second G_1 mating. As in the first double mutant mating scheme, progeny from these matings (G_2) were scored for sex and phenotypic markers upon eclosure. In contrast to the first scheme, all G_2 matings produced *cac*^{ts2} ; *mle*^{napts} double mutants (1/4 = 25%).

cac^{s} ; *mle*^{napts} double mutants were also produced according to the second mating scheme using the *cac*^{s} strain from Dr. J.C. Hall's lab but they died before heartbeat recordings could be performed.

Heartbeat Recordings, Temperature Step Protocols, and Data Analysis

Heartbeat was recorded from translucent "white", P1 pupae (Ashburner, 1989) and data were analyzed using the same methods as were used for wild-type and *cac* strains (Materials and Methods, Chapter 1). As mentioned, additional statistical analyses were performed on *cac* ; *mle*^{napts} double mutants to determine whether they were eclosing

in the expected segregation and sex ratios, based on emergence scores for sex and genotype of G_2 progeny. Data for both alleles of both double mutant mating schemes were evaluated by chi square analysis.

RESULTS

Statistical Analyses of *cac ; mle^{napts}* Double Mutants

There was a slight deficiency of *cac^{s}* ; *mle^{napts}* double mutant progeny produced by the first double mutant mating scheme, indicated by an unexpected segregation ratio (130 expected, 108 observed, $X^2_{total} = 4.96 > X^2_{crit} = 3.84$). Sex ratios were as expected for this double mutant, indicating that approximately the expected numbers of males and females were produced. Like *cac^{s}* ; *mle^{napts}* double mutants, there was a deficieny of *cac^{ts2}*; *mle^{napts}* double mutants produced by this scheme (198 expected, 164 observed, $X^2_{total} = 7.79 > X^2_{crit} = 3.84$). Unlike the *cac^{s}* ; *mle^{napts}* double mutants, however, male *cac^{ts2}* ; *mle^{napts}* double mutants did not eclose as frequently as females (355 males, 437 females, $X^2_{total} = 8.49 > X^2_{crit} = 3.30$).

In contrast to these results, the segregation and sex ratios for double mutants produced by to the second scheme were as expected. The only exception to this trend concerned the sex ratio of *cac^{ts2}* ; *mle^{napts}* double mutant produced according to the second scheme, which showed a deficiency of males (116 males, 192 females, $X^2_{total} = 18.8 > X^2_{crit} = 3.84$), similar to the deficiency of males of this genotype observed according to the first mating scheme. Due to the contradictory nature of the X^2 test

results and the experimental weakness introduced by utilizing two different double mutant mating schemes, it is difficult to draw conclusions from these results.

General Observations of *cac* Mutants in a *mle*^{napts} Background

Both double mutants produced from the first mating scheme developed into healthy stocks. For *cac*^{ts2} ; *mle*^{napts} double mutants an additional barrier was overcome because the *cac*^{ts2} stock used in G_0 had lower viability compared to the *cac*^{s} stock. We do not know the reason for the *cac*^{ts2} stock's decreased ability to thrive.

Although all segregation and sex ratios indicated that double mutants from the second mating scheme eclosed in the expected frequencies, both *cac*^{s} ; *mle*^{napts} and *cac*^{ts2} ; *mle*^{napts} stocks survived poorly. The *cac*^{s} ; *mle*^{napts} stock from the second mating scheme died before heartbeat recordings could be performed. Even though enough flies eclosed as G_2 progeny to produce a self-maintaining *cac*^{s} ; *mle*^{napts} double mutant stock (333 *cac*^{s} ; *mle*^{napts} progeny, compared to 154 *cac*^{ts2} ; *mle*^{napts} progeny), and though double mutants were able to reproduce, albeit not very well (relatively few double mutant progeny eclosed), and despite the special care (i.e. covering the medium with yeast and changing the stocks once a day) given the cultures, it was not possible to generate a thriving stock. In comparison to wild-type and *cac*^{ts2} flies, the *cac*^{s} flies used in G_0 of this double mutant cross spent an abnormally large quantity of time on the surface of the medium. Because of this behavior they often got stuck in the medium and perished, which resulted in the stock having comparatively low viability. In congruence with observations of the parental single mutant *cac*^{s} homozygous stock, this behavior was also evident in *cac*^{s} ; *mle*^{napts} double mutant progeny, and may have contributed to their poor viability.

However, cac^{ts2} ; mle^{napts} flies did not survive well either, despite the robustness of the cac^{ts2} stock used in G_0 of this double mutant mating. The cac^{ts2} ; mle^{napts} stock survived long enough for pupal heartbeats to be recorded, but they dwindled and died soon after. It was evident that a major contributing factor to the double mutants' inability to thrive was their poor reproductive ability. Preliminary analysis showed that cac^{ts2} ; mle^{napts} females had poorly developed ovaries, which was at least partly a cause of the stock's low productivity.

Effect of mle^{napts} on Heartbeat Frequency

The mle^{napts} mutant's heart phenotype was reported in detail in Dowse *et al.* (1995). Data from the current study mostly confirm results from this earlier work. Pupae homozygous for the mle^{napts} mutation exhibit lower heart rates than wild-type pupae, although only significantly so at 37°C (37°C: F = 5.72, P = 0.0221) (Tables 3, 4; Fig. 11). However, raw data and MESA plots at 25°C and at 40°C show that heart rate in mle^{napts} mutants is noticeably lower than wild-type across temperature (Figs. 1ab, 2ab, 9ab, 10ab). In addition, homozygous mle^{napts} mutants' heart rates do not respond consistently to temperature changes (Tables 3, 4; Fig. 11).

The mle^{napts} mutation's effect on heart rate is recessive, as heterozygotes have heartbeat frequencies that are not significantly different from wild-type at temperatures $\geq$ 25, except at 37°C (25°C: F = 2.40, P = 0.1396; 30°C: F = 1.20, P = 0.2895; 35°C: F = 3.75, P = 0.0696; 37°C: F = 6.82, P = 0.0132; 39°C: F = 3.32, P = 0.0872; 40°C: F = 2.77, P = 0.1156; 41°C: F = 0.13, P = 0.7270; 42°C: F = 0.78, P = 0.3898) (Tables 3, 4). The phenotypic dominance value for wild-type over mle^{napts} is very strong, at 4.36.

Heterozygotes have heartbeat frequencies higher than homozygotes, significantly so at 35°C to 39°C (35°C: $F = 6.23$, $P = 0.0225$; 37°C: $F = 14.94$, $P = 0.0004$; 39°C: $F = 8.09$, $P = 0.0112$) (Tables 3, 4). Furthermore, heterozygotes have heartbeat frequencies significantly higher overall than homozygotes at temperatures ≥20°C ($F = 30.18$, $P = 0.0001$), which supports that *mle*^{napts} is recessive (Tables 3, 4). This result is contrary to the results of Dowse *et al.* (1995), where *mle*^{napts} was dominant for the temperature-insensitive heart rate phenotype. Such a discrepancy could be due to the potential accumulation of genetic modifiers in the *mle*^{napts} strain between the two study dates. However, the recessive nature of the heart rate effect observed in this study is consistent with research on *mle*^{napts} mutants' paralytic phenotype, which is also recessive (Kernan *et al.*, 1991).

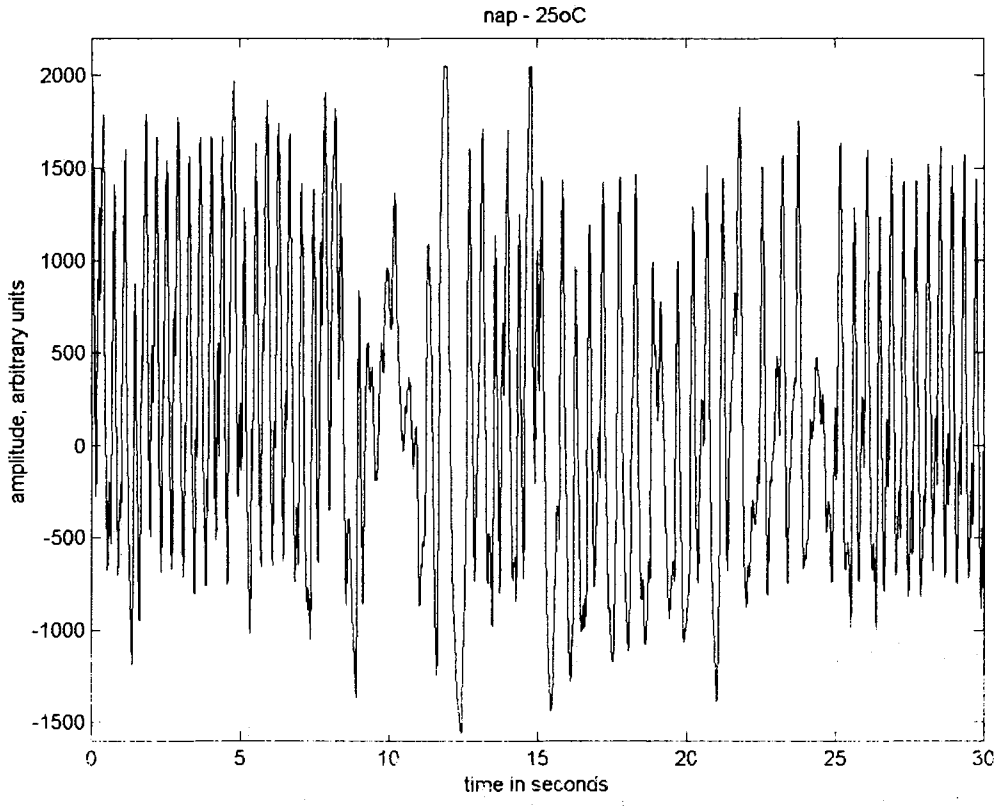

Figure 9. Example of the complete set of analyses performed on heartbeat data from a singie *mle*^{napts} pupa at 25°C.

a) Output of the optical recording device (raw data) for heartbeat of typical *mle*^{napts} *Drosophila melanogaster* at 25°C. The beat is fairly arrhythmic throughout the 30 s test period (Tables 3, 6; Figs. 11, 16) but has about the same frequency as wild-type at the same temperature (Fig. 1a).

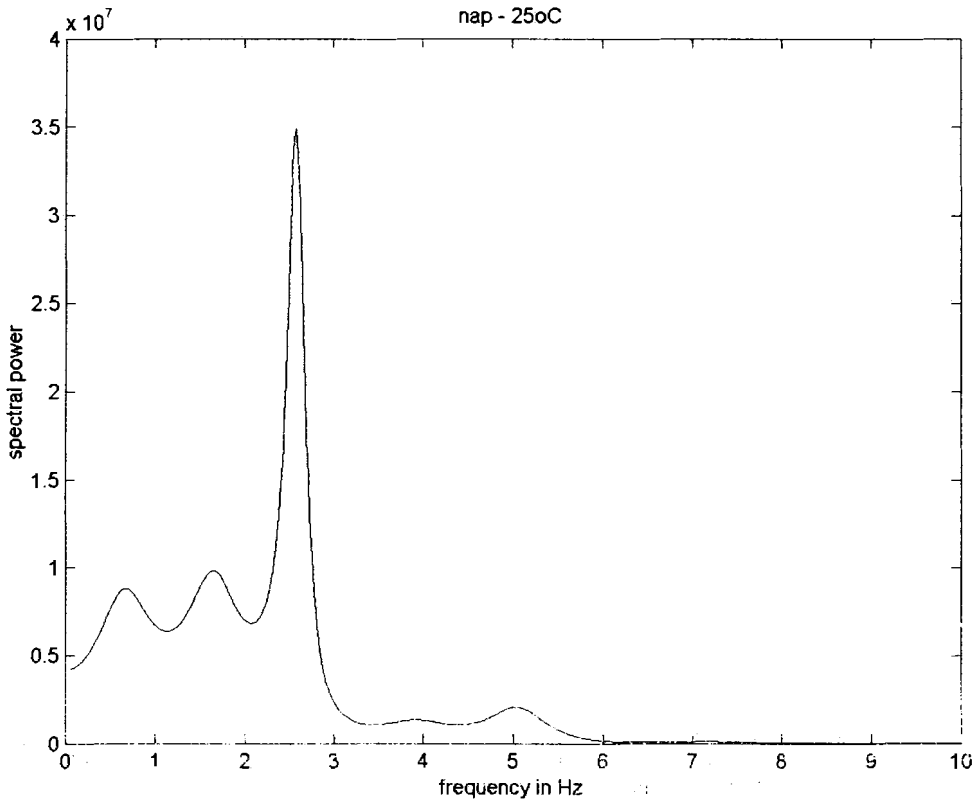

Figure 9. Continued.

b) Heartbeat of *mle*^{napts} *Drosophila melanogaster* at 25°C. Power spectrum derived from Maximum Entropy Spectral Analysis (MESA) for the same *mle*^{napts} pupa tested at 25°C, indicating the estimated frequency of the heartbeat. As mentioned previously (Chapter 1), any less pronounced additional peaks are reflections of irregularities in the raw data. Because there is a huge range of spectral power magnitudes among records, they are not all to the same scale (see ordinate scale at left of spectrum). The heartbeat frequency for this pupa is 2.58 Hz. The mean heart rate for *mle*^{napts} pupae at 25°C is 2.17 Hz (Tables 3, 4), which is almost identical to wild-type's at the same temperature (Tables 3, 4; Figs. 1b, 11).

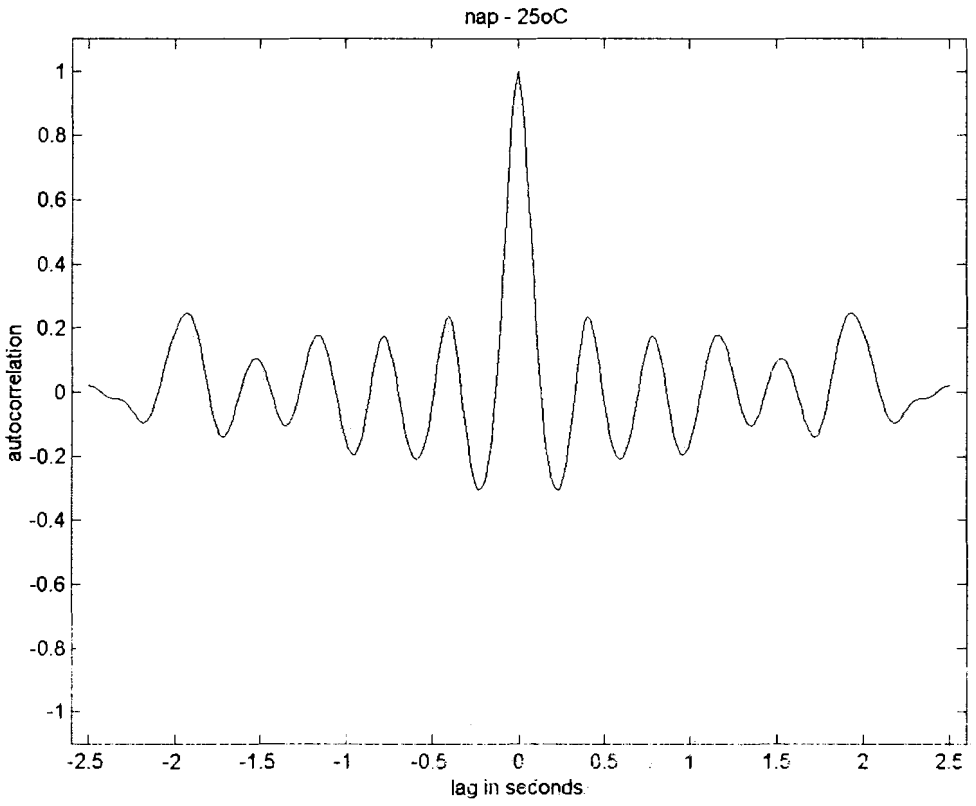

Figure 9. Continued.

c) Heartbeat of *mle*^{napts} *Drosophila melanogaster* at 25°C. Autocorrelogram for the same *mle*^{napts} pupa tested at 25°C. As explained in Chapter 1, decay of the autocorrelation function, in conjunction with results of the raw data plot and MESA spectrum, indicate heartbeat regularity. The height of the third peak, expressed as a fraction of the height of the first peak, is a good measure of the rhythmicity index score. The rhythmicity index is 0.17 for this pupa. The average rhythmicity index score for *mle*^{napts} pupae at 25°C is 0.31, which is slightly lower than wild-type pupae's at this temperature (Tables 6, 7; Figs 1c, 16).

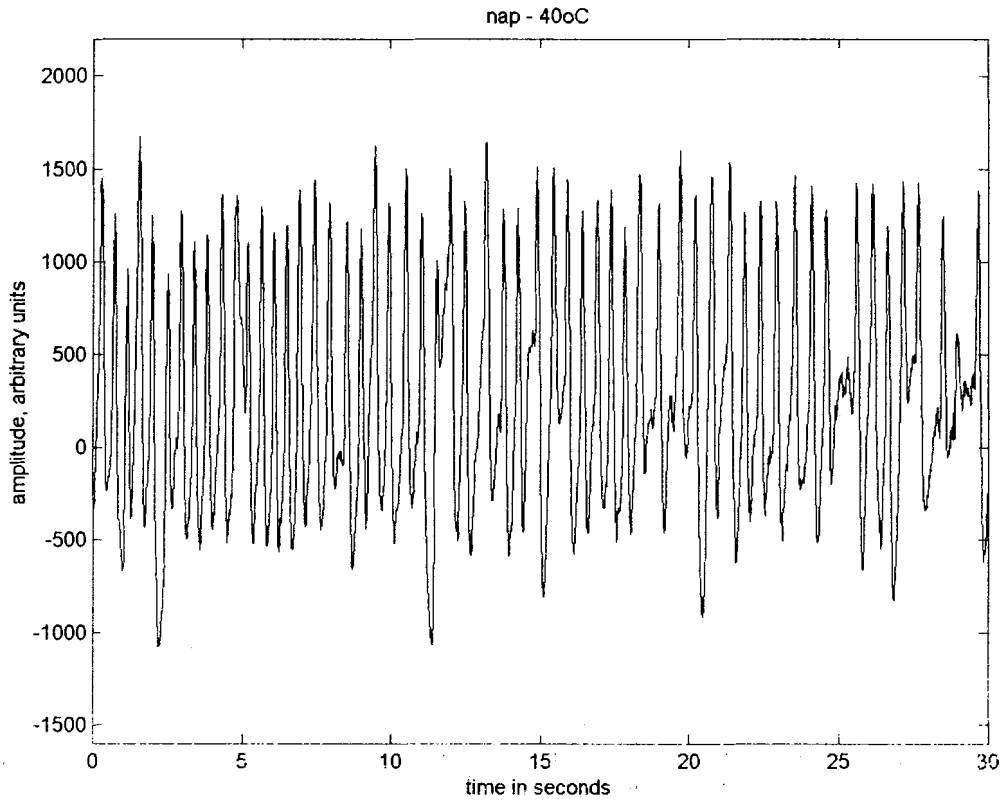

Figure 10. Example of the complete set of analyses performed on heartbeat data from a single *mle*^{napts} pupa at 40°C.

a) Output of the optical recording device (raw data) for heartbeat of typical *mle*^{napts} *Drosophila melanogaster* at 40°C. The heartbeat is even more irregular than it was at 25°C, having become almost chaotic (Tables 6, 7; Figs. 9a, 16). The heart rate has increased slightly, but not as much as wild-type pupae (Tables 3, 4; Figs. 9a, 11). The heartbeat's arrhythmicity is made more compelling by comparison with that of wild-type at the same temperature (Fig. 2a).

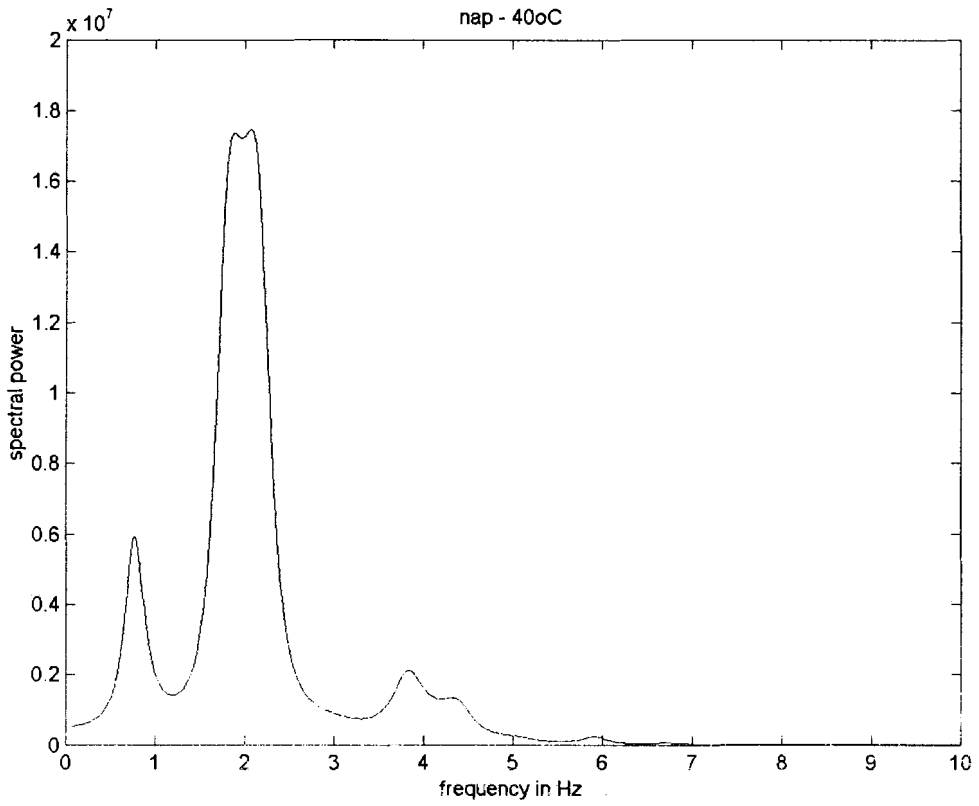

Figure 10. Continued.

b) Heartbeat of *mle*^{napts} *Drosophila melanogaster* at 40°C. Power spectrum derived from MESA for the same *mle*^{napts} pupa tested at 40°C, indicating the average frequency of the heartbeat, 2.08 Hz. The mean heart rate for *mle*^{napts} pupae at 40°C is 2.29 Hz, which has only slightly increased from 25°C (Tables 3, 4; Fig. 9b, 11), and is slightly lower than wild-type pupae at the same temperature (Tables 3, 4; Fig 2b).

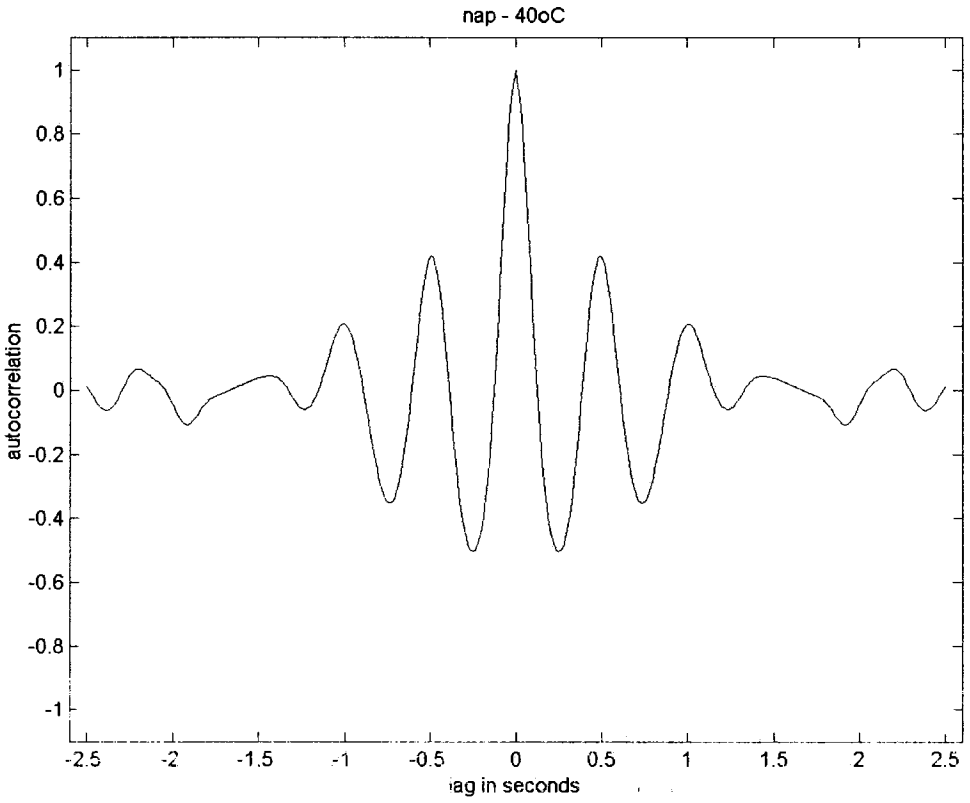

Figure 10. Continued.

c) Heartbeat of *mle*^{napts} *Drosophila melanogaster* at 40°C. Autocorrelogram for the same *mle*^{napts} pupa tested at 40°C. The autocorrelogram indicates that the heartbeat of this pupa is much less rhythmic at high temperature than it was at 25°C (Fig. 9c). At 40°C, the rhythmicity score is 0.21 for this pupa. The average rhythmicity score for *mle*^{napts} pupae at 40°C is 0.15, which is drastically lower than wild-type pupae (Tables 6, 7; Figs. 2c, 16).

FR Genotype	Temperature 20	25	30	35	37	39	40	41	42	Over-all FR across temp
mle^{napts}	1.82	2.17	2.58	2.42	2.15	1.81	2.29	2.27	1.44	2.10^{A}
+/- SEM	0.15	0.21	0.13	0.23	0.21	0.34	0.29	0.32	0.34	
N	15	10	10	10	20	10	10	10	10	
wild-type	1.80	2.18	2.44	2.63	2.73	2.39	2.38	2.36	1.84	2.32^{B}
	0.10	0.19	0.19	0.20	0.09	0.24	0.25	0.30	0.36	
	14	9	9	9	18	9	9	9	9	
mle^{napts}/+	2.16	2.52	2.71	3.08	3.06	2.94	2.87	2.50	2.28	2.69^{C}
	0.13	0.12	0.16	0.13	0.09	0.19	0.15	0.27	0.35	
	15	10	10	10	19	9	9	9	9	

Table 3. Mean heartbeat frequency of *mle*^{napts} strains and wild-type. Mean heartbeat frequency ± standard error of the mean (SEM) at medium and high temperatures, determined by univariate analyses for all genotypes tested. As mentioned in Materials and Methods, Chapter 1, heart rates and rhythmicity indices of genotypes at low temperatures were not included in statistical analyses because heartbeats of most pupae were arrhythmic at these temperatures so data were not informative. Strains are ordered according to their overall heart rate values across temperature (column at right). Extraneous genotypes were omitted from the table for clarity.

Heartbeat frequencies of strains were initially compared across temperature by ANOVA and then ranked by Ryan-Einot-Gabriel-Welsch multiple F test (REGWF, Einot and Gabriel, 1975) ($\alpha = 0.05$). There is a significant difference between genotypes ($F = 16.21$, $P = 0.0001$), and groupings are indicated by letter superscript (A, B, or C) in the overall frequency column. Means that share a superscript are not significantly different. SEM = standard error of the mean, N = number of pupae tested and analyzed for given strain at each temperature.

Figure 11. Comparison of the relationship between rate of pupal heartbeat and temperature. Increase in heart rates with rising temperature of wild-type (solid line), mle^{napts} (line with triangles), cac^{s} (line with circles), cac^{s} ; mle^{napts} (line with stars), cac^{ts2} (line with asterisks), and cac^{ts2} ; mle^{napts} (line with diamonds) pupae. Mean heart rates were determined by univariate analyses and are listed in Table 4. Bars representing standard error of the mean were omitted for clarity, but are listed in Table 4.

Regression analyses results for these data are misleading because they omit the non-linearity of temperature variations, as explained in Chapter 1, so they were not included. Figure 11 provides a much more accurate depiction of the relationship of heart rate to changing temperature for critical strains. However, to ensure that the current study's recorded mle^{napts} mutants' heartbeat phenotype is consistent with that previously reported, heart rate was regressed on temperature for mle^{napts} pupae, yielding a slope of –0.0008 and an intercept of 2.1229. This indicates that there is a negative relationship between heartbeat frequencies and temperature for this strain, which is consistent with previously reported results (Dowse *et al.*, 1995).

Homogeneity of slopes analysis was performed on heart rate data for the same three genotypes and there were significant genotype ($F = 75.27$, $P = 0.0001$), temperature ($F = 102.24$, $P = 0.0001$), and temperature x genotype ($F = 6.54$, $P = 0.0001$) effects. Apparently, different genotypes have different heart rates, altering temperature causes changes in heart rate, and genotype affects how heart rate changes in response to temperature. Conclusions drawn from these results are clearly depicted in Figure 11.

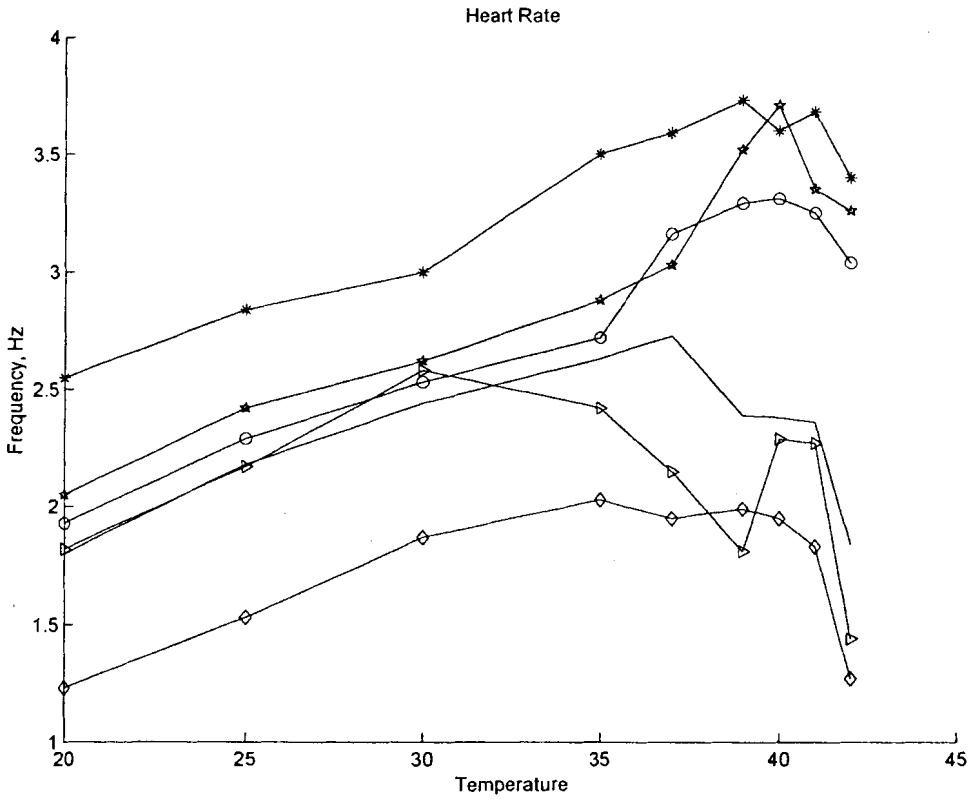
Heart Rate
Frequency, Hz
Temperature
4
3.5
3
2.5
2
1.5
1
20
25
30
35
40
45

FR	Temperature									Over-all FR across temp
Genotype	20	25	30	35	37	39	40	41	42	
cac^{ts2} ; *mle*^{napts}	1.23	1.53	1.87	2.03	1.95	1.99	1.95	1.83	1.27	1.73^{A}
+/- SEM	0.13	0.22	0.22	0.23	0.19	0.27	0.27	0.27	0.25	
N	30	18	18	18	36	18	18	18	18	
mle^{napts}	1.82	2.17	2.58	2.42	2.15	1.81	2.29	2.27	1.44	2.10^{B}
	0.15	0.21	0.13	0.23	0.21	0.34	0.29	0.32	0.34	
	15	10	10	10	20	10	10	10	10	
wild-type	1.80	2.18	2.44	2.63	2.73	2.39	2.38	2.36	1.84	2.32^{B}
	0.10	0.19	0.19	0.20	0.09	0.24	0.25	0.30	0.36	
	14	9	9	9	18	9	9	9	9	
mle^{napts}/+	2.16	2.52	2.71	3.08	3.06	2.94	2.87	2.50	2.28	2.69^{C}
	0.13	0.12	0.16	0.13	0.09	0.19	0.15	0.27	0.35	
	15	10	10	10	19	9	9	9	9	
cac^{s}	1.93	2.29	2.53	2.72	3.16	3.29	3.31	3.25	3.04	2.79^{C}
	0.11	0.15	0.18	0.21	0.13	0.22	0.23	0.25	0.30	
	29	19	19	19	37	16	16	16	16	
cac^{s}/+	2.01	2.29	2.64	2.88	3.10	3.21	3.18	3.09	3.03	2.80^{C}
	0.07	0.11	0.13	0.36	0.10	0.11	0.10	0.12	0.12	
	28	17	17	9	33	16	16	16	16	
cac^{s} ; *mle*^{napts}	2.05	2.42	2.62	2.90	3.03	3.52	3.71	3.35	3.26	2.87^{C,D}
	0.17	0.25	0.35	0.16	0.29	0.25	0.18	0.44	0.42	
	19	9	9	17	17	8	8	8	8	
cac^{ts2}/+	2.28	2.64	3.00	3.32	3.47	3.59	3.59	3.18	2.97	
	0.04	0.07	0.10	0.09	0.07	0.07	0.09	0.24	0.30	3.10^{D,E}
	30	19	19	19	38	19	19	19	19	
cac^{ts2}	2.55	2.84	3.00	3.50	3.59	3.73	3.60	3.68	3.40	
	0.08	0.14	0.19	0.17	0.14	0.17	0.24	0.19	0.28	
	30	20	20	20	40	20	20	20	20	3.31^{E}

Effect of *cac*^{s} with *mle*^{napts} on Heartbeat Frequency

In contrast to the heart rate decrease in *mle*^{napts} pupae is the increase exhibited by pupae homozygous for both *cac*^{s} and *mle*^{napts} mutations that is clearly shown across temperature in raw data and MESA plots of *cac*^{s} ; *mle*^{napts} double mutants, as compared to those of wild-type at 25°C and 40°C (Tables 4, 5; Figs. 1ab, 2ab, 11, 12ab, 13ab). *cac*^{s}; *mle*^{napts} double mutants have heart rates that are significantly higher than wild-type at temperatures ≥39°C, except at 41°C (39°C: F = 10.49, P = 0.0055; 40°C: F = 17.30, P = 0.0008; 41°C: F = 3.58, P = 0.0778; 42°C: F = 6.65, P = 0.0210) (Tables 4, 5; Fig. 11), similarly to *cac*^{s} in a wild-type background (as shown in Chapter 1 Results – Table 1 ; Fig. 7).

Homozygous *cac*^{s} in a homozygous *mle*^{napts} background has the same effect of increasing heart rate as *cac*^{s} alone (Figs. 7, 11). Because heart rates of *cac*^{s} mutants and *cac*^{s} double mutants with *mle*^{napts} have heart rates that are not significantly different, it appears that *cac*^{s} is not interacting with *mle*^{napts} for heart rate (20°C: F = 0.38, P = 0.5390; 25°C: F = 0.23, P = 0.6378; 30°C: F = 0.06, P = 0.8080; 35°C: F = 0.15, P = 0.7000; 37°C: F = 0.22, P = 0.6393; 39°C: F = 0.40, P = 0.5360; 40°C: F = 1.22, P = 0.2812; 41°C: F = 0.04, P = 0.8352; 42°C: F = 0.18, P = 0.6748) (Tables 4, 5; Fig. 11). That *cac*^{s} is not interacting with *mle*^{napts} is supported by overall heartbeat frequencies of strains heterozygous for either or both *cac*^{s} and *mle*^{napts} that are not significantly different from those of *cac*^{s} homozygotes (F = 0.62, P = 0.6002) (Table 5).

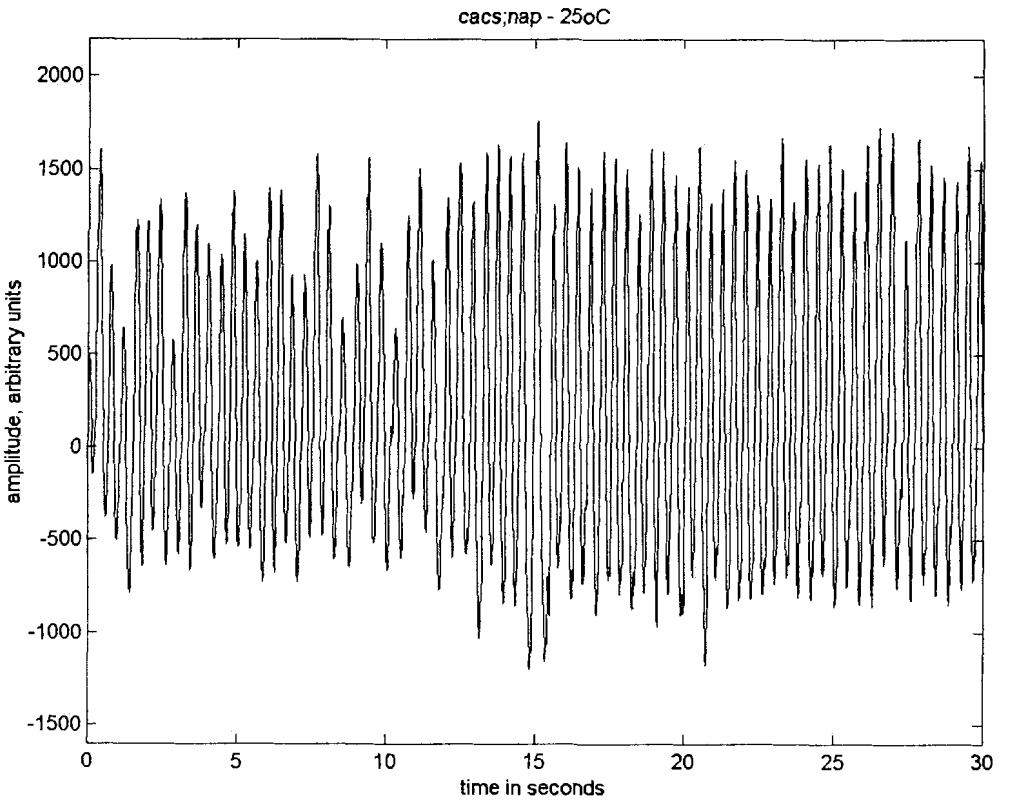

Figure 12. Example of the complete set of analyses performed on heartbeat data from a single *cac*^{s} ; *mle*^{napts} pupa at 25°C.

a) Output of the optical recording device (raw data) for heartbeat of typical *cac*^{s} ; *mle*^{napts} *Drosophila melanogaster* at 25°C. Heart rate is moderately higher than wild-type (Fig. 1a) at the same temperature, and is even slightly higher than *cac*^{s} (Tables 4, 5; Figs. 3a, 11). Rhythmicity is almost like wild-type but slightly higher (Tables 7, 8; Figs. 1a, 16).

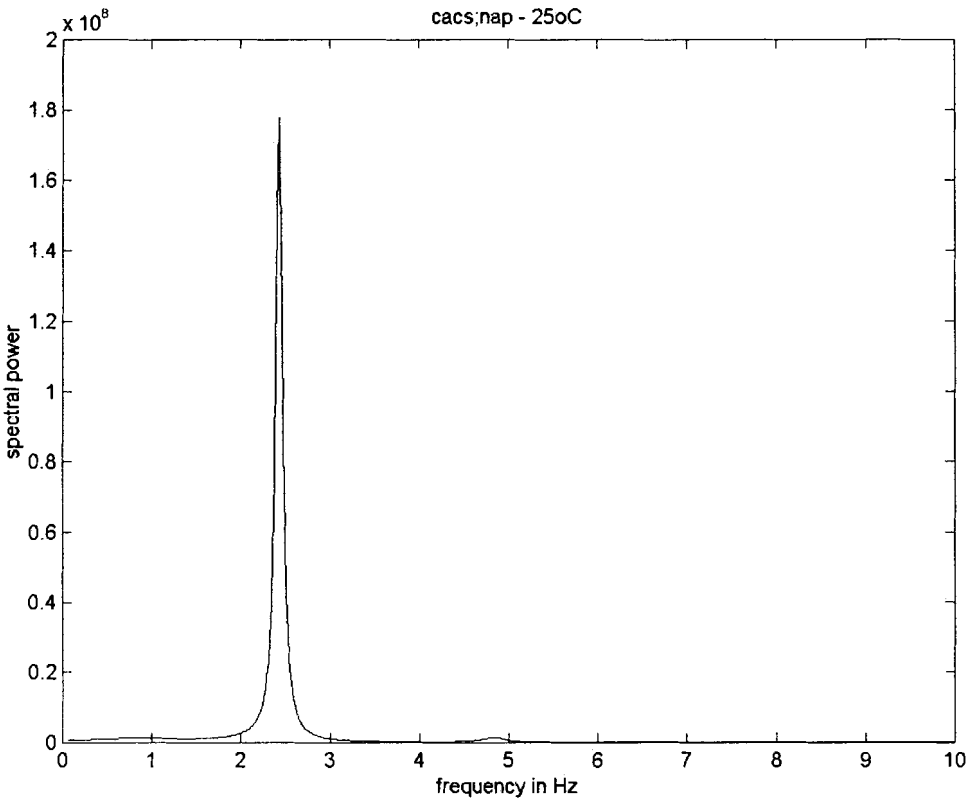

Figure 12. Continued.

b) Heartbeat of *cac*^{s} ; *mle*^{napts} *Drosophila melanogaster* at 25°C. Power spectrum derived from MESA for the same *cac*^{s} ; *mle*^{napts} pupa tested at 25°C, indicating the average frequency of the heartbeat, which is 2.43 Hz. The mean heart rate for *cac*^{s} ; *mle*^{napts} pupae at 25°C is 2.42 Hz (Tables 4, 5). The heartbeat frequency is much higher than for wild-type, and noticeably higher than *cac*^{s} pupae at the same temperature (Tables 4, 5; Figs. 1b, 11).

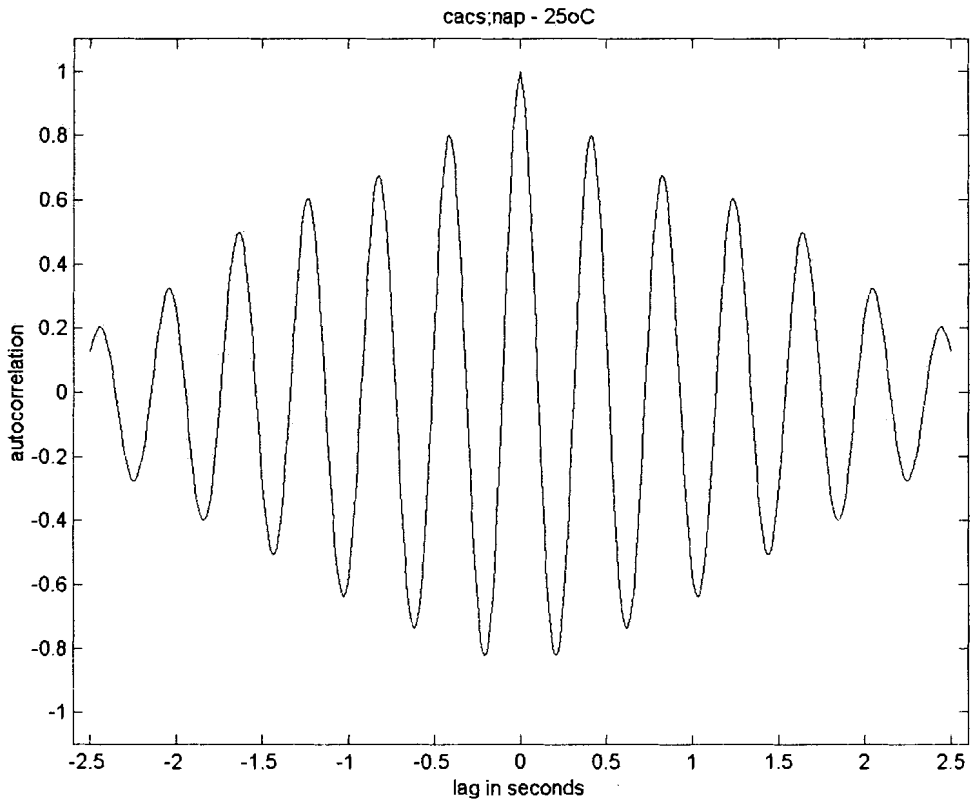

Figure 12. Continued.

c) Heartbeat of *cac*^{s} ; *mle*^{napts} *Drosophila melanogaster* at 25°C. Autocorrelogram for the same *cac*^{s} ; *mle*^{napts} pupa tested at 25°C. The rhythmicity index score is 0.68 for this pupa. The average rhythmicity score for *cac*^{s} ; *mle*^{napts} pupae at 25°C is 0.42, which is very similar to that of wild-type pupae at 25°C (Tables 7, 8; Fig. 1c, 16).

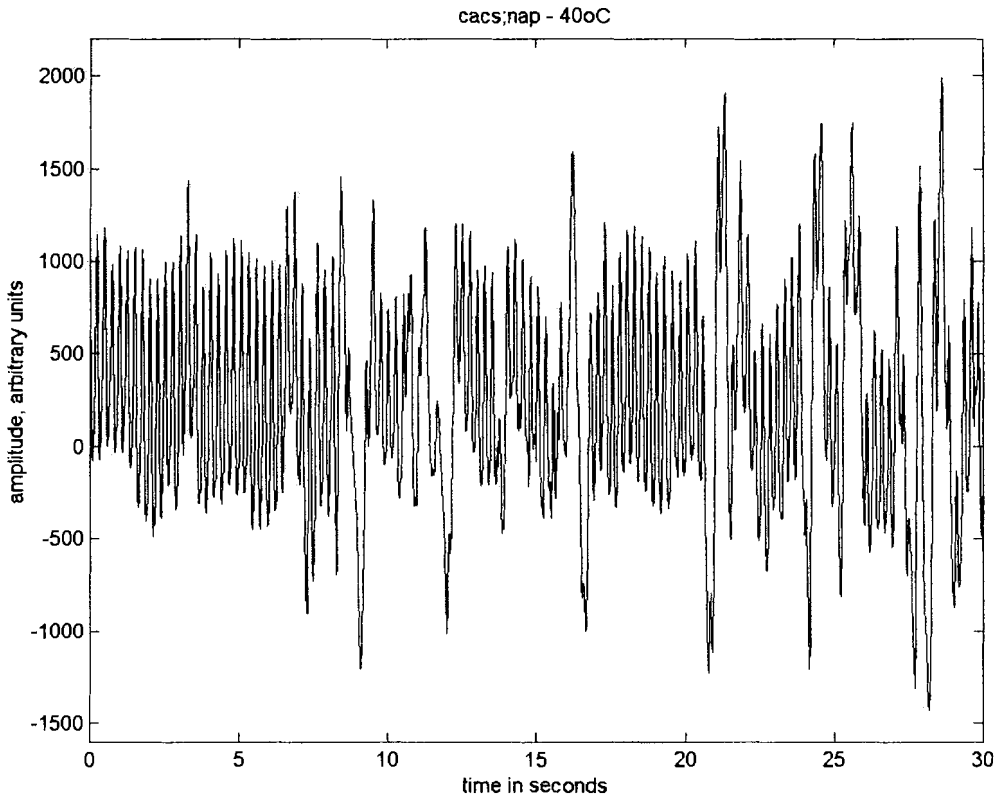

Figure 13. Example of the complete set of analyses performed on heartbeat data from a single cac^{s} ; mle^{napts} pupa at 40°C.

a) Output of the optical recording device (raw data) for heartbeat of typical cac^{s} ; mle^{napts} *Drosophila melanogaster* at 40°C. The heartbeat is more irregular than it was at 25°C, but only slightly so (Tables 7, 8; Figs. 12a, 16). Rhythmicity is still very much like wild-type (Fig. 2a). Heartbeat frequently has increased drastically from 25°C (Fig. 12a) and has increased even more greatly compared to wild-type than it was at the lower temperature (Tables 4, 5; Fig. 11).

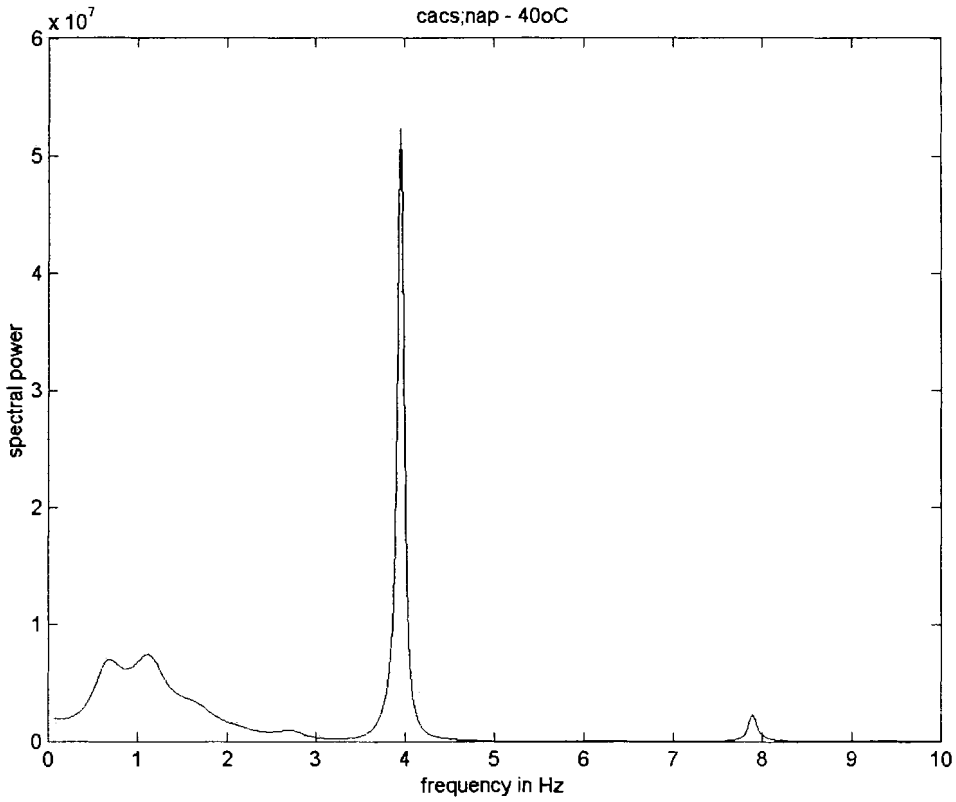

Figure 13. Continued.

b) Heartbeat of *cac*^{s} ; *mle*^{napts} *Drosophila melanogaster* at 40°C. Power spectrum derived from MESA for the same *cac*^{s} ; *mle*^{napts} pupa tested at 40°C, indicating the average frequency of the heartbeat, which has massively increased from 25°C. The frequency of heartbeat for this pupa is 3.96 Hz. The mean heart rate for *cac*^{s} ; *mle*^{napts} pupae at 40°C is 3.71 Hz, indicating a further divergence from wild-type pupae (Tables 4, 5; Figs. 12b, 11).

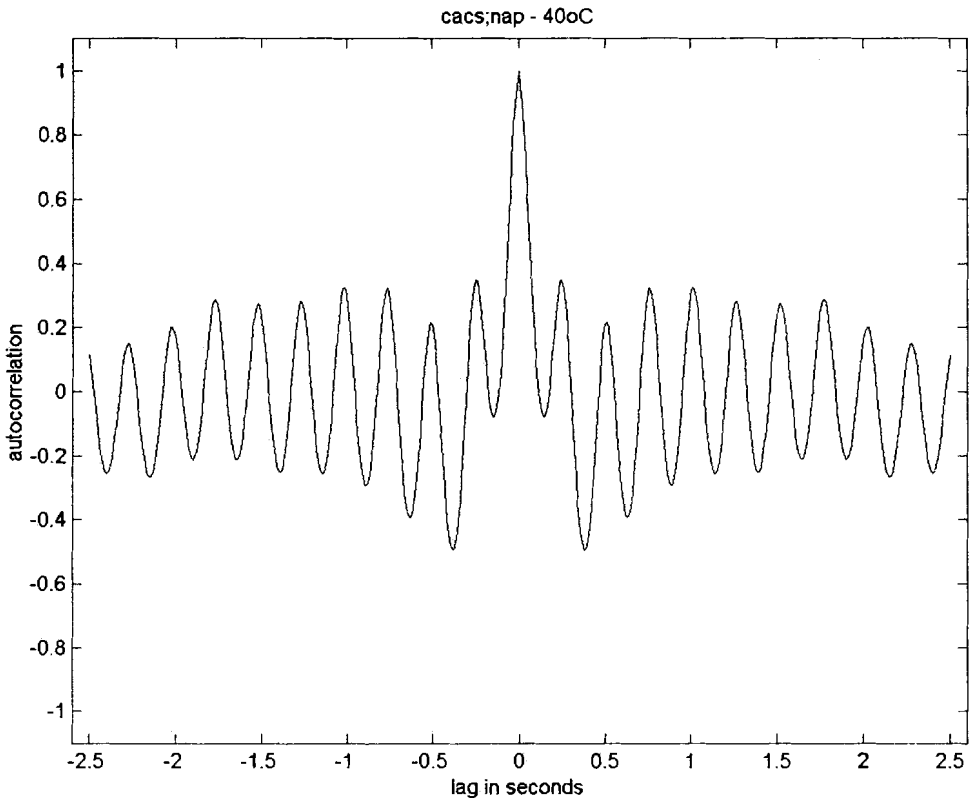

Figure 13. Continued.

c) Heartbeat of *cac*^{s} ; *mle*^{napts} *Drosophila melanogaster* at 40°C. Autocorrelogram for the same *cac*^{s} ; *mle*^{napts} pupa tested at 40°C. The autocorrelogram indicates that the heartbeat of this pupa is only very slightly less rhythmic at high temperature than it was at 25°C. At 40°C, the rhythmicity score is 0.22 for this pupa. The average rhythmicity score for *cac*^{s} ; *mle*^{napts} pupae at 40°C is 0.42, which is barely higher than wild-type pupae (Tables 7, 8; Fig. 2c, 12c, 16).

FR	Temperature									Over-all FR across temp
Genotype	20	25	30	35	37	39	40	41	42	
mle^{napts}	1.82	2.17	2.58	2.42	2.15	1.81	2.29	2.27	1.44	2.10^{A}
+/- SEM	0.15	0.21	0.13	0.23	0.21	0.34	0.29	0.32	0.34	
N	15	10	10	10	20	10	10	10	10	
wild-type	1.80	2.18	2.44	2.63	2.73	2.39	2.38	2.36	1.84	2.32^{A,B}
	0.10	0.19	0.19	0.20	0.09	0.24	0.25	0.30	0.36	
	14	9	9	9	18	9	9	9	9	
cac^{s}/+ ; *mle*^{napts}/+	2.10	2.33	2.62	2.81	2.81	2.81	2.91	2.87	2.88	
	0.21	0.17	0.14	0.12	0.08	0.15	0.12	0.12	0.24	2.66^{B,C}
	5	3	3	3	6	3	3	3	3	
cac^{s}	1.93	2.29	2.53	2.72	3.16	3.29	3.31	3.25	3.04	
	0.11	0.15	0.18	0.21	0.13	0.22	0.23	0.25	0.30	2.79^{C}
	29	19	19	19	37	16	16	16	16	
cac^{s}/+	2.01	2.29	2.64	2.90	3.10	3.21	3.18	3.09	3.03	
	0.07	0.11	0.13	0.16	0.10	0.11	0.10	0.12	0.12	2.80^{C}
	28	17	17	17	33	16	16	16	16	
cac^{s}/+ ; *mle*^{napts}	2.66	2.36	2.98	2.31	3.22	3.22	3.35	3.16	2.26	
	0.10	0.54	0.17	0.71	0.07	0.12	0.27	0.35	0.54	2.84^{C}
	5	4	4	4	7	3	3	3	3	
cac^{s} ; *mle*^{napts}	2.05	2.42	2.62	2.88	3.03	3.52	3.71	3.35	3.26	
	0.17	0.25	0.35	0.36	0.29	0.25	0.18	0.44	0.42	2.87^{C}
	19	9	9	9	17	8	8	8	8	
cac^{s} ; *mle*^{napts}/+	2.20	2.55	2.81	3.04	3.04	3.29	3.16	3.26	2.89	
	0.22	0.19	0.29	0.31	0.23	0.11	0.14	0.15	0.28	2.89^{C}
	13	9	9	9	17	8	8	8	8	

Effect of cac^{ts2} with mle^{napts} on Heartbeat Frequency

cac^{ts2} ; mle^{napts} homozygous mutants have a much different heart rate phenotype than the double mutant strain carrying cac^{s}. Heartbeat frequency of cac^{ts2} ; mle^{napts} mutants is lower than that of wild-type, significantly so at 20°C and 37°C (20°C: F = 7.58, P = 0.0087; 37°C: F = 8.12, P = 0.0063 (Table 4; Fig. 11). Reduced frequency of cac^{ts2} ; mle^{napts} mutant heartbeat is evident across temperature in raw data and MESA figures of double mutants compared to those of wild-type at 25°C and 40°C (Figs. 1ab, 2ab, 14ab, 15ab).

Although cac^{ts2} ; mle^{napts} mutants are similar to mle^{napts} homozygotes because they both have decreased heartbeat frequencies, double mutants have even lower heart rates, albeit only significantly so at 20°C and 30°C (20°C: F = 7.45, P = 0.0092; 30°C: F = 5.22, P = 0.0308) (Table 4; Fig. 11). This result suggests that there is an interaction between cac^{ts2} and mle^{napts}, and specifically that mle^{napts} is epistatic over cac^{ts2} for the heart rate phenotype.

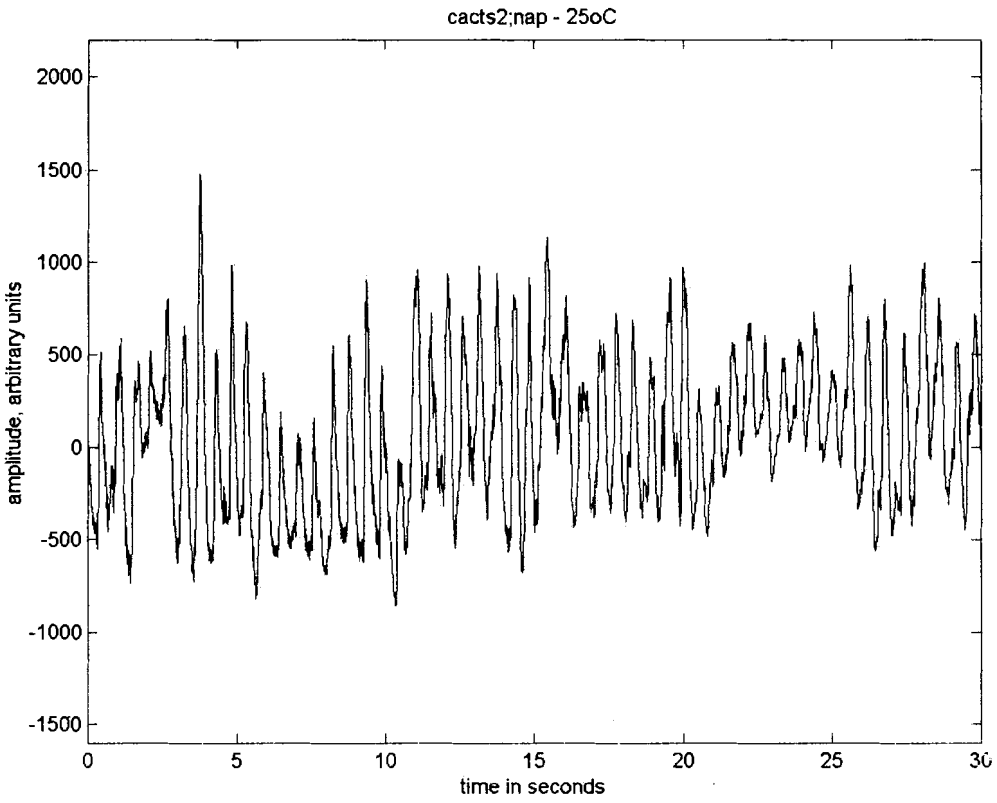

Figure 14. Example of the complete set of analyses performed on heartbeat data from a single cac^{ts2} ; mle^{napts} pupa at 25°C.

a) Output of the optical recording device (raw data) for heartbeat of typical cac^{ts2} ; mle^{napts} *Drosophila melanogaster* at 25°C. The heartbeat frequency is much slower than wild-type at the same temperature, but in contrast rhythmicities of the two strains are similar (Tables 4, 7; Fig. 1a).

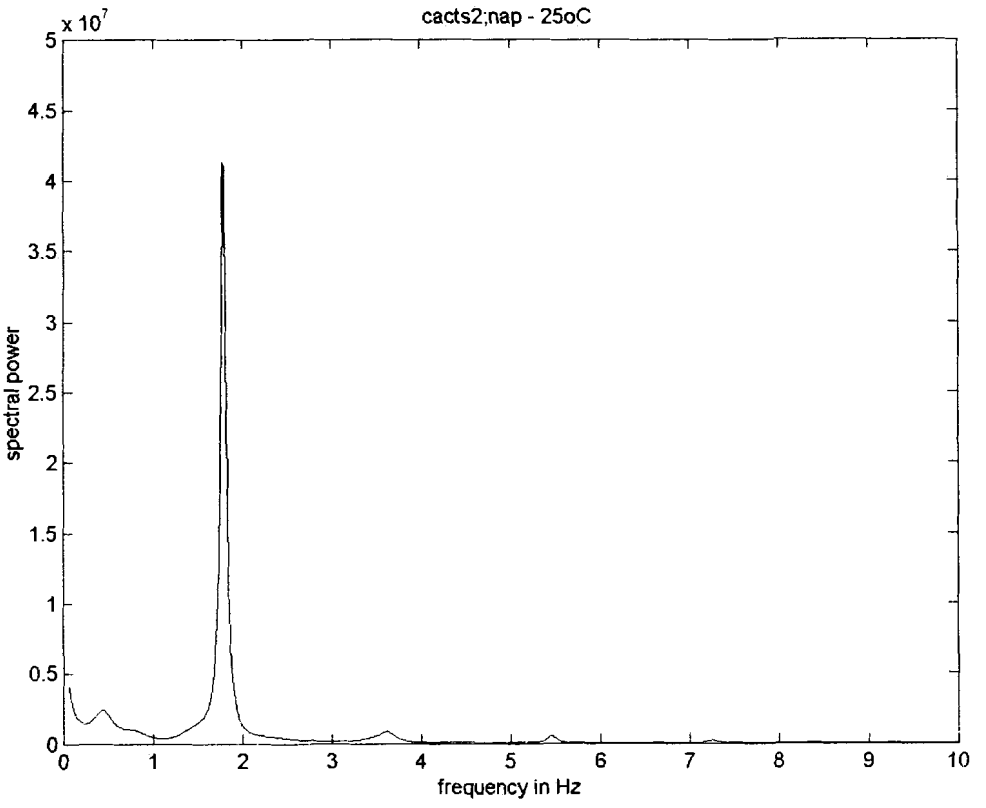

Figure 14. Continued.

b) Heartbeat of cac^{ts2} ; mle^{napts} *Drosophila melanogaster* at 25°C. Power spectrum derived from MESA for the same cac^{ts2} ; mle^{napts} pupa tested at 25°C, indicating the average frequency of the heartbeat, which is 1.78 Hz. The mean heart rate for cac^{ts2} ; mle^{napts} pupae at 25°C is 1.53 Hz (Table 4). The heartbeat frequency is considerably lower than for wild-type pupae at the same temperature (Table 4; Figs. 1b, 11).

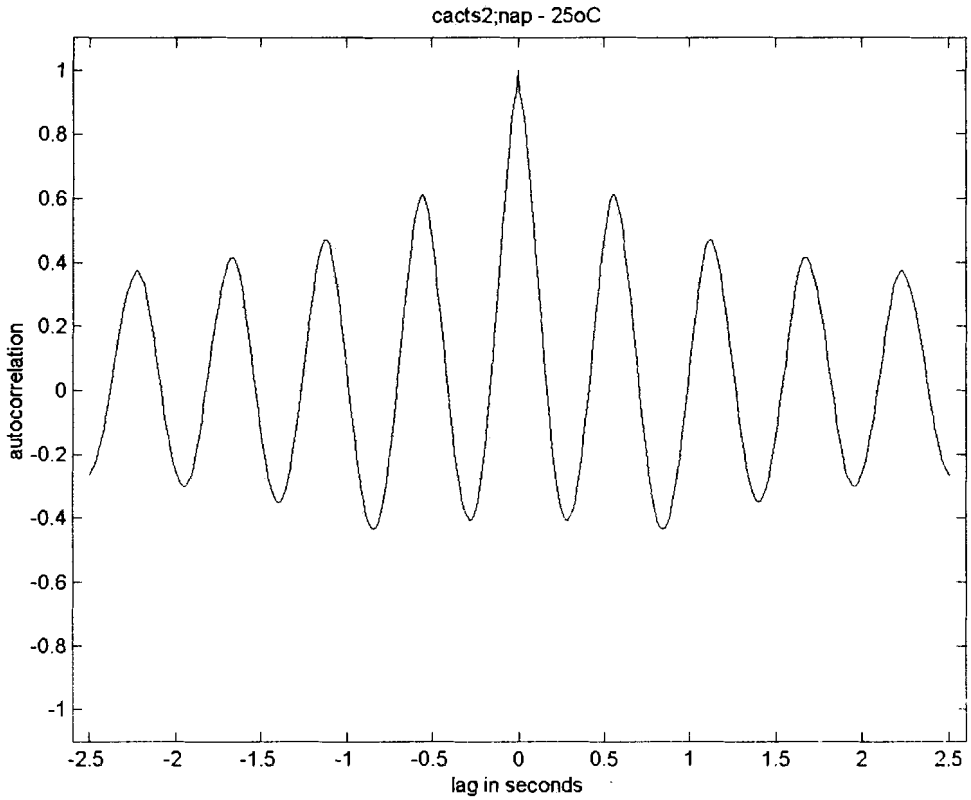

Figure 14. Continued.

c) Heartbeat of cac^{ts2} ; mle^{napts} *Drosophila melanogaster* at 25°C. Autocorrelogram for the same cac^{ts2} ; mle^{napts} pupa tested at 25°C. The rhythmicity index score is 0.47 for this pupa. The average rhythmicity score for cac^{ts2} ; mle^{napts} pupae at 25°C is 0.42, which is very similar to that of wild-type at the same temperature (Table 7; Figs. 1c, 16).

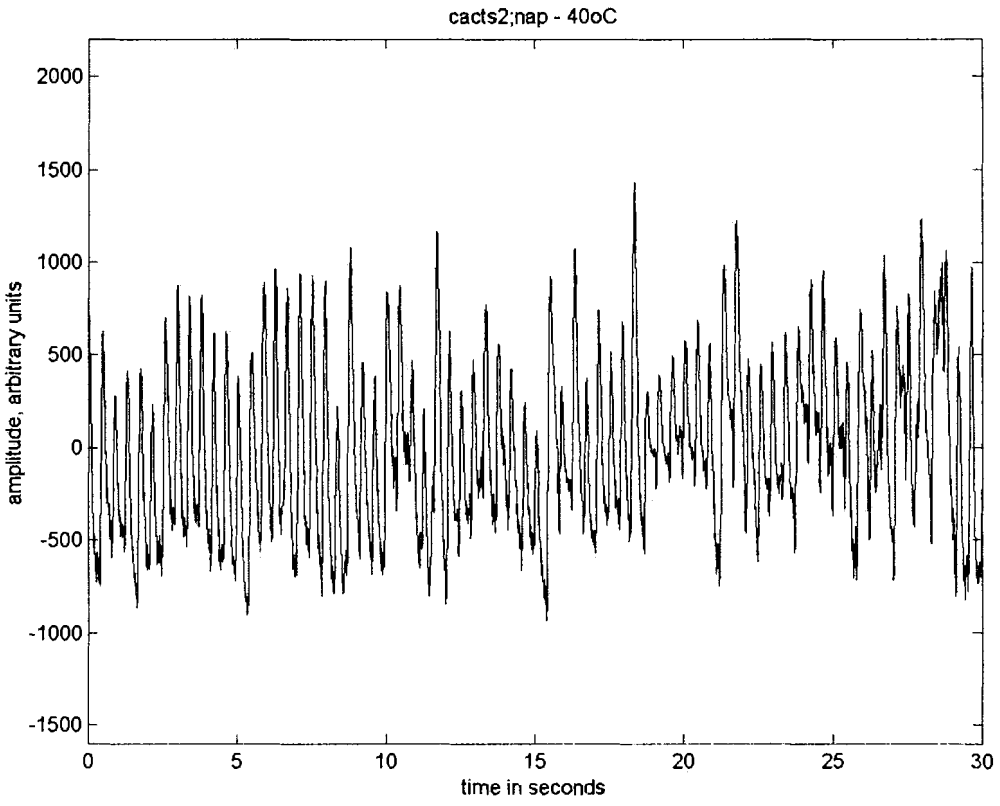

Figure 15. Example of the complete set of analyses performed on heartbeat data from a single cac^{ts2} ; mle^{napts} pupa at 40°C.

a) Output of the optical recording device (raw data) for heartbeat of typical cac^{ts2} ; mle^{napts} *Drosophila melanogaster* at 40°C. The heartbeat frequency has slightly increased from 25°C (Table 4; Figs. 14a) but is still much slower than wild-type at the same temperature (Fig. 2a). Heartbeat rhythmicity is still like that of wild-type, and is slightly lower than it was at 25°C (Table 7; Figs. 2a, 14a, 16).

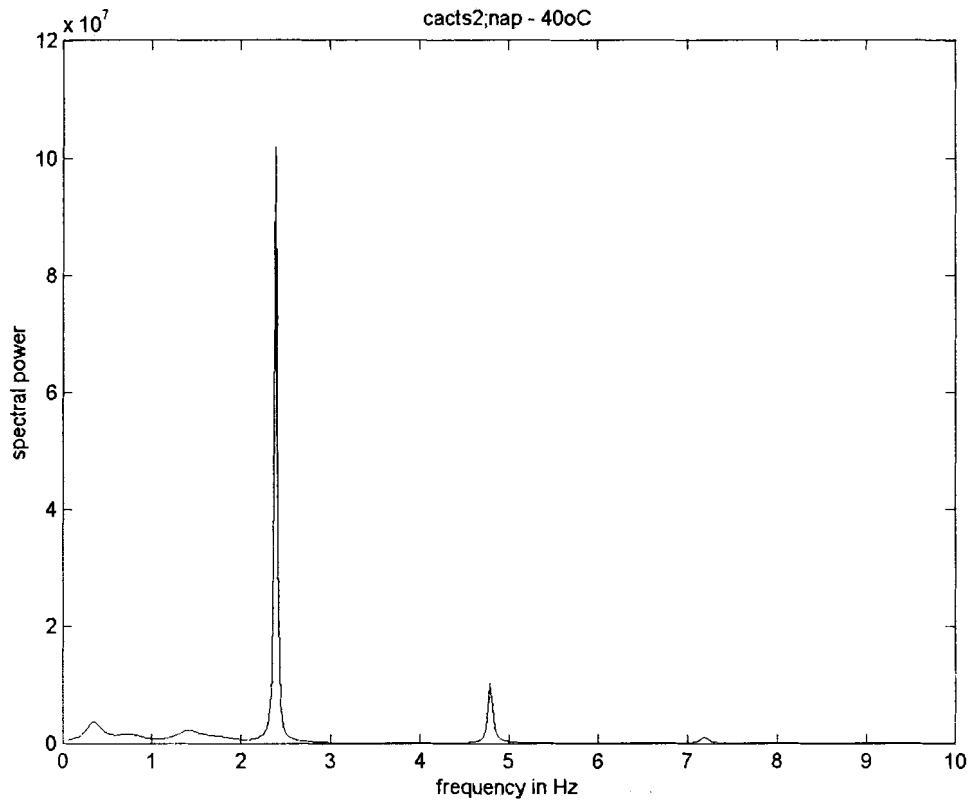

Figure 15. Continued.

b) Heartbeat of cac^{ts2} ; mle^{napts} *Drosophila melanogaster* at 40°C. Power spectrum derived from MESA for the same cac^{ts2} ; mle^{napts} pupa tested at 40°C, indicating the average frequency of the heartbeat, which has increased from 25°C (Tables 4, 6; Figs. 11, 14b). The frequency of heartbeat for this pupa is 2.40 Hz. The mean heart rate for cac^{ts2} ; mle^{napts} pupae at 40°C is 1.95 Hz (Table 4). Heart rate is still quite a bit lower than wild-type, but not as much as it was at 25°C (Table 4; Figs. 2b, 11).

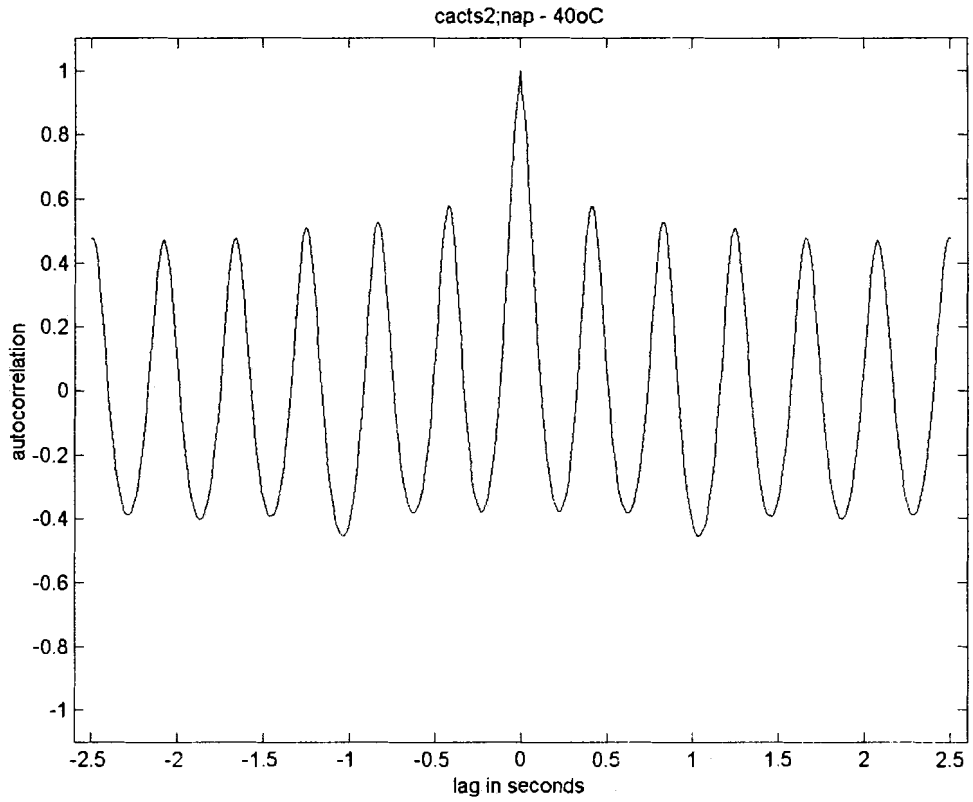

Figure 15. Continued.

c) Heartbeat of cac^{ts2} ; mle^{napts} *Drosophila melanogaster* at 40°C. Autocorrelogram for the same cac^{ts2} ; mle^{napts} pupa tested at 40°C. The autocorrelogram indicates that the heartbeat of this pupa is similar in rhythmicity at this temperature to its score at 25°C (Table 7; Figs. 14c, 16). At 40°C, the rhythmicity score is 0.53 for this pupa. The average rhythmicity score for cac^{ts2} ; mle^{napts} pupae at 40°C is 0.34 (Table 7). Rhythmicity is very close to that of wild-type at high temperature (Table 7; Figs. 2c, 16).

Effect of *mle*^{napts} on Heartbeat Rhythmicity Index

mle^{napts} homozygotes have decreased rhythmicity indices as compared to wild-type but only significantly so at temperatures ≥40°C (40°C: F = 11.17, P = 0.0041; 41°C: F = 5.38, P = 0.0349; 42°C: F = 9.05, P = 0.0132). However, *mle*^{napts} homozygotes have significantly decreased rhythmicity indices overall as compared to wild-type at temperatures ≥20°C (F = 16.13, P = 0.0001) (Tables 6, 7; Fig. 16). Raw data and autocorrelation plots at 25°C and 40°C for *mle*^{napts} versus wild-type emphasize *mle*^{napts} homozygotes' reduced rhythmicity across temperature (Figs. 1ac, 2ac, 9ac, 10ac).

Just as *mle*^{napts} is recessive for the heart rate phenotype, it is also recessive for rhythmicity, in accordance with the study by Dowse *et al.* (1995). *mle*^{napts} heterozygotes have heartbeat rhythmicities that are not significantly different from wild-type at temperatures ≥20°C (20°C: F = 0.31, P = 0.5854; 25°C: F = 3.20, P = .0913; 30°C: F = 0.45, P = 0.5130; 35°C: F = 0.07, P = 0.7912; 37°C: F = 2.42, P = 0.1290; 39°C: F = 0.05, P = 0.8318; 40°C: F = 0.13, P = 0.7254; 41°C: F = 3.35, P = 0.0885; 42°C: F = 0.67, P = 0.4318) (Tables 6, 7). *mle*^{napts} heterozygotes have significantly higher heartbeat rhythmicities than *mle*^{napts} homozygotes at several temperatures ≥25°C (25°C: F = 6.48, P = 0.0216; 30°C: F = 1.84, P = 0.1922; 35°C: F = 1.75, P = 0.2033; 37°C: F = 10.97, P = 0.0022; 39°C: F = 2.00, P = 0.1811; 40°C: F = 8.14, P = 0.0110; 41°C: F = 0.24, P = 0.6320; 42°C: F = 1.34, P = 0.2722) (Tables 6, 7). However, *mle*^{napts} heterozygotes have higher heartbeat rhythmicities overall than *mle*^{napts} homozygotes at temperatures ≥20°C (F = 25.22, P = 0.0001) (Tables 6, 7).

RI Genotype	Temperature 20	25	30	35	37	39	40	41	42	Over-all RI across temp
mle^{napts}	0.43	0.31	0.35	0.27	0.18	0.18	0.15	0.16	0.11	0.25^{A}
+/- SEM	0.05	0.08	0.08	0.05	0.04	0.02	0.02	0.03	0.04	
N	13	8	10	9	17	6	10	9	6	
wild-type	0.52	0.39	0.42	0.36	0.29	0.33	0.32	0.35	0.30	0.37^{B}
	0.08	0.08	0.07	0.09	0.04	0.08	0.05	0.08	0.05	
	14	9	9	8	18	9	8	8	6	
mle^{napts}/+	0.58	0.58	0.48	0.40	0.40	0.31	0.35	0.18	0.22	0.41^{B}
	0.07	0.07	0.07	0.08	0.06	0.07	0.07	0.04	0.08	
	14	10	10	10	19	9	9	8	7	

Table 6. Mean rhythmicity indices of *mle*^{napts} strains and wild-type. Mean rhythmicity indices ± standard error of the mean (SEM) at medium and high temperatures, determined by univariate analyses for all genotypes tested. As mentioned earlier, rhythmicity indices of genotypes at low temperatures were not included in statistical analyses. Strains are ordered according to their overall rhythmicity index values across temperature (column at right). Extraneous genotypes were omitted from the table for clarity.

Rhythmicity indices of strains were compared across temperature by ANOVA and then ranked by REGWF test ($\alpha = 0.05$) (Einot and Gabriel, 1975). There is a significant difference between genotypes ($F = 13.40$, $P = 0.0001$), and groupings are indicated by letter superscript in the overall frequency column. Means that share a superscript are not significantly different. SEM = standard error of the mean, N = number of pupae tested and analyzed for given strain at each temperature.

Figure 16. Comparison of the relationship between rhythmicity index of pupal heartbeat and temperature. Heart rhythmicity versus temperature in wild-type (solid line), *mle*^{napts} (line with triangles), *cac*^{s} (line with circles), *cac*^{s} ; *mle*^{napts} (line with stars), *cac*^{ts2} (line with aterisks), and *cac*^{ts2} ; *mle*^{napts} (line with diamonds) pupae. Mean rhythmicity indices were determined by univariate analyses and are listed in Table 7. Bars representing standard error of the mean were omitted for clarity, but are listed in Table 7.

Regression analyses results for rhythmicity index data of these strains are omitted because they are misleading, just as they were for heart rate data, and for consistency of data analysis. Figure 16 provides a clear depiction of the relationship of rhythmicity index to changing temperature for critical strains. As was done for heart rate, rhythmicity index was regressed on temperature for *mle*^{napts} mutants to ensure consistency of heartbeat recording results from this study with those previously reported. Regression analysis resulted in a slope of –0.0134 and an intercept of 0.6957 (SAS). This indicates that there is a negative relationship between rhythmicity index and temperature for this strain, which is consistent with previously reported results (Dowse *et al.*, 1995).

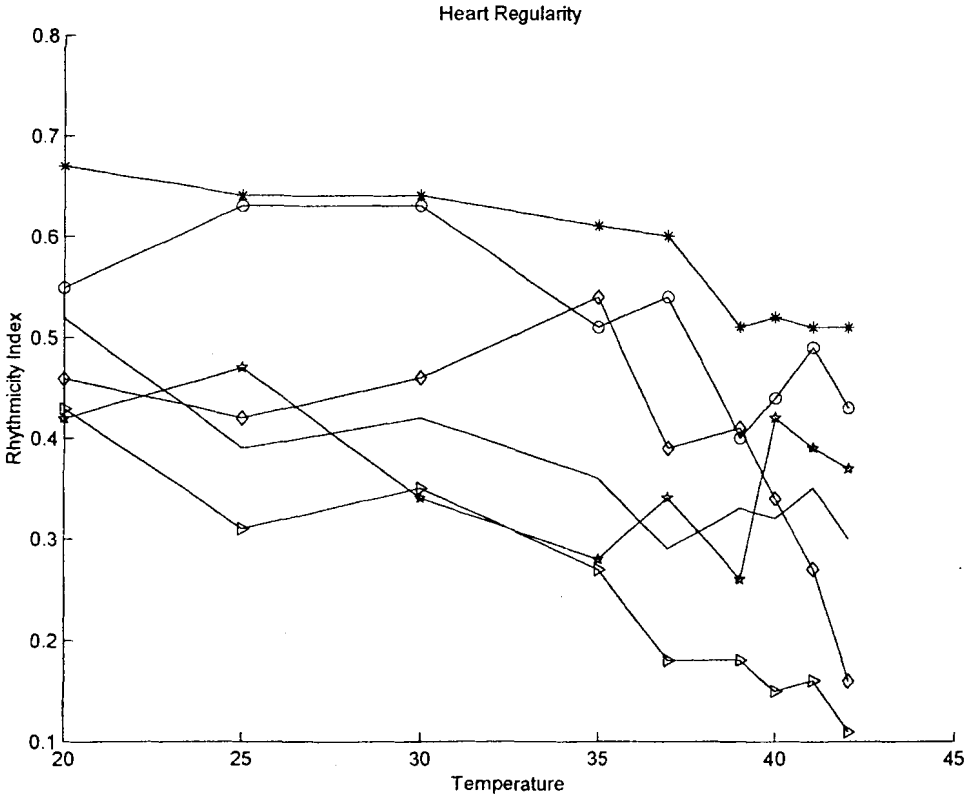

Figure 16. Continued.

Homogeneity of slopes analysis was performed on heart rate data for the same three genotypes and there were significant genotype ($F = 36.14$, $P = 0.0001$) and temperature ($F = 45.86$, $P = 0.0001$) effects, but the temperature x genotype effect ($F = 0.95$, $P = 0.4482$) was non-significant. These results indicate that genotypes have characteristic rhythmicity indices, and that temperature changes affect heartbeat rhythmicity. However, it does not appear that genotype affects how rhythmicity index changes in response to temperature. This could be because when temperature is altered rhythmicity changes are fairly erratic, in comparison to heart rate adjustments, which makes it difficult to uncover trends specific to genotype. Conclusions drawn from these results are depicted in Figure 16.

Table 7. Mean rhythmicity indices of mle^{napts}, *cac* strains, *cac* strains in a mle^{napts} background, and wild-type. Mean rhythmicity indices ± standard error of the mean (SEM) at medium and high temperatures, determined by univariate analyses for all genotypes tested. As mentioned earlier, rhythmicity indices of genotypes at low temperatures were not included in statistical analyses. Data from certain strains included in Table 6 are repeated here for ease of comparison. Strains are ordered according to their overall rhythmicity index values across temperature (column at right).

Rhythmicity indices of strains were initially compared across temperature by ANOVA and then ranked by REGWF test ($\alpha = 0.05$) (Einot and Gabriel, 1975). Genotype has a significant effect ($F = 34.15$, $P = 0.0001$) and groupings are indicated by letter superscript in the overall frequency column. Means that share a superscript are not significantly different. SEM = standard error of the mean, N = number of pupae tested and analyzed for given strain at each temperature.

RI	Temperature									Over-all RI across temp
Genotype	20	25	30	35	37	39	40	41	42	
mle^{napts}	0.43	0.31	0.35	0.27	0.18	0.18	0.15	0.16	0.11	0.25^{A}
+/- SEM	0.05	0.08	0.08	0.05	0.04	0.02	0.02	0.03	0.04	
N	13	8	10	9	17	6	10	9	6	
wild-type	0.52	0.39	0.42	0.36	0.29	0.33	0.32	0.35	0.30	0.37^{B}
	0.08	0.08	0.07	0.09	0.04	0.08	0.05	0.08	0.05	
	14	9	9	8	18	9	8	8	6	
cac^{s} ; *mle*^{napts}	0.42	0.47	0.34	0.28	0.34	0.26	0.42	0.39	0.37	0.37^{B}
	0.06	0.08	0.07	0.10	0.07	0.10	0.09	0.09	0.09	
	19	9	9	9	16	8	8	8	6	
cac^{ts2} ; *mle*^{napts}	0.46	0.42	0.46	0.54	0.39	0.41	0.34	0.27	0.16	0.40^{B}
	0.05	0.07	0.07	0.06	0.04	0.05	0.05	0.05	0.03	
	19	11	14	11	25	12	12	11	8	
mle^{napts}/+	0.58	0.58	0.48	0.40	0.40	0.31	0.35	0.18	0.22	0.41^{B}
	0.07	0.07	0.07	0.08	0.06	0.07	0.07	0.04	0.08	
	14	10	10	10	19	9	9	8	7	
cac^{s}	0.55	0.63	0.63	0.51	0.54	0.40	0.44	0.49	0.43	0.53^{C}
	0.05	0.06	0.06	0.06	0.04	0.06	0.05	0.06	0.06	
	28	19	19	19	34	15	15	15	14	
cac^{s}/+	0.63	0.60	0.58	0.60	0.56	0.53	0.46	0.43	0.46	0.55^{C,D}
	0.05	0.07	0.06	0.06	0.04	0.06	0.06	0.05	0.06	
	28	17	16	16	33	16	16	16	16	
cac^{ts2}	0.67	0.64	0.64	0.61	0.60	0.51	0.52	0.51	0.51	
	0.05	0.06	0.07	0.06	0.04	0.06	0.06	0.06	0.05	0.59^{C,D}
	29	20	19	20	39	20	19	20	17	
cac^{ts2}/+	0.67	0.67	0.68	0.65	0.60	0.58	0.62	0.55	0.62	
	0.04	0.06	0.05	0.05	0.04	0.05	0.05	0.07	0.06	
	30	19	19	19	38	19	19	17	16	0.63^{D}

Effect on Heartbeat Rhythmicity of *cac* Mutations in a *mle^{napts}* Background

Hearts of flies homozygous for both *cac^{s}* and *mle^{napts}* mutations have rhythmicities that are not significantly different from wild-type at temperatures ≥20°C (20°C: F = 1.17, P = 0.2880; 25°C: F = 0.56, P = 0.4635; 30°C: F = 0.67, P = 0.4247; 35°C: F = 0.37, P = 0.5522; 37°C: F = 0.33, P = 0.5722; 39°C: F = 0.32, P = 0.5775; 40°C: F = 0.88, P = 0.3634; 41°C: F = 0.12, P = 0.7332; 42°C: F = 0.61, P = 0.4512) (Tables 7, 8; Fig. 16). Similarly, *cac^{ts2}* ; *mle^{napts}* double mutants have rhythmicity indices that are not significantly different from wild-type at temperatures ≥20°C, except at 42°C (20°C: F = 0.60, P = 0.4455; 25°C: F = 0.09, P = 0.7650; 30°C: F = 0.19, P = 0.6633; 35°C: F = 2.82, P = 0.1112; 37°C: F = 2.57, P = 0.1166; 39°C: F = 0.74, P = 0.3989; 40°C: F = 0.08, P = 0.7841; 41°C: F = 0.72, P = 0.4065; 42°C: F = 5.85, P = 0.0324) (Table 7; Fig. 16). Raw data and autocorrelation plots of double mutants at 25°C and 40°C emphasize that their rhythmicity indices as not different from those of wild-type across temperature (Figs. 1ac, 2ac, 12ac, 13ac, 14ac, 15ac).

cac mutant homozygotes have significantly increased rhythmicity indices at certain temperatures whereas *mle^{napts}* homozygotes have decreased heartbeat rhythmicities at most temperatures. The intermediate nature of double mutant heartbeat rhythmicity implies that *cac* and *mle^{napts}* may have additive effects for the rhythmicity phenotype. Strains heterozygous for either/and *cac^{s}* or *mle^{napts}* reflect this result because the majority of them (only one exception) have overall rhythmicity indices that are not significantly different from wild-type (F = 3.19, P = 0.0245) (Table 8).

Table 8. Mean rhythmicity indices of *mle*^{napts}, all *cac*^{s} strains, *cac*^{s} strains in a *mle*^{napts} background, and wild-type. Mean rhythmicity index ± standard error of the mean (SEM) at medium and high temperatures, determined by univariate analyses for all genotypes tested. Additional stipulations concerning temperature inclusions are like those of Table 6. Strains are ordered according to their overall heart rate values across temperature (column at right). This table contains all heterozygous combinations of *cac*^{s} and *mle*^{napts}. Certain strains are also listed in Tables 6 and 7.

Heartbeat frequencies of strains were compared across temperature by ANOVA and then ranked by REGWF test ($\alpha = 0.05$) (Einot and Gabriel, 1975). There is a significant difference between genotypes ($F = 21.93$, $P = 0.0001$), and groupings are indicated by letter superscript in the overall frequency column. Means that share a superscript are not significantly different. SEM = standard error of the mean, N = number of pupae tested and analyzed for given strain at each temperature.

RI	Temperature									Over-all RI across temp
Genotype	20	25	30	35	37	39	40	41	42	
mle^{napts}	0.43	0.31	0.35	0.27	0.18	0.18	0.15	0.16	0.11	0.25^{A}
+/- SEM	0.05	0.08	0.08	0.05	0.04	0.02	0.02	0.03	0.04	
N	13	8	10	9	17	6	10	9	6	
cac^{s}/+ ; *mle*^{napts}	0.42	0.43	0.32	0.40	0.24	0.37	0.36	0.24	0.22	0.33^{A,B}
+/- SEM	0.12	0.04	0.08	0.05	0.06	0.07	0.09	0.10	0.08	
N	5	4	4	3	7	3	3	3	2	
cac^{s} ; *mle*^{napts}/+	0.53	0.46	0.54	0.38	0.34	0.33	0.26	0.20	0.16	
	0.07	0.10	0.08	0.07	0.05	0.05	0.05	0.05	0.03	0.37^{B}
	12	9	9	8	17	8	8	8	8	
wild-type	0.52	0.39	0.42	0.36	0.29	0.33	0.32	0.35	0.30	
	0.08	0.08	0.07	0.09	0.04	0.08	0.05	0.08	0.05	0.37^{B}
	14	9	9	8	18	9	8	8	6	
cac^{s} ; *mle*^{napts}	0.42	0.47	0.34	0.28	0.34	0.26	0.42	0.39	0.37	
	0.06	0.08	0.07	0.10	0.07	0.10	0.09	0.09	0.09	0.37^{B}
	19	9	9	9	16	8	8	8	6	
cac^{s}/+ ; *mle*^{napts}/+	0.75	0.79	0.69	0.60	0.37	0.36	0.34	0.29	0.19	
	0.05	0.05	0.10	0.13	0.11	0.16	0.11	0.07	0.09	0.49^{C}
	5	3	3	3	6	3	3	3	3	
cac^{s}	0.55	0.63	0.63	0.51	0.54	0.40	0.44	0.49	0.43	
	0.05	0.06	0.06	0.06	0.04	0.06	0.05	0.06	0.06	0.53^{C}
	28	19	19	19	34	15	15	15	14	
cac^{s}/+	0.63	0.60	0.58	0.60	0.56	0.53	0.46	0.43	0.46	
	0.05	0.07	0.06	0.06	0.04	0.06	0.06	0.05	0.06	0.55^{C}
	28	17	16	16	33	16	16	16	16	

DISCUSSION

The *cac* gene encodes a calcium ion channel that may participate in the cardiac pacemaker, and *mle* encodes a dsRNA helicase involved in mRNA splicing (Reenan *et al.*, 2000) that has effects on heartbeat when mutated (mle^{napts}) (Dowse *et al.*, 1995). From the results of Dowse *et al.*'s (1995) study it was hypothesized that mle^{napts} affects the heart either by indirectly interacting with the pacemaker or by influencing the impact of neurotransmitters. Further studies helped isolate necessary pacemaker components consisting of *eag*, *slo*, and *Sh* potassium channels, and an unknown calcium channel (Johnson *et al.*, 1998). However, interactions between identified pacemaker channels and mle^{napts} could not account for the heartbeat defects of this helicase mutant. This left the possibility that the unidentified calcium channel in the pacemaker may interact with mle^{napts} in a manner causative of the latter's defective heartbeat. Pharmacological evidence excluded L-type (Dmca1D) and T-type channels, and implicated Dmca1A (*cac*) as providing the necessary Ca^{2+} current to fulfill pacemaker function (Johnson *et al.*, 1998). A later study reinforced the hypothesis that *cac* and mle^{napts} may interact (Johnson *et al.*, 2001). Actually, the interaction hypothesis stemmed from this study of shi^{ts} ; mle^{napts} double mutants, where aberrant heartbeat of the dynamin mutant (shi^{ts}) was restored to a wild-type state, potentially due to a direct interaction of the helicase protein mutant (mle^{napts}) with *cac* calcium channel transcripts (Johnson *et al.*, 2001). The combination of these results set the background for future work to establish whether an interaction between mle^{napts} and *cac* exists, and if so, the mechanism by which the heart is affected.

I performed heartbeat recordings of flies mutant for lesions in both *cac* and *mle* genes. The results of this study uncovered an interaction between the two genes, but do not support the hypothesis that the interaction causes heartbeat defects in mle^{napts} flies. Therefore, further investigation is required to determine details about the relationship between mle^{napts} and *cac*.

The Effect of mle^{napts} on Heartbeat

mle^{napts} mutants show a recessive, temperature-dependent decrease in heartbeat frequency, and more drastically in rhythmicity compared to wild-type. In addition, mle^{napts} mutants' heart rates do not respond to temperature changes, while their rhythmicities continuously decrease with rising temperature. These results are mostly consistent with those of prior studies of this mutant (Dowse *et al.*, 1995; Johnson *et al.*, 2001), except that the previously observed lack of response of mle^{napts} mutants' heart rates to alterations in temperature occurred in a dominant fashion, and this result was only subtly evident in this study. In the current study mle^{napts} homozygotes were marginally unresponsive to changes in temperature, but heartbeat of heterozygotes lacked this result completely. Differences in results between studies could be due to mle^{napts} mutants having different genetic backgrounds from one study to the next.

***cac* and mle^{napts} Double Mutants**

Based on the hypothesis that mle^{napts} reduces *cac* calcium channel number, (established by work on shi^{ts}), and the finding that these channels allow a greater overall Ca^{2+} current in cac^{s} and cac^{ts2} mutants (this study), I would expect *cac* ; mle^{napts} double

mutants to have wild-type heartbeats due to counteraction of these effects. The current work makes it unclear whether an interaction between mle^{napts} and *cac* exists. cac^{s} ; mle^{napts} double mutants have heart rates that are not significantly different from wild-type, except at very high temperatures ($\geq$39°C) (Tables 4, 5; Fig. 11). However, cac^{s} single mutants exhibit a similar heart rate phenotype, only diverging from wild-type at temperatures slightly lower than double mutants ($\geq$37°C) (Table 4; Fig. 11). Heartbeat frequencies of cac^{s} mutants and cac^{s} ; mle^{napts} mutants are both higher than mle^{napts} single mutants' heart rates at all temperatures, and not significantly different from each other, although on average double mutants' heart rates are slightly higher than single mutants' (Table 4; Fig. 11) . These findings suggest that cac^{s} is not interacting with mle^{napts} for heart rate. However, based on Chapter 1 conclusions to explain dominance of cac^{s} mutants' heartbeat frequency increase, there is another possibility. Even if mle^{napts} causes a reduction in calcium channels, those channels allowing a greater overall Ca^{2+} current may be sufficient to cause some degree of tachycardia. Under this hypothesis, heartbeat of cac^{s} ; mle^{napts} double mutants should be more nearly normal than in cac^{s} single mutants. This expectation is potentially confirmed by the rhythmicity phenotypes of these genotypes. Heartbeat rhythmicities of double mutant flies are no different from wild-type at any temperature, whereas those of cac^{s} mutants are increased when averaged across temperature and at specific temperatures (25°C, 37°C; Table 1; Fig. 7). If there are fewer overactive calcium channels in double mutants then there would be a less significant increase in inward Ca^{2+} current compared to cac^{s} mutants, which would result in a much less pronounced, or perhaps completely non-evident, increase in heartbeat strength (Johnson *et al.*, 1997). Therefore, the rhythmicity phenotype of double mutants

suggests that MLE may be interacting with cac^{s} or at least that their effects on heartbeat are additive. Other results, however, restore skepticism to the theory that cac^{s} and mle^{napts} interact. It would be surprising that cac^{s} ; mle^{napts} double mutants have higher heart rates than cac^{s} single mutants if this hypothesis were true, but this is only a slight and non-significant effect and so may be due to differences in experimental method like the use of varied sample sizes between genotypes. The effect of sample size was already noted by the conclusion as to why this study's cac^{s} mutant heartbeat results contradict those of a past study (Johnson *et al.*, 1998). An interesting tangent to these findings is that mle^{napts} being homo- or heterozygous appears to inconsistently, albeit subtly, affect rhythmicity (Table 8). This observation is perplexing considering that cac^{s} may be epistatic over mle^{napts} for heartbeat frequency and may again allude to an interaction between the genes.

Determining the presence of an interaction between mle^{napts} and the *cac* gene becomes even more complex when considering the other allele under scrutiny, cac^{ts2}. Although heartbeat rhythmicity results for cac^{ts2} ; mle^{napts} double mutants are statistically indistinguishable from those of cac^{s} ; mle^{napts} double mutants (Table 7), as expected, their heart rates are very different (Table 4). cac^{ts2} ; mle^{napts} double mutants have much lower heart rates than wild-type flies, and even lower than mle^{napts} mutants, when averaged across temperature and at specific temperatures (Table 4; Fig. 11). This result is remarkable considering that cac^{ts2} mutant flies have drastic heart rate changes in the opposite direction (Table 4; Fig. 11). This phenotype is difficult to explain at the physiological level, especially when considering that cac^{ts2} mutants may have more aberrant channel inactivation properties than cac^{s} mutants. Based on this information I

would expect cac^{ts2} ; mle^{napts} double mutants to have heart rates at least slightly more increased than the double mutant strain carrying cac^{s} because inactivation of these calcium channels is more defective. That heart rates of cac^{ts2} and mle^{napts} double mutants are severely decreased implies an interaction, but different from that between mle^{napts} and *para*.

An unfortunate factor that adds confusion to this discussion is that strains of double mutants for each *cac* allele and mle^{napts} were isolated using different mating schemes. Until double mutants of both *cac* alleles are isolated using the same process and their heartbeats recorded, it will not be possible to draw reliable conclusions.

REFERENCES

Alberts, B., D. Bray, A. Johnson, J. Lewis, M. Raff, K. Roberts, and P. Walter. 1998. *Essential Cell Biology: An Introduction to the Molecular Biology of the Cell.* Garland. New York.

Alberts, B., D. Bray, J. Lewis, M. Raff, K. Roberts, and J.D. Watson. 2002. *Molecular Biology of the Cell,* 4th Ed. Garland. New York.

Amichot, M., C. Castella, J.-B. Bergé, and D. Pauron. 1993. Transcription analysis of the *para* gene by *in situ* hybridization and immunological characterization of its expression product in wild-type and mutant strains of *Drosophila*. *Insect Biochem. Molec. Biol.* 23: 381-390.

Ashcroft, F.M. 2000. *Ion Channels and Disease.* Academic. Boston.

Atkinson, N.S., G. Robertson, and B. Ganetzky. 1991. A component of calcium – activated potassium channels encoded by the *Drosophila slo* locus. *Science.* 253: 551-555.

Barinaga, M. 1998. Tracking down mutations that can stop the heart. *Science.* 281: 32-34.

Bodmer, R. 1993. The gene *tinman* is required for specification of the heart and visceral muscles in *Drosophila*. *Development.* 118: 719-729.

Brooks, I.M., R. Felling, F. Kawasaki, and R.W. Ordway. 2003. Genetic analysis of a synaptic calcium channel in *Drosophila*: intragenic modifiers of a temperature-sensitive paralytic mutant of *cacophony*. *Genetics.* 164: 163-171.

Brüggemann, A., L.A. Pardo, W. Stühmer, and O. Pongs. 1993. *Ether a go-go* encodes a voltage-gated channel permeable to K^+ and Ca^{2+} and modulated by cAMP. *Nature.* 365: 445-448.

Chan, B., A. Villella, P. Funes, and J.C. Hall. 2002. Courtship and other behaviors affected by a heat-sensitive, molecularly novel mutation in the *cacophony* calcium-channel gene of *Drosophila*. *Genetics.* 162: 135-153.

Chang, H., and D.D. Miller. 1978. Courtships and mating sounds in species of the *Drosophila affinis* subgroup. *Evolution.* 32: 540-550.

Clancy, C.E., and Y. Rudy. 1999. Linking a genetic defect to its cellular phenotype in a cardiac arrhythmia. *Nature.* 400: 566-569.

Curran, M., I. Splawski, K. Timothy, G. Vincent, E. Green, and M. Keating. 1995. A molecular basis for cardiac arrhythmia: HERG mutations cause long QT syndrome. *Cell.* 80: 795-803.

Curtis, N., J. Ringo, and H. Dowse. 1999. Morphology of the pupal heart, adult heart, and associated tissues in the fruit fly (*Drosophila melanogaster). J. Morphol.* 240: 225-235.

Dascal, N., T.P. Snutch, H. Lübbert, N. Davidson, and H.A. Lester. 1986. Expression and modulation of voltage-gated calcium channels after RNA injection in Xenopus oocytes. *Science.* 231: 1147-1150.

Davenport, C.B. 1941. The early history of research with Drosophila. *Science.* 93: 305-306.

Day, N.C., S.J. Wood, P.G. Ince, S.G. Volsen, W. Smith, C.R. Slater, and P.J. Shaw. 1997. Differential localization of voltage-dependent calcium channel α_1 subunits at the human and rate neuromuscular junction. *J. Neurosci.* 17: 6226-6235.

de Leon, M., Y. Wang, L. Jones, E. Perez-Rey, X. Wei, T.W. Soong, T.P. Snutch, and D.T. Yue. 1995. Essential Ca^{2+}-binding motif for Ca^{2+}-sensitive inactivation of L-type Ca^{2+} channels. *Science.* 270: 1502-1506.

Dellinger, B.B., R. Felling, and R.W. Ordway. 2000. Genetic modifiers of the *Drosophila* NSF mutant, *comatose*, include a temperature-sensitive paralytic allele of the calcium channel $\alpha 1$ subunit gene, *cacophony. Genetics.* 155: 203-211.

DeMaria, C.D., T.W. Soong, B.A. Alseikhan, R.S. Alvania, and D.T. Yue. 2001. Calmodulin bifurcates the local Ca^{2+} signal that modulates P/Q-type Ca^{2+} channels. *Nature.* 411: 484-489.

Dowse, H., J. Ringo, J. Power, E. Johnson, K. Kinney, and L. White. 1995. A congenital heart defect in *Drosophila* caused by an action potential mutation. *J. Neurogenet.* 10: 153-168.

Eberl, D., D. Ren, G. Feng, L. Lorenz, D. VanVactor, and L. Hall. 1998. Genetic and developmental characterization of *Dmca1D*, a calcium channel α_1 subunit gene in *Drosophila melanogaster. Genetics.* 148: 1159-1169.

Einot, I., and K. Gabriel. 1975. A study of the powers of several methods of multiple comparisons. *J. Am. Stat. Assoc.* 70: 351.

Elkins, T., B. Ganetzky, and C.-F. Wu. 1986. A *Drosophila* mutation that eliminates a calcium-dependent potassium current. *Proc. Natl. Acad. Sci. USA.* 83: 8415-8419.

Engel, J.E., and C.-F. Wu. 1992. Interactions of membrane excitability mutations affecting potassium and sodium currents in the flight and giant fiber escape systems of *Drosophila*. *J. Comp. Physiol. A.* 171: 93-104.

Ewing, A.W., and H.C. Bennet-Clark. 1968. The courtship songs of *Drosophila*. *Behaviour*. 31: 288-301.

Fletcher, C.F., N.G. Copeland, and N.A. Jenkins. 1998. Genetic analysis of voltage-dependent calcium channels. *J. Bioenerg. Biomem.* 30: 387-398.

Fozzard, H., and M. Arnsdorf. 1992. Cardiac electrophysiology. In: *The heart and cardiovascular system*, 2nd Ed. H. Fozzard (ed.). Raven. New York. pp 63-98.

Ganetzky, B. 1984. Genetic studies of membrane excitability in *Drosophila*: lethal interaction between two temperature-sensitive paralytic mutations. *Genetics*. 108: 897-911.

Gibbs, F.P. 1981. Temperature-dependence or rat circadian pacemaker. *Am. Phys. Soc.* R17-R20.

Gielow, M., G.-G. Gu, and S. Singh. 1995. Resolution and pharmacological analysis of the voltage-dependent calcium channels of *Drosophila*'s larval muscles. *J. Neurosci.* 15: 6085-6093.

Gilbert, S.F. 2000. *Developmental Biology,* 6th Ed. Sinauer. Sunderland.

Greenberg, R.M., J. Streissnig, A. Koza, P. Devay, H. Glossman, and L.M. Hall. 1989. Native and detergent-solubilized membrane extracts from *Drosophila* heads contain binding sites for the phenylalkylamine calcium channel blockers. *Insect Biochem.* 19: 309-322.

Greenspan, R.J., and J.-F. Ferveur. 2000. Courtship in *Drosophila*. *Annu. Rev. Genet.* 34: 205-232.

Gu, G.-G., and S. Singh. 1995. Pharmacological analysis of heartbeat in *Drosophila*. *J. Neurobiol.* 28: 269-280.

Guillén, A., J.-M. Jallon, J.-A. Fehrentz, C. Pantaloni, J. Bockaert, and V. Homburger. 1990. A G_o-like protein in *Drosophila melanogaster* and its expression in memory mutants. *EMBO J.* 9: 1449-1455.

Guyton, A.C., and J.E. Hall. 2000. *Textbook of Medical Physiology,* 10th Ed. W.B. Saunders. Philadelphia.

Hall, J.C. 1994. The mating of a fly. *Science*. 264: 1702-1714.

Hanrahan, C.J., M.J. Palladino, B. Ganetzky, and R.A. Reenan. 2000. RNA editing of the *Drosophila para* Na^+ channel transcript: evolutionary conservation and developmental regulation. *Genetics*. 155: 1149-1160.

Heisenberg, M., and K.G. Götz. 1975. The use of mutations for the partial degradation of vision in *Drosophila melanogaster*. *J. Comp. Physiol.* 98: 217-241.

Hering, S., S. Aczél, M. Grabner, F. Döring, S. Berjukow, J. Mitterdorfer, M. J. Sinnegger, J. Striessnig, V. E. Degtiar, Z. Wang, and H. Glossman. 1996. Transfer of high sensitivity for benzothiazepines from L-type to class A (BI) calcium channels. *J. Bio. Chem.* 271: 24471-24475.

Hering, S., S. Berjukow, S. Aczél, and E.N. Timin. 1998. Ca^{2+} channel block and inactivation: common molecular determinants. *Trends Pharmacol. Sci.* 19: 439-443.

Hering, S., S. Berjukow, S. Sokolov, R. Marksteiner, R.G. Weiss et al., 2000. Molecular determinants of inactivation in voltage-gated Ca^{2+} channels. *J. Physiol.* 528: 237-249.

Hille, B. 2001. *Ionic Channels of Excitable Membranes*, 3rd Ed. Sinauer. Sunderland.

Homyk, Jr. T., and Q. Pye. 1989. Some mutations affecting neural or muscular tissues alter the physiological components of the electroretinogram in *Drosophila*. *J. Neurogenet.* 5: 37-48.

Horowitz, D.S., and A.R. Krainer. 1994. Mechanisms for selecting 5' splice sites in mammalian pre-mRNA splicing. *Trends Genet.* 10: 100-106.

Hüser, J., L.A. Blatter, and S.L. Lipsius. 2000. Intracellular Ca^{2+} release contributes to automaticity in cat atrial pacemaker cells. *J. Physiol.* 524: 414-422.

Irisawa, H., H.F. Brown, and W. Giles. 1993. Cardiac pacemaking in the sinoatrial node. *Phys. Rev.* 73: 197-227.

Jackson, F.R., S.D. Wilson, G.R. Strichartz, and L.M. Hall. 1984. Two types of mutants affecting voltage-sensitive sodium channels in *Drosophila melanogaster*. *Nature*. 308: 189-191.

Jeziorski, M.C., R.M. Greenberg, and P.A.V. Anderson. 2000. The molecular biology of invertebrate voltage-gated Ca^{2+} channels. *J. Exp. Biol.* 203: 841-856.

Jiang, Y., A. Lee, J. Chen, V. Ruta, M. Cadene, B.T. Chait, and R. MacKinnon. 2003a. X-ray structure of a voltage-dependent K^+ channel. *Nature*. 423: 33-41.

Jiang, Y., V. Ruta, J. Chen, A. Lee, and R. MacKinnon. 2003b. The principle of gating charge movement in a voltage-dependent K^+ channel. *Nature*. 423: 42-48.

Johnson, E., J. Ringo, and H. Dowse. 1997. Modulation of *Drosophila* heartbeat by neurotransmitters. *J. Comp. Physiol. B*. 167: 89-97.

Johnson, E., J. Ringo, N. Bray, and H. Dowse. 1998. Genetic and pharmacological identification of ion channels central to *Drosophila*'s cardiac pacemaker. *J. Neurogenet.* 12: 1-24.

Johnson, E., J. Ringo, and H. Dowse. 2000. Native and heterologous neuropeptides are cardioactive in *Drosophila melanogaster*. *J. Insect Physiol.* 46: 1229-1236.

Johnson, E., J. Ringo, and H. Dowse. 2001. Dynamin, encoded by the gene *shibire*, is essential for cardiac function. *J. Exp. Zool.* 289: 81-89.

Johnson, E., T. Sherry, J. Ringo, and H. Dowse. 2002. Modulation of the cardiac pacemaker of *Drosophila*: Cellular Mechanisms. *J. Comp. Physiol. B*. 172: 227-236.

Jones, J.C. 1977. *The Circulatory System of Insects*. Charles C. Thomas. Springfield.

Kaplan, W., and W. Trout. 1968. The behavior of four neurological mutants of *Drosophila*. *Genetics*. 61: 399-409.

Kardong, K.V. 2002. *Vertebrates: Comparative Anatomy, Function, Evolution*, 3rd Ed. McGraw-Hill. Boston.

Kawasaki, F., F. Felling, and R.W. Ordway. 2000. A temperature-sensitive paralytic mutant defines a primary synaptic calcium channel in *Drosophila*. *J. Neurosci.* 20: 4885-4889.

Kawasaki, F., S.C. Collins, and R.W. Ordway. 2002. Synaptic calcium channel function in *Drosophila*: Analysis and transformation rescue of temperature-sensitive paralytic and lethal mutations of *cacophony*. *J. Neurosci.* 22: 5856-5864.

Keating, M., and M. Sanguinetti. 1996. Molecular genetic insights into cardiovascular disease. *Science*. 272: 681-685.

Kernan, M., M. Kuroda, R. Kreber, B. Baker, and B. Ganetzky. 1991. nap^{ts}, a mutation affecting sodium channel activity in *Drosophila*, is an allele of *mle*, a regulator of dosage compensation. *Cell*. 66: 949-959.

Kim, Y., and M. Nirenberg. 1989. *Drosophila* NK-homeobox genes. *Proc. Natl. Acad. Sci. USA*. 86: 7716-7720.

Koch, W.J., P.T. Ellinor, and A. Schwartz. 1990. cDNA cloning of a dihydropyridine-sensitive calcium channel from rat aorta: Evidence for the existence of alternatively spliced forms. *J. Biol. Chem.* 265: 17786-17791.

Krauss, G. 2001. *Biochemistry of Signal Transduction and Regulation*, 2nd Ed. Sinauer. Sunderland.

Kulkarni, S.J., and J.C. Hall. 1987. Behavioral and cytogenetic analysis of the *cacophony* courtship song mutant and interacting genetic variants in *Drosophila melanogaster*. *Genetics*. 115: 461-475.

Lee, A., S.T. Wong, D. Gallagher, B. Li, D.R. Storm, T. Scheuer, and W.A. Catterall. 1999. Ca^{2+}/calmodulin binds to and modulates P/Q-type calcium channels. *Nature*. 399: 155-158.

Levine, J.D., P. Funes, H.B. Dowse, and J.C. Hall. 2002. Signal analysis of behavioral and molecular cycles. *BMC Neurosci*. 3: 1471-22-2.

Lewin, B. 2000. *Genes VII*. Oxford. New York.

Lipsius, S.L., J. Hüser, and L.A. Blatter. 2001. Intracellular Ca^{2+} release sparks atrial pacemaker activity. *News Physiol. Sci.* 16: 101-106.

Littleton, J.T., and B. Ganetzky. 2000. Ion channels and synaptic organization: analysis of the *Drosophila* genome. *Neuron*. 26: 35-43.

Loughney, K., R. Kreber, and B. Ganetzky. 1989. Molecular analysis of the *para* locus, a sodium channel gene in *Drosophila*. *Cell*. 58: 1143-1154.

MacPherson, M.R., V.P. Pollock, K.E. Broderick, L. Kean, F.C. O'Connell, J.A.T. Dow, and S.A. Davies. 2001. L-type calcium channels regulate epithelial fluid transport in *Drosophila melanogaster*. *Am. J. Physiol.* 280: C394-C407.

Markou, T., and G. Theophilidis. 2000. The pacemaker activity generating the intrinsic myogenic contraction of the dorsal vessel of *Tenebrio molitor* (coleoptera). *J. Exp. Biol.* 203: 3471-3483.

McCann, F.V. 1969. The heart as a model for electrophysiological studies. In: *Experiments in Physiology and Biochemistry, VII*. G.A. Kerkut (ed.). Academic. London. pp 59-88.

Metcalf, R., M. Winton, and T. Fukuto. 1964. The effects of cholinergic substances upon the isolated heart of *Periplaneta americana*. *J. Insect Physiol.* 10: 353-361.

Miller, C. 1978. Voltage-gated cation conductance channel from fragmented sarcoplasmic reticulum: steady-state electrical properties. J. *Membr. Biol.* 40: 1-23.

Miller, T.A. 1985. Structure and physiology of the circulatory system. In:. *Comprehensive insect physiology, biochemistry, and pharmacology*, Vol. III. Kerkut, G.A., and L. Gilbert (eds.). Pergamon. New York. pp 289-353.

Moczydlowski, E., K., Lucchesi, and A. Ravindran. 1988. An emerging pharmacology of peptide toxins targeted against potassium channels. J. *Membr. Biol.* 105: 95-111.

Navaratnam, V. 1987. *Heart muscle: ultrastructural studies*. Cambridge Uni. New York.

Neely, A., X. Wei, R. Olcese, L. Birnbaumer, and E. Stefani. 1993. Potentiation by the beta subunit of the ratio of the ionic current to the charge movement in the cardiac calcium channel. *Science*. 262: 575-578.

Nunoki, K., V. Florio, and W. A. Catterall. 1989. Activation of purified calcium channels by stoichiometric protein phosphorylation. *Proc. Natl. Acad. Sci. USA*. 86: 6816-6820.

Olivera, B., G. Miljanich, J. Ramachandran, and M. Adams. 1994. Calcium channel diversity and neurotransmitter release: The ω-Conotoxins and ω-Agatoxins. *Annu. Rev. Biochem*. 63: 823-867.

Pak, W.L. 1970. Mutants of the visual pathway of *Drosophila melanogaster*. *Nature*. 227: 518-520.

Palladino, M.J., L.P. Keegan, M.A. O'Connell, and R.A. Reenan. 2000. A-to-I pre-mRNA editing in *Drosophila* is primarily involved in adult nervous system function and integrity. *Cell*. 102: 437-449.

Papaefthimiou, C., and G. Theophilidis. 2001. An *in vitro* method for recording the electrical activity of the isolated heart of the adult *Drosophila melanogaster*. *In Vitro Cell. Dev. Biol.-Animal*. 37: 445-449.

Park, M., C. Lewis, D. Turbay, A. Chung, J.-N. Chen, S. Evans, R.E. Breitbart, M.C. Fishman, S. Izumo, and R. Bodmer. 1998. Differential rescue of visceral and cardiac defects in *Drosophila* by vertebrate *tinman*-related genes. *Proc. Natl. Acad. Sci.* USA. 95: 9366-9371.

Peixoto, A.A., and J.C. Hall. 1998. Analysis of temperature-sensitive mutants reveals new genes involved in the courtship song of *Drosophila*. *Genetics*. 148: 827-838.

Peixoto, A.A., L.A. Smith, and J.C. Hall. 1997. Genomic organization and alternative exons in a *Drosophila* calcium channel gene. *Genetics*. 145: 1003-1013.

Peixoto, A.A., R. Costa, and J.C. Hall. 2000. Molecular and behavioral analysis of sex-linked courtship song variation in a natural population of *Drosophila melanogaster*. *J. Neurogenet.* 14: 245-256.

Peterson, B.Z., J.S. Lee, J.G. Mulle, Y. Wang, M. de Leon, and D.T. Yue. 2000. Critical determinants of Ca^{2+}-dependent inactivation within an EF-hand motif of L-type Ca^{2+} channels. *Biophys. J.* 78: 1906-1920.

Poulson, D.F. 1994. Histogenesis, organogenesis, and differentiation in the embryo of *Drosophila melanogaster*. In: *Biology of Drosophila*, facsimile edition. M. Demerec (ed.). Cold Spring Harbor Laboratory. Cold Spring Harbor. pp 168-274.

Reenan, R.A., C.J. Hanrahan, and B. Genetzky. 2000. The *mle^{napts}* RNA helicase mutation in *Drosophila* results in a splicing catastrophe of the *para* Na^{+} channel transcript in a region of RNA editing. *Neuron.* 25: 139-149.

Rigg, L., B.M. Heath, Y. Cui, and D.A. Terrar. 2000. Localisation and functional significance of ryanodine receptors during β-adrenoceptor stimulation in the guinea-pig sino-atrial node. *Cardio. Res.* 48: 254-264.

Rigg, L., P.A.D. Mattick, B.M. Heath, and D.A. Terrar. 2003. Modulation of the hyperpolarization-activated current (I_f) by calcium and calmodulin in the guinea-pig sino-atrial node. *Cardio. Res.* 57: 497-504.

Rigg, L., and D.A. Terrar. 1996. Possible role of calcium release from sarcoplasmic reticulum in pacemaking in guinea-pig sino-atrial node. *Exp. Physiol.* 81: 877-880.

Rizki, T.M. 1978. The circulatory system and associated cells and tissues. In: *The Genetics and Biology of Drosophila*. Ashburner, M., and T.R.F. Wright (eds.). Cold Spring Harbor. Cold Spring Harbor. pp 1839-1845.

Robbins, J., R. Aggarwal, R. Nichols, and G. Gibson. 1999. Genetic variation affecting heart rate in *Drosophila melanogaster*. *Genet. Res. Camb.* 74: 121-128.

Rubin, G.M., M.D. Yandell, J.R. Wortman, G.L.G. Miklos, C.R. Nelson, I.K. Hariharan, M.E. Fortini, P.W. Li, R. Apweiler, W. Fleischmann, J.M. Cherry, S. Henikoff, M.P. Skupski, S. Misra, M. Ashburner, E. Birney, M.S. Boguski, T. Brody, P. Brokstein, S.E. Celniker, S.A. Chervitz, D. Coates, A. Cravchik, A. Gabrielian, R.F. Galle, W.M. Gelbart, R.A. George, L.S.B. Goldstein, F. Gong, P. Guan, N.L. Harris, B.A. Hay, R.A. Hoskins, J. Li, Z. Li, R.O. Hynes, S.J.M. Jones, P.M. Kuehl, B. Lemaitre, J.T. Littleton, D.K. Morrision, C. Mungall, P.H. O'Farrell, O.K. Pickeral, C. Shue, L.B. Vosshall, M. Sanguinetti, C. Jiang, M. Curran, and M. Keating. 1995. A mechanistic link between an inherited and an acquired cardiac arrhythmia: HERG encodes the Ikr potassium channel. *Cell.* 81: 299-307.

Schilcher, F.v. 1976. The behavior of *cacophony*, a courtship song mutant in *Drosophila melanogaster*. *Behav. Biol.* 17: 187-196.

Schott, J-J., D. Benson, C. Bason, W. Pease, G. Silberbach, J. Moak, B. Maron, C. Seidman, and J. Seidman. 1998. Congenital heart disease caused by mutations in the transcription factor NKX2-5. *Science*. 281: 108-111.

Sigworth, F.J. 2003. Life's transistors. *Nature*. 423: 21-22.

Simon, M., M. Strathmann, and N. Gautam. 1991. Diversity of G proteins in signal transduction. *Science*. 252: 802-808.

Smith, L.A., A.A. Peixoto, E.W. Kramer, A. Villella, and J.C. Hall. 1998. Courtship and visual defects of *cacophony* mutants reveal functional complexity of a calcium-channel α_1 subunit in *Drosophila*. *Genetics*. 149: 1407-1426.

Smith, L., X. Wang, A. Peixoto, E. Neumann, L.M. Hall, and J. Hall. 1996. A *Drosophila* calcium channel α-1 subunit gene maps to a genetic locus associated with behavioral and visual defects. *J. Neurosci.* 16: 7868-7879.

Snutch, T.P., J.P. Leonard, M.M. Gilbert, H.A. Lester, and N. Davidson. 1990. Rat brain expresses a heterogeneous family of calcium channels. *Proc. Natl. Acad. Sci. USA*. 87: 3391-3395.

Sokal, R., and F.J. Rohlf. 1995. *Biometry*. Freeman. New York.

Speith, H.T., and J.M. Ringo. 1983. Mating behavior and sexual isolation in Drosophila. In: *The Genetics and Biology of Drosophila*, Vol. 3c. Ashburner, M., H.L. Carson, and J.N. Thompson, Jr. (eds.). Academic Press. New York.

Strong, M., K.G. Chandy, and G. Gutman. 1993. Molecular evolution of voltage-sensitive ion channel genes: On the origin of electrical excitability. *Mol. Biol. Evol.* 10: 221-242.

Suzuki, D.T., T. Grigliatti, and R. Williamson. 1971. Temperature-sensitive mutations in *Drosophila melanogaster*., VII. A mutation (*para*^{ts}) causing a reversible adult paralysis. *Proc. Nat. Acad. Sci. USA*. 68: 890-893.

Terrar, D., and L. Rigg. 2000. What determines the initiation of heartbeat? *J. Physiol.* 524: 316.

The FlyBase Consortium. 2003. The FlyBase database of the *Drosophila* genome projects and community literature. *Nucleic Acids Res.* 31: 172-175. http://flybase.org/

Thompson, S. 1977. Three pharmacologically distinct potassium channels in molluscan neurons. *J. Physiol.* 265: 465-488.

Timpe, L., T. Schwarz, B. Tempel, D. Papazian, Y-N. Jan, and L. Jan. 1988. Expression of functional potassium channels from *Shaker* cDNA in *Xenopus* oocytes. *Nature.* 331: 143-145.

Tsien, R.W., P. Hess, E.W. McCleskey, and R.L Rosenberg. 1987. Calcium channels: Mechanisms of selectivity, permeation, and block. *Annu. Rev. Biophys. Chem.* 16: 265-290.

Warmke, J., R. Drysdale, and B. Ganetzky. 1991. A distinct potassium channel polypeptide encoded by the *Drosophila eag* locus. *Science.* 252: 1560-1562.

Warmke, J., and B. Ganetzky. 1994. A family of potassium channel genes related to *eag* in *Drosophila* and mammals. *Proc. Natl. Acad. Sci. USA.* 91: 3438-3442.

Weinreich, F., and T.J. Jentsch. 2000. Neurological diseases caused by ion channel mutations. *Curr. Op. Neurobiol.* 10: 409-415.

Wheeler, D.A., S.J. Kulkarni, D.A. Gailey, and J.C. Hall. 1989. Spectral analysis of courtship songs in behavioral mutants of *Drosophila melanogaster*. *Behav. Genet.* 19: 503-528.

White, L., J. Ringo, and H. Dowse. 1992. A circadian clock of *Drosophila*: effects of deuterium oxide and mutations at the *period* locus. *Chronobiology International.* 9: 250-259.

Wu, C. -F., B. Ganetzky, Y. Jan, L. Jan., and S. Benzer. 1978. A *Drosophila* mutant with a temperature-sensitive block in nerve conduction. *Proc. Natl. Acad. Sci. USA.* 75: 4047-4051.

Yamamoto, D., J.-M. Jallon, and A. Komatsu. 1997. Genetic dissection of sexual behavior in *Drosophila melanogaster*. *Annu. Rev. Entomol.* 42: 551-585.

Zhang, J.F., P.T. Ellinor, R.W. Aldrich, and R.W. Tsien. 1994. Molecular determinants of voltage-dependent inactivation in calcium channels. *Nature.* 372: 97-100.

Zhang, Q., X. Zhao, H. Zheng, F. Zhong, W. Zhong, R. Gibbs, J.C. Venter, M.D. Adams, and S. Lewis. 2000. Comparative genomics of the eukaryotes. *Science.* 287: 2204-2215.

Zhong, Y., and C.-F. Wu. 1991. Alteration of four identified K^+ currents in *Drosophila* muscle by mutations in *eag*. *Science.* 252: 1562-1564.

Zhou, J., R. Olcese, N. Quin, F. Noceti, L. Birnbaumer, and E. Stefani. 1997. Feedback inhibition of Ca^{2+} channels by Ca^{2+} depends on the short sequence of the C terminus that does not include the Ca^{2+}-binding function of a motif with similarity to Ca^{2+}-binding domains. *Proc. Natl. Acad. Sci. USA.* 94: 2301-2305.

Zühlke, R.D., G.S. Pitt, K. Deisseroth, R.W. Tsien, and H. Reuter. 1999. Calmodulin supports both inactivation and facilitation of L-type calcium channels. *Nature*. 399: 159-162

BIOGRAPHY OF THE AUTHOR

Vanessa McGowan was born and raised in Sault Ste. Marie, Ontario, Canada on April 19, 1977. She attended Sir James Dunn high school in the city of her birth. She then attended the University of Maine in Orono, Maine on an athletic scholarship. She graduated with a Bachelor of Science degree in Biology with a Chemistry minor in May, 2000. She participated in the Honors Program while doing her undergraduate work, earning Highest Honors after completing an Honor's Thesis under the tutelage of Dr. Harold B. Dowse and Erik Johnson. During that time, she competed as a varsity athlete and captain on the University of Maine's Cross Country, and Track and Field teams.

Upon completion of her undergraduate degree she began graduate work at the University of Maine with Harold B. Dowse as her major advisor. After receiving her degree, she will seek employment in commercial biological research in the Portland, Maine area, before continuing her studies in the medical field.

Vanessa is a candidate for the Master of Science degree in Zoology from The University of Maine in December, 2003.